Status of SNPP VIIRS Instrument Operations

VIIRS Characterization Support Team (VCST)

June 6, 2016

Outline

- Status of SNPP/VIIRS Operations:
  - SNPP Burn Maneuvers
  - SNPP/VIIRS Calibration Maneuvers
  - Spacecraft and VIIRS Anomalies
  - VIIRS Flight Software Update
  - Warm-Up/Cool-Down Operations
  - DNB VROP Operations
  - VIIRS Telemetry

Spacecraft Burn Maneuvers

- **Drag Make-Up (DMU) Maneuvers**
  - Purpose: To keep near orbital period to ~101.5 minutes.
  - 23 DMUs since launch, most recent March 24, 2016.
- **Inclination Adjustment Maneuvers (IAM)**
  - Purpose: To keep equator crossing time between 1325 and 1330.
  - 5 IAMs since launch, most recent September 23, 2015.
- **Risk Mitigation Maneuvers (RMM)**
  - Purpose: For collision avoidance.
  - 5 RMMs since launch, most recent November 15, 2015.

Spacecraft Calibration Maneuvers

- **VIIRS Lunar Roll Maneuvers (LRM)**
  - To observe the Moon through the Space View at near-constant lunar phase. ~9 times/year.
  - 37 LRMs since launch, most recent May 17, 2016.
  - Sector Rotation to put data nadir at center of SV beginning with the April 2, 2012 event (5th event).

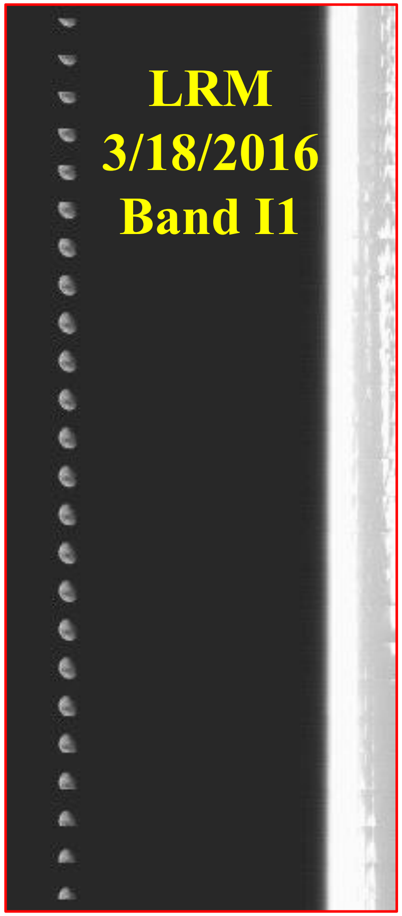

- **SNPP Yaw Maneuvers**
  - VIIRS: 14 Maneuvers for SD/SDSM Screen Cal., Feb. 15-16, 2012.
  - OMPS/CERES: February 17, 2012 & March 4, 2014.
- **SNPP Pitch Maneuver**
  - Nighttime, for VIIRS, CERES, & ATMS Cal., February 20, 2012.

Spacecraft & VIIRS Anomalies

- **Spacecraft Anomalies**
  - Sun Pointing: March 24, 2012, effects to some VIIRS band trends.
  - Earth Pointing: June 21, 2012, ~20 hours offline.
- **VIIRS "Petulant Mode"**
  - Single Board Computer (SBC) lock-up.
  - 8 Events since launch, most recent October 9, 2014.
  - Roughly 2-4 hours to get back online, sometimes longer.
  - None since FSW 0x4016 update in December 2014.
- **VIIRS Scan Sync Loss**
  - Mirror sync loss between RTA and HAM for short (~2-3 minutes). periods resulting in poor geolocation accuracy.
  - 63 Events since launch, most recent May 16, 2016.

VIIRS Flight Software Update

(Information courtesy of SNPP MOT)

- **VIIRS FSW 0x4016**
  - **Uploaded on December 10, 2014.**
  - **Implemented software watchdog timer that could assist in understanding and/or preventing SBC lock-up occurrences.**

- **VIIRS FSW 0x4017**
  - **Uploaded on April 19, 2016.**
  - **Perform robust indices checks before accessing out-of-bound memory locations. Prevent DAS upload error similar to Op-Night/Op-Day incident on June 12, 2014.**
  - **Trade band M7 for M11 at night per scientist request.**
  - **Fix segmentation dump and clear fault log in Safe Mode event.**
  - **M11 at night cannot accomplished until SNPP Block 2.0 is operational.**

VIIRS BB Warm-Up/Cool-Down

- **WUCD Events for TEB Calibration:**
  - **17 Events since launch, most recent March 14-16, 2016.**
  - **8 temperature steps: Min/Max T_{BB} = 272.5 to 315.0 K.**
  - **Complete in 46 hours.**

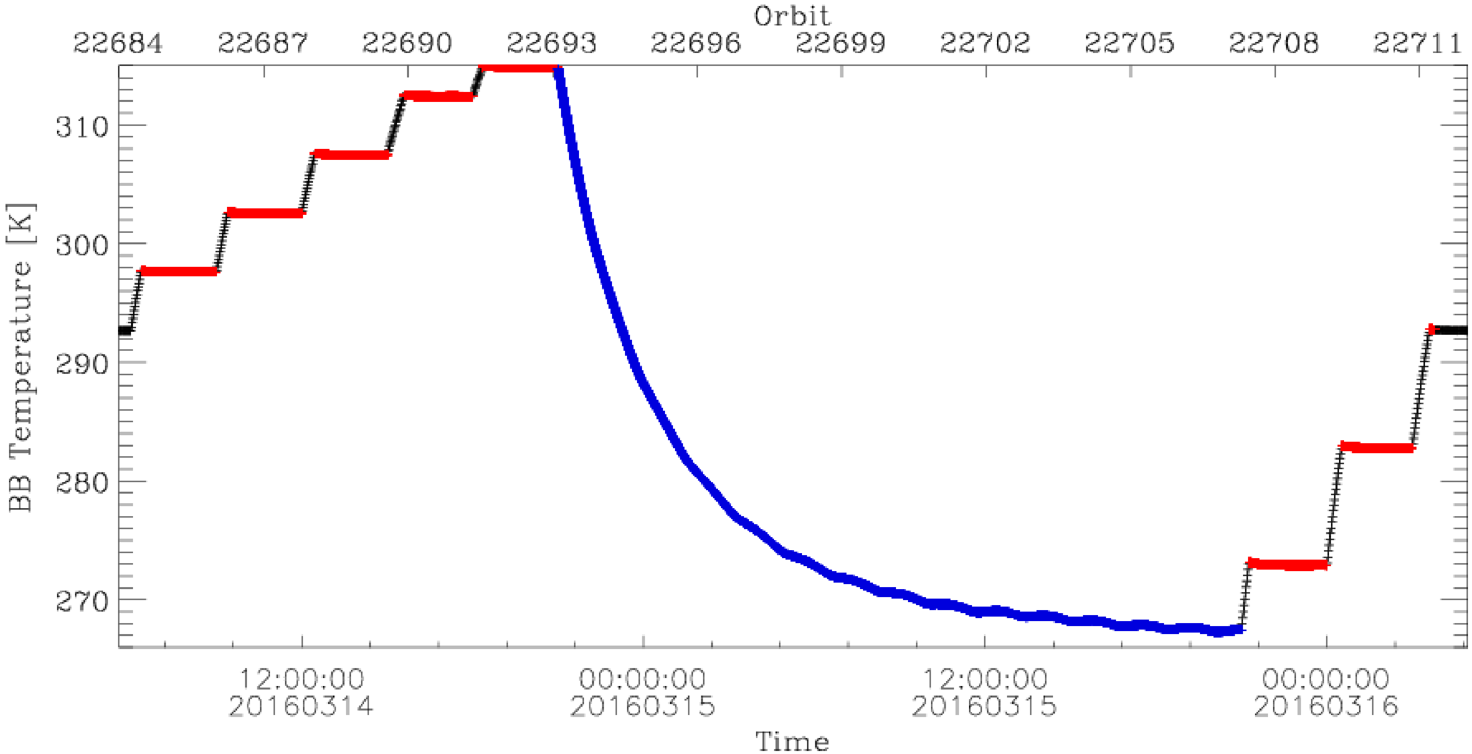

VIIRS DNB VROP Calibrations

- **VROP for DNB Calibration:**
  - Monthly events since launch, most recent June 4, 2016.
  - Occurs during New Moon, at night, over the central Pacific.
  - Calibration of DNB Offset, Dark, and Gain Ratios.

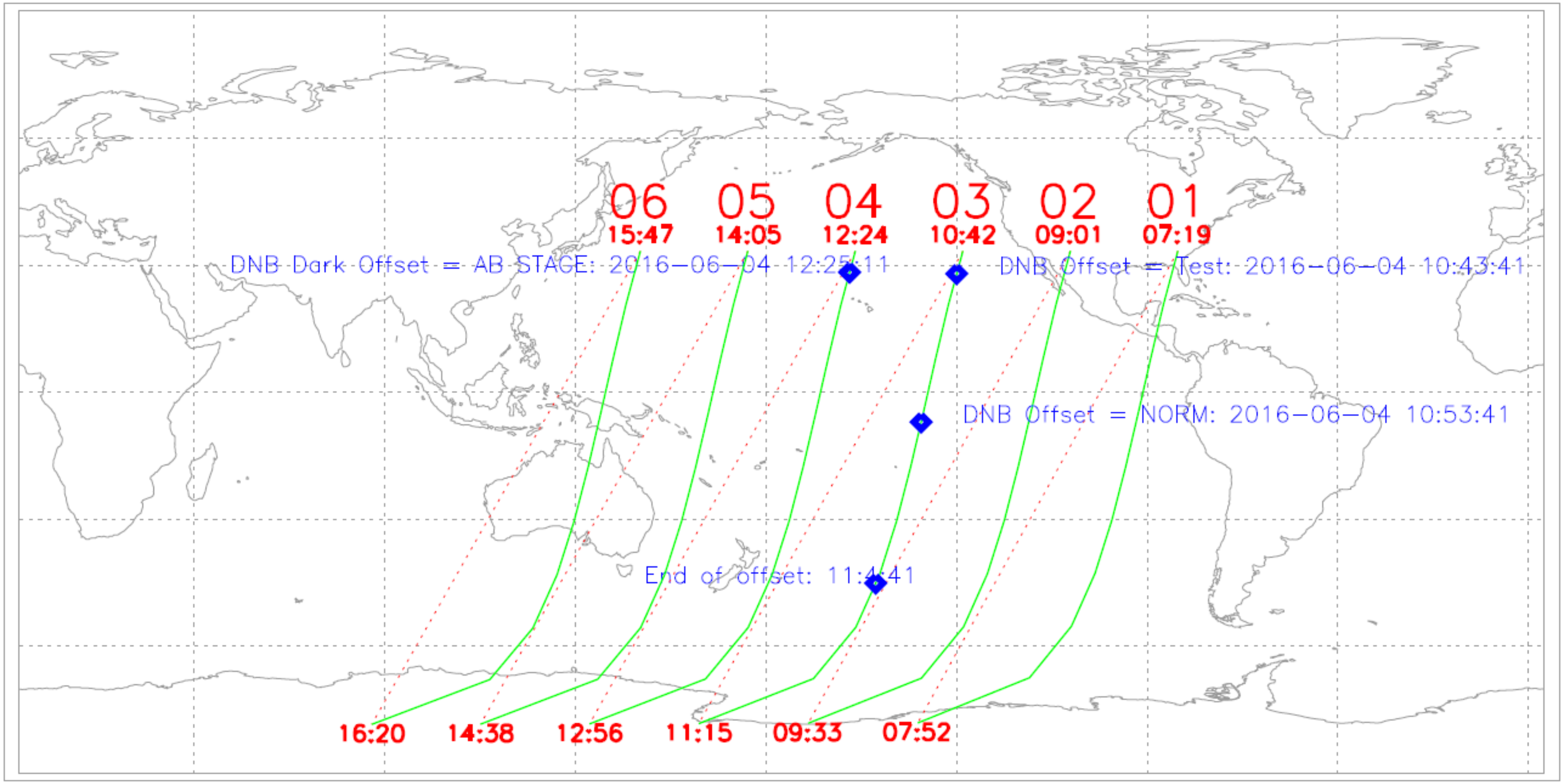

VIIRS Telemetry

- **Telemetry Monitored Continually:**
  - **Focal Plane Array Temperatures.**
  - **On-board blackbody Temperatures.**
  - **Other temperatures, voltages, etc.**
  - **No unusual trending seen currently.**

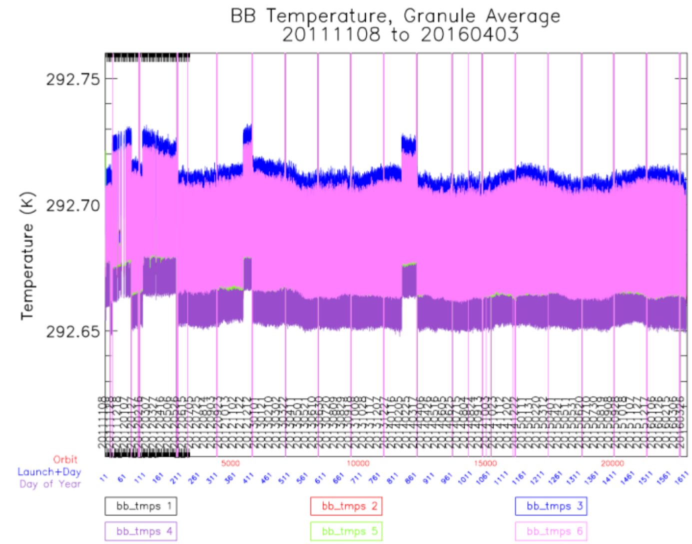

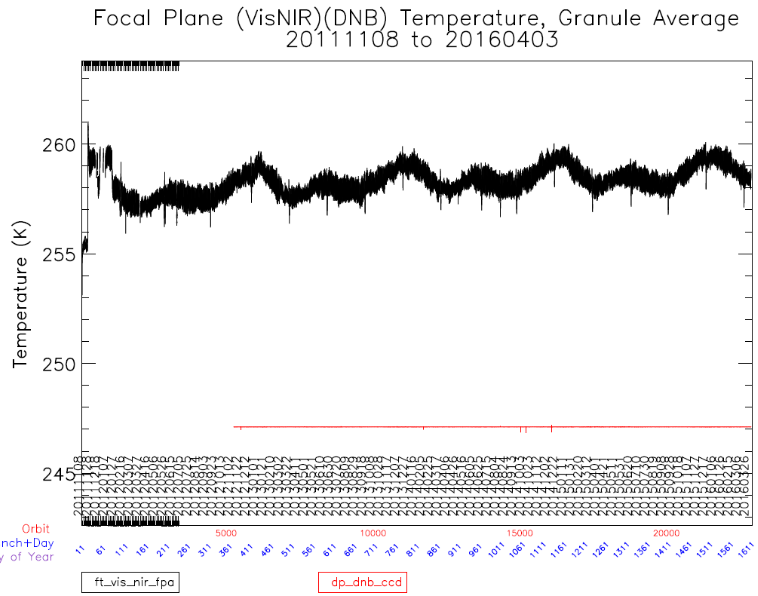

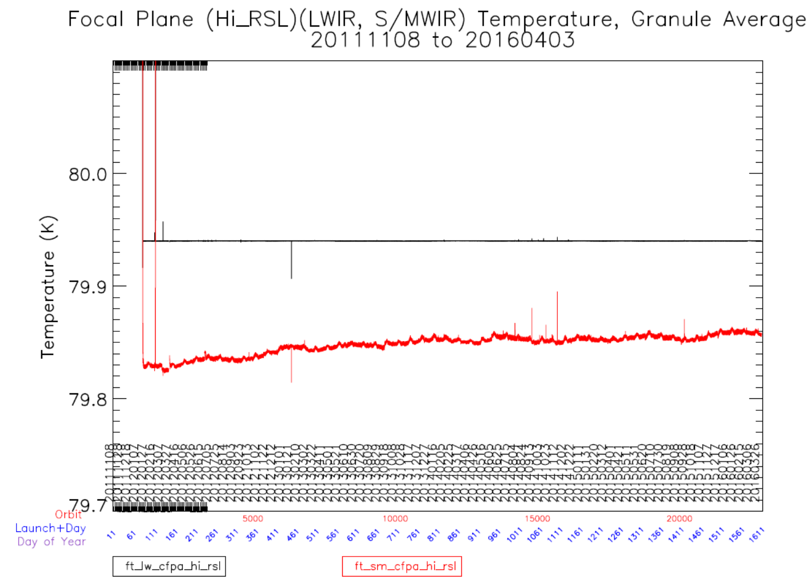

Summary

- **Status of SNPP/VIIRS Operations:**
  - SNPP Orbit maintenance continuing.
  - No Petulant SBC lock-up since Oct 9, 2014.
  - RTA/HAM Scan Sync Loss anomalies still occurring.
  - Spacecraft maneuvers for calibration (LRM, etc.) are ongoing.
  - Warm-Up/Cool-Down activities for TEB Cal occur quarterly.
  - DNB VROP operations occur during new moon monthly.
  - VIIRS telemetry being monitored, not showing unusual trends.
  - Swapping M11 for M7 at night after Block 2.0 operation.

NASA VIIRS Level-1 Version-2 Calibration Software

June 6, 2016

Sam Anderson, Chengbo Sun

VCST / NASA GSFC

NASA VIIRS L1B Version-2 Software Objectives Overview

- Apply running average of TEB F-factor over scans instead of per-scan value
- Apply a time-dependent modulated RSR in the calibration algorithm
- Use solar irradiance at 1 AU to avoid computations of large numbers
- Temperature dependent calibration coefficients for the RSBs
- Alternative blackbody thermistor weighting scheme to decrease orbital variation present in the F-factor
- Improved handling of saturation thresholds and radiance range
- General clean-up and consolidation to improve performance and facilitate maintenance

NASA VIIRS L1B Version-2 Software Objectives With Performance Impact

- Enhancements to time-dependent netCDF4 LUTs
  - Added time-dependent Relative Spectral Response LUT
  - Pre-compute integrated/normalized Solar Irradiance
  - Use Astronomical Units (AU) rather than meters to avoid imprecision arising from use of large numbers
- Apply Finite Impulse Response (FIR) filter to all SV and TEB F-Factor data
  - 201-tap FIR Filter
  - Bandwidth of passband is configurable
  - Requires sequence of three consecutive granules for proper moving averaging
- Revise handling of saturated and out-of-range pixels
- Add optional new diagnostic group to L1B format

Filter TEB F-Factors

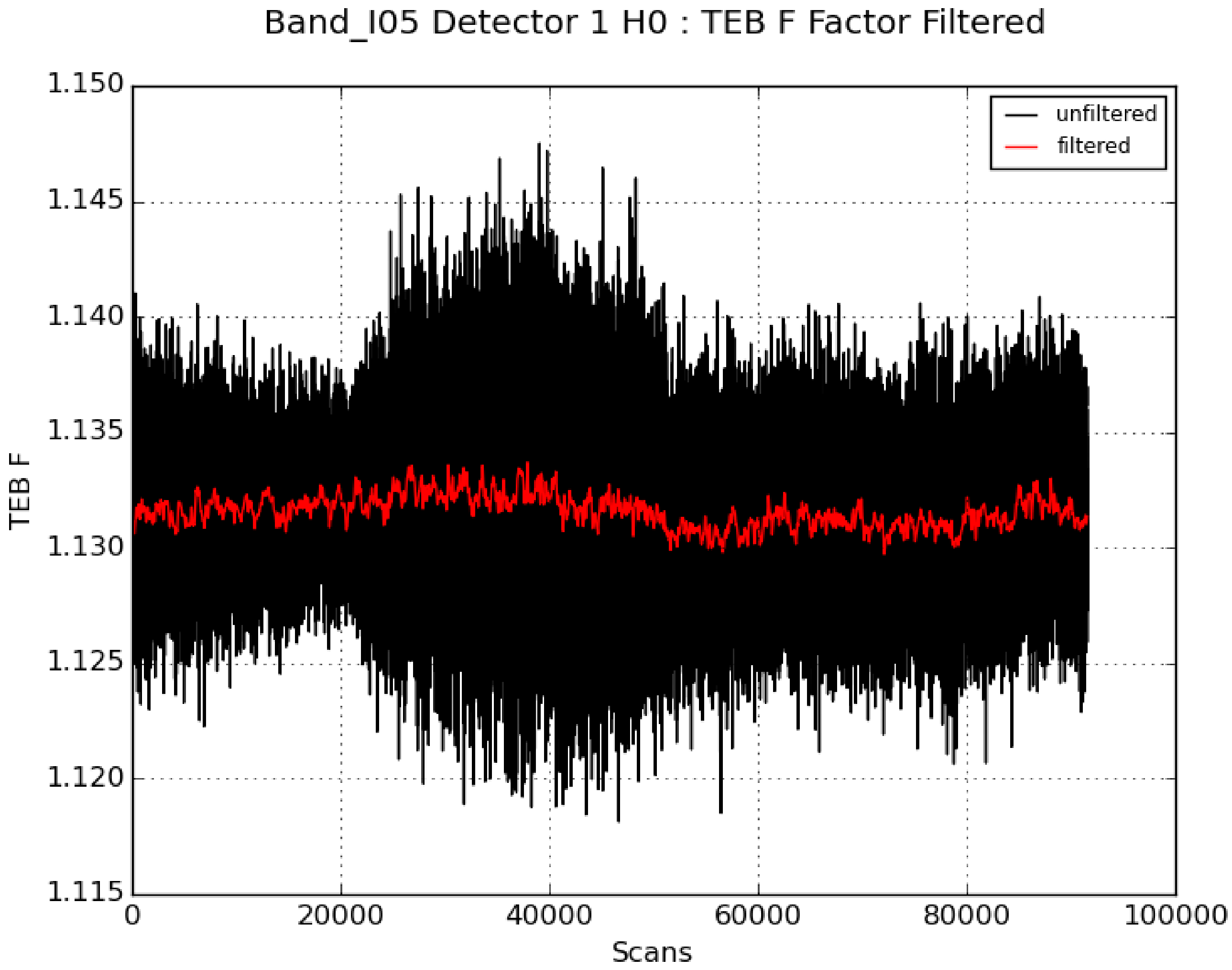

Black Body warm-up/cool-down cycle 12-14-2015 thru 12-17-2105

Filter SV with DC Restore Correction

- 4-day Warm-Up/Cool-Down cycle
- RSB SV exhibits occasional DC Restore fluctuations
- DCR Correction removes discontinuities in SV time series caused by DC Restore offsets (blue)
- Filter is applied (red)
- DC Restore offsets are restored in final time series (black)

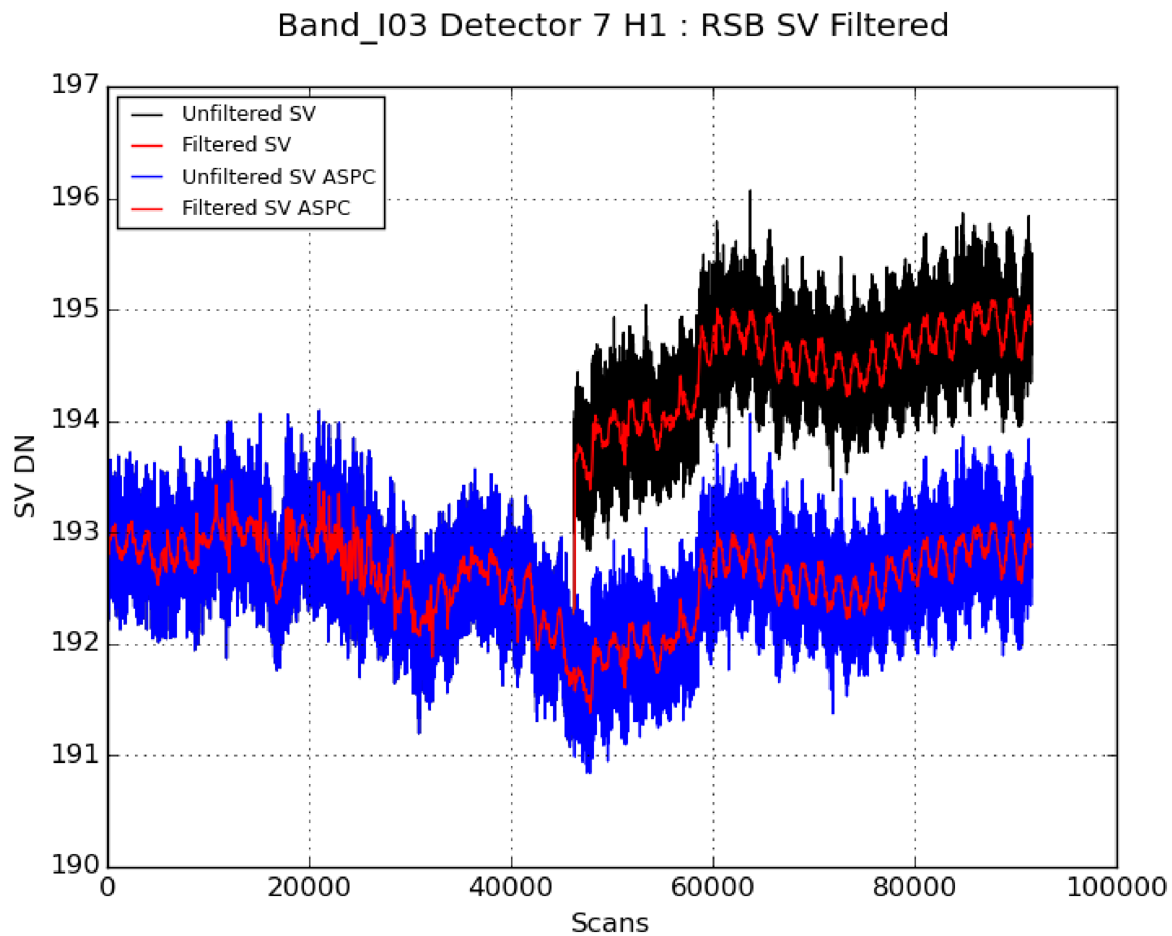

Black Body warm-up/cool-down cycle 12-14-2015 thru 12-17-2105

Filter SV with DC Restore Correction (cont.)

- 4-day Warm-Up/Cool-Down cycle
- TEB SV exhibits frequent and substantial DC Restore fluctuations, especially during warm-up/cool-down cycle
- ASP Offset Corrections are applied first
- Filter is then applied
- DC Restore offsets are restored

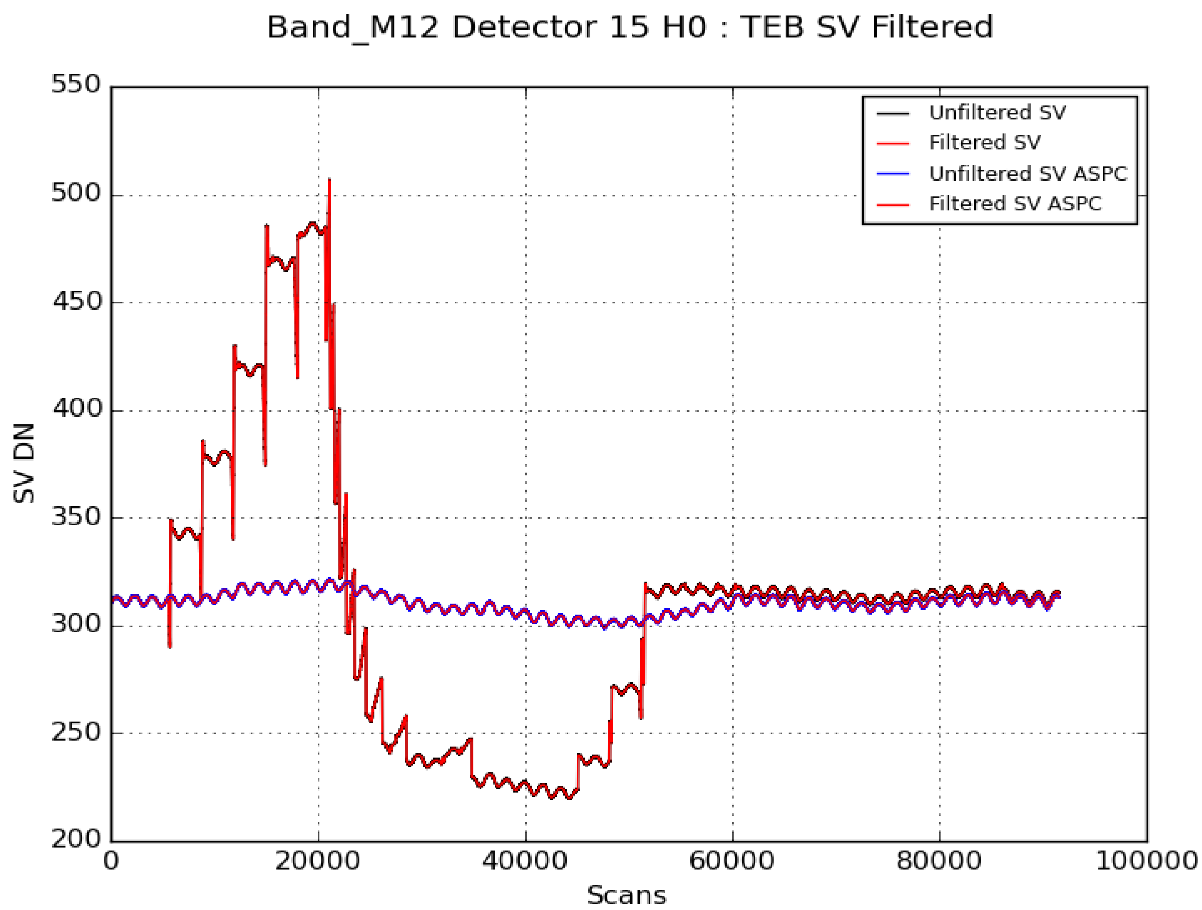

Black Body warm-up/cool-down cycle 12-14-2015 thru 12-17-2105

Effect of SV Noise on Calibrated Products

- True-Color rendering of the difference between L1B products with and without SV filtering
- Units of radiance scaled to reflectance and then scaled to 16-bit integer

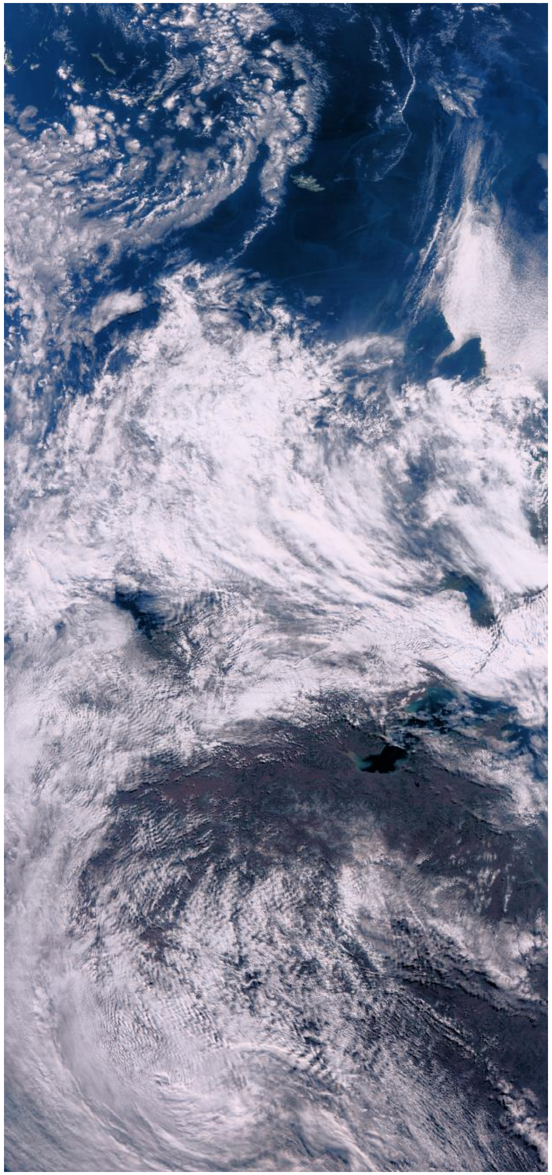

Estimate of Difference Between Filtered and Unfiltered RSB Products

- Analysis based on differences observed in a single granule
  - V2015262003600.L1B-M_SNPP.nc
  - V2015262003600.L1B-I_SNPP.nc
- Statistics based on the difference between L1B products with and without space view filtering
- Units of radiance scaled to reflectance and then to 16-bit integer
- Results show the benefit of SV noise filtering is not extraordinary

Band	Standard Deviation of Difference	Minimum	Maximum	Mean
I01	1.28	-8	7	-0.0073
I02	1.75	-9	8	-0.0024
I03	3.39	-18	18	0.0335
M01	0.94	-5	5	-0.0157
M02	0.97	-4	6	-0.0032
M03	0.98	-5	5	-0.0063
M04	1.05	-6	5	0.0109
M05	1.22	-7	6	0.0090
M06	0.50	-2	2	-0.0003
M07	1.36	-8	7	-0.0028
M08	1.41	-6	6	0.0061
M09	1.60	-7	6	-0.0026
M10	1.13	-6	4	-0.0221
M11	1.75	-7	8	-0.0016

Estimate of Difference Between Filtered and Unfiltered TEB Products

- Analysis based on differences observed in a single granule
  - V2015262003600.L1B-M_SNPP.nc
  - V2015262003600.L1B-I_SNPP.nc
- Statistics based on the difference between L1B products with and without space view filtering and TEB F-Factor Filtering
- Units of radiance scaled to 16-bit integer
- Results show the benefit of SV and TEB F-Factor noise filtering is more significant for some Long-Wave Infrared (LWIR) Bands

Band	Standard Deviation of Difference	Minimum	Maximum	Mean
I04	3.49	-43	44	0.0182
I05	14.39	-174	163	-0.4033
M12	2.28	-21	19	-0.0112
M13	0.098	-1	1	0.0000
M14	9.23	-44	47	0.0023
M15	4.08	-25	22	-0.1704
M16	3.23	-16	20	-0.1519

New Saturation Threshold and Radiance Range Processing

- The maximum radiance supported on a given band may increase substantially with time due to degradation of optical pathway
- The maximum usable DN on any band, however, is invariant
- Consequently, we prefer to use DN to establish saturation thresholds and radiance ranges
- Effective saturation thresholds for some bands are lower than the digital saturation threshold currently used
- Revised saturation thresholds
  - Imagery Reflective Solar Bands: 3400 DN
  - Imagery Thermal Emissive Bands: 4095 DN (digital saturation)
  - Moderate Dual-Gain Reflective Solar Bands: 3700 DN
  - Moderate Dual-Gain Thermal Emissive Bands (M13) : 4095 DN (digital saturation)
  - Moderate Single-Gain Reflective Solar Bands: 4095 DN (digital saturation)
  - Moderate Single-Gain Thermal Emissive Bands : 4095 DN (digital saturation)
  - Day-Night Band: 7872 DN (digital saturation occurs at 8191 DN)

Revised Saturation Thresholds for Moderate Dual-Gain Bands

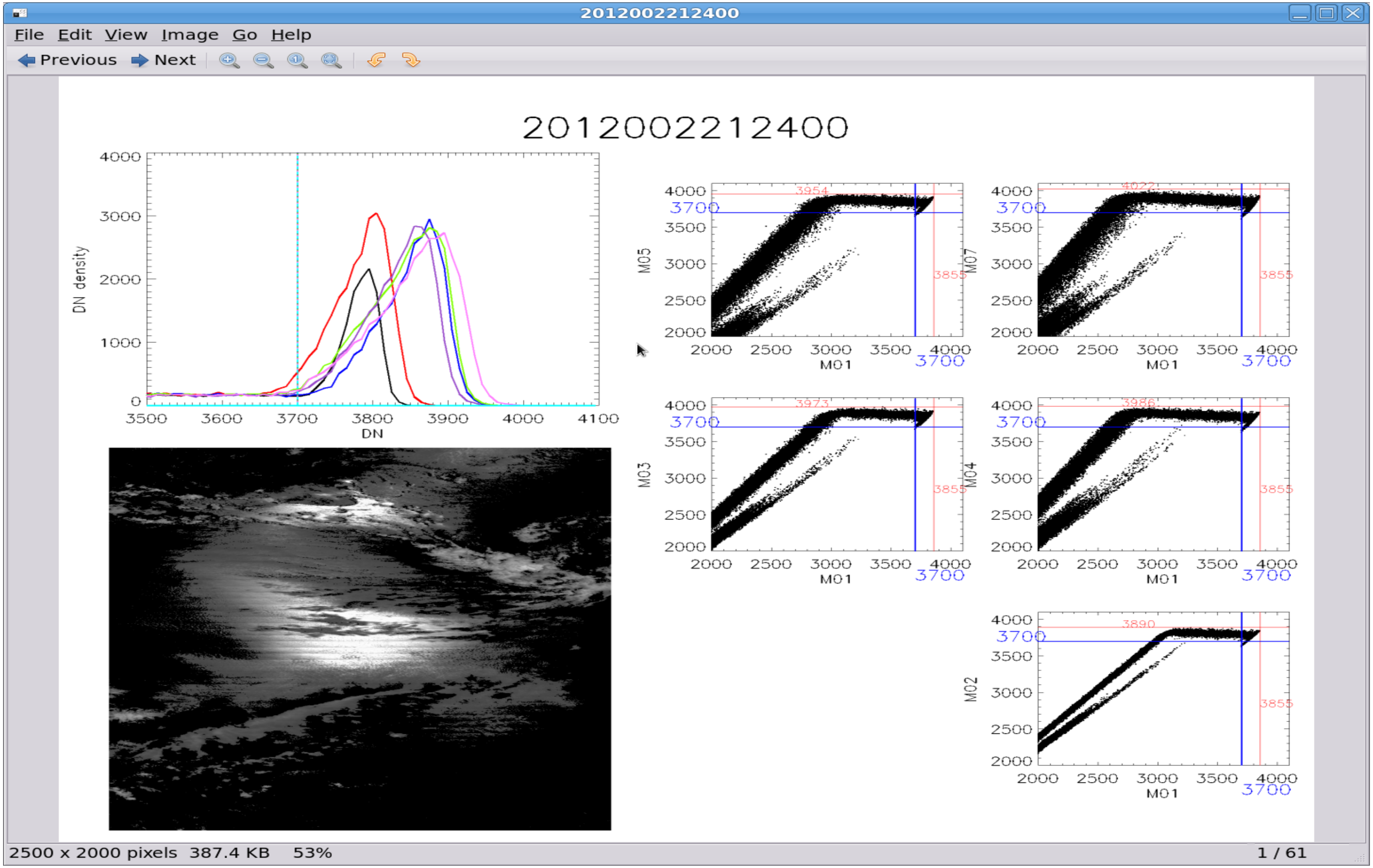

Add Optional Diagnostic Array Group

- A set of optional diagnostic arrays has been added to M-band and I-band products
  - Required for testing
  - Useful for analysis
- Imagery (I) Bands
  - SV and TEB_F arrays
  - Dimensions: band x time series x scan x detector x aggregation zone x parity
- Moderate (M) Bands
  - SV_DG, SV_SG, TEB_F_DG, and TEB_F_SG arrays
  - Dimensions: band x time series x scan x detector x gain state*
- Multiple time series show the sequence of filter processing stages
  - Input (after validation and replacement of corrupted SV scans with granule average)
  - DC Restore effects removed to restore continuous time series
  - 201-tap FIR filter applied
  - DC Restore effects restored

Space View Diagnostic Array

- Moon-in-SV Example
- Input to filter has scans contaminated with moonlight removed and replaced with granule-average SV
- DCR Correction removes discontinuities in SV time series caused by DC Restore offsets
- 201-tap FIR filter is applied to the central, current granule
- DC Restore offsets are restored in final time series

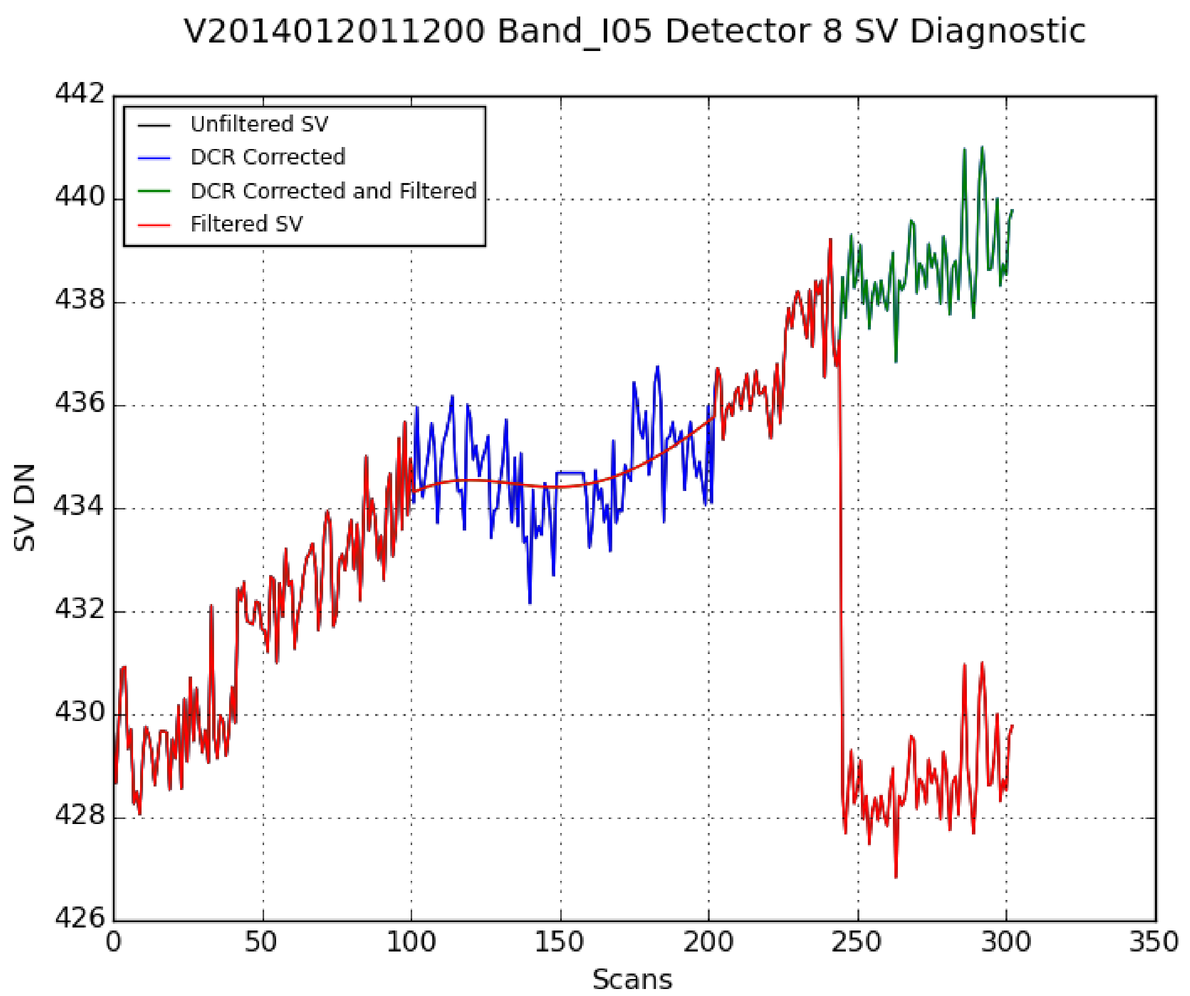

TEB F-Factor Diagnostic Array

- Moon-in-SV Example
- Calculation of F Factor uses SV background reference
- SV scans with lunar contamination are replaced with granule average
- Raw F Factors are computed
- 201-tap FIR filter is applied to the central, current granule

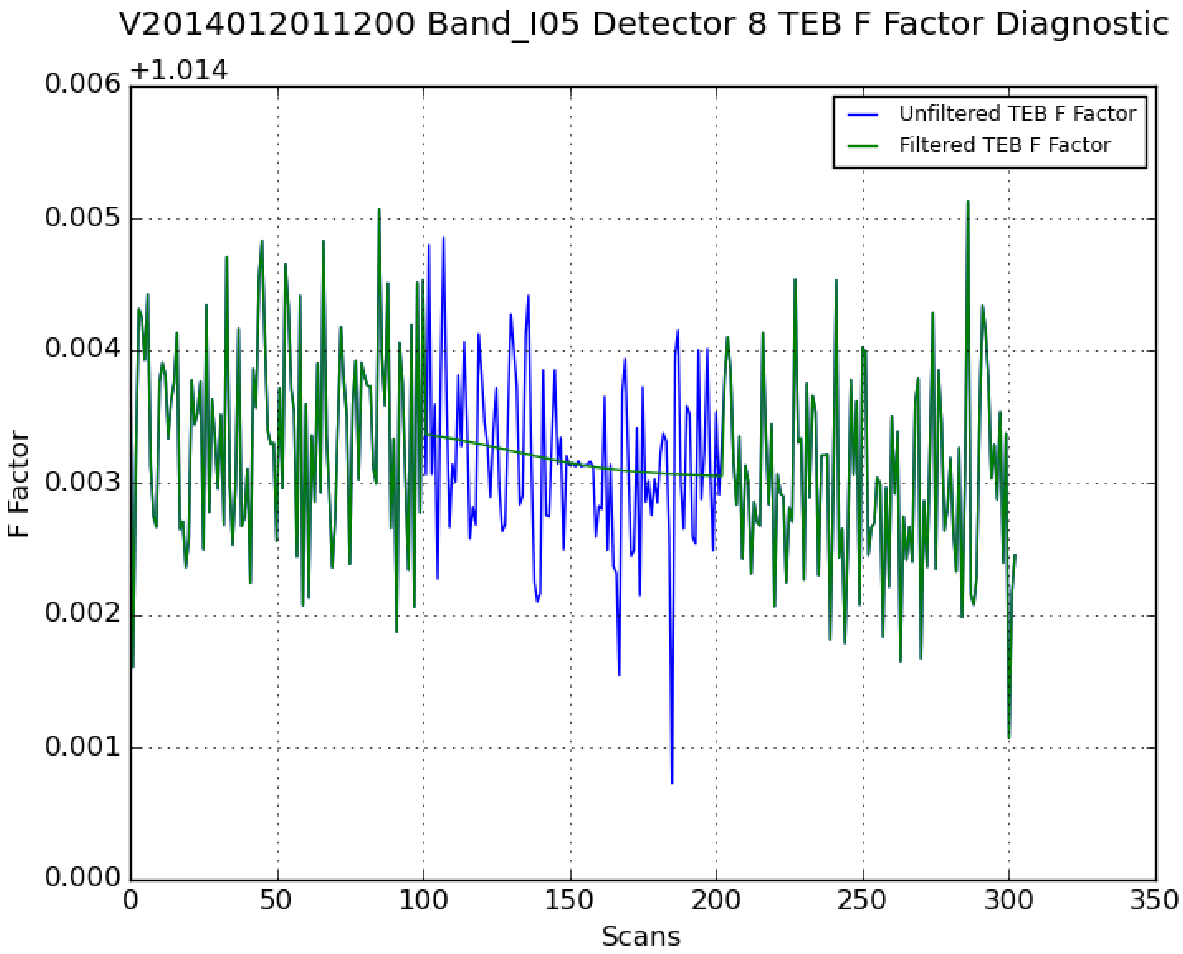

SNPP VIIRS Reflective Solar Bands On-orbit Radiometric Calibration Performance and Improvements

Ning Lei[1], Xuexia Chen[1], Zhipeng Wang[1], and Jack Xiong[2]

1. VIIRS Characterization and Support Team (VCST), SSAI, Lanham, MD, USA
2. NASA GSFC, Greenbelt, MD, USA

June 6, 2016

VIIRS RSB Spectral Responses

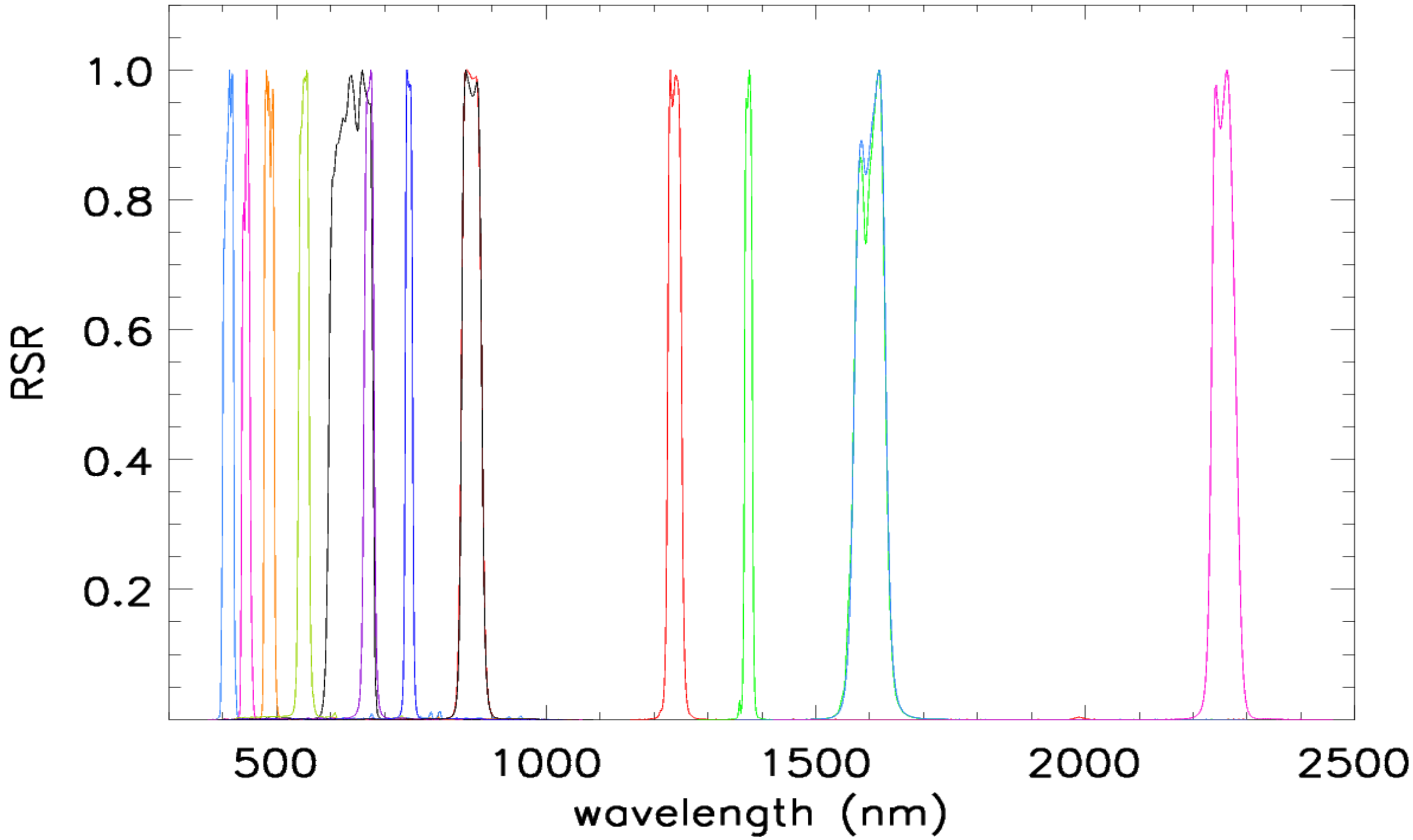

C. Moeller, J. McIntire, T. Schwarting, and D. Moyer, “VIIRS F1 “best” relative spectral response characterization by the Government Team”, in *Proc. SPIE*, 2011, vol. 8153, Paper 0K.

VIIRS RSB L1B Product

TOA spectral hemispherical reflectance is estimated by (Eq. 81, ATBD)

$$\rho(\lambda_{\mathrm{B}}) = \frac{\pi F(B) \times \left(c_0 + c_1 dn_{\mathrm{EV}} + c_2 dn_{\mathrm{EV}}^2\right)}{\mathrm{RVS}(\theta_{\mathrm{EV}}, B) \cos\theta_{\mathrm{sun-earth}} \overline{E_{\mathrm{sun}}}(\lambda_{\mathrm{B}}, d_{\mathrm{sc}})} \quad (1)$$

Calibration performance means how accurately the reflectance is measured

- Error in dn_{EV} : SNR
- Error in F
- Error in RVS
- Error in the quadratic polynomial

SNR

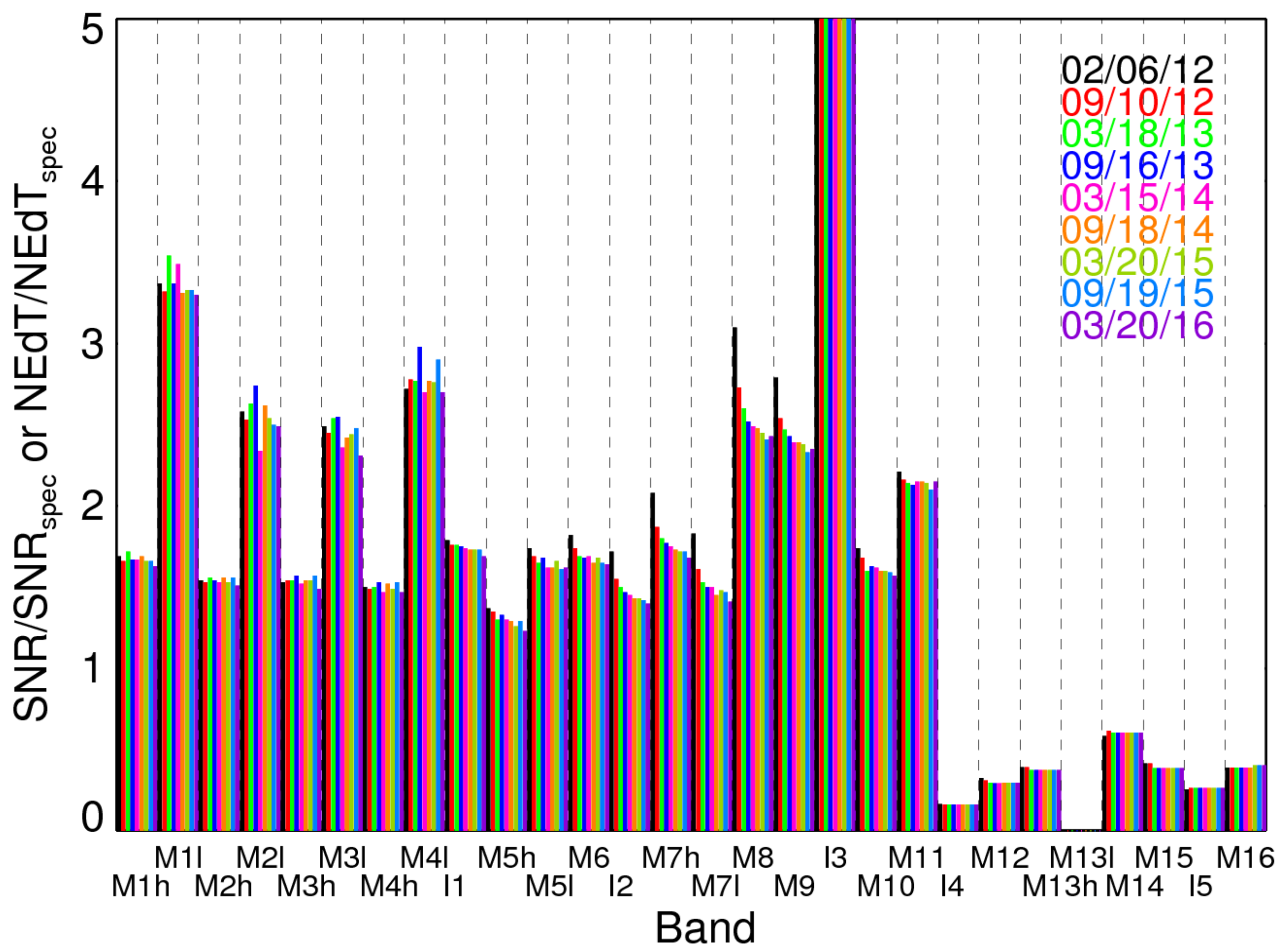
SNR/SNR$_{spec}$ or NEdT/NEdT$_{spec}$
0
1
2
3
4
5
02/06/12
09/10/12
03/18/13
09/16/13
03/15/14
09/18/14
03/20/15
09/19/15
03/20/16
M1l M2l M3l M4l M5h M6 M7h M8 I3 M11 M12 M13l M15 M16
M1h M2h M3h M4h I1 M5l I2 M7l M9 M10 I4 M13h M14 I5
Band

SNR projection

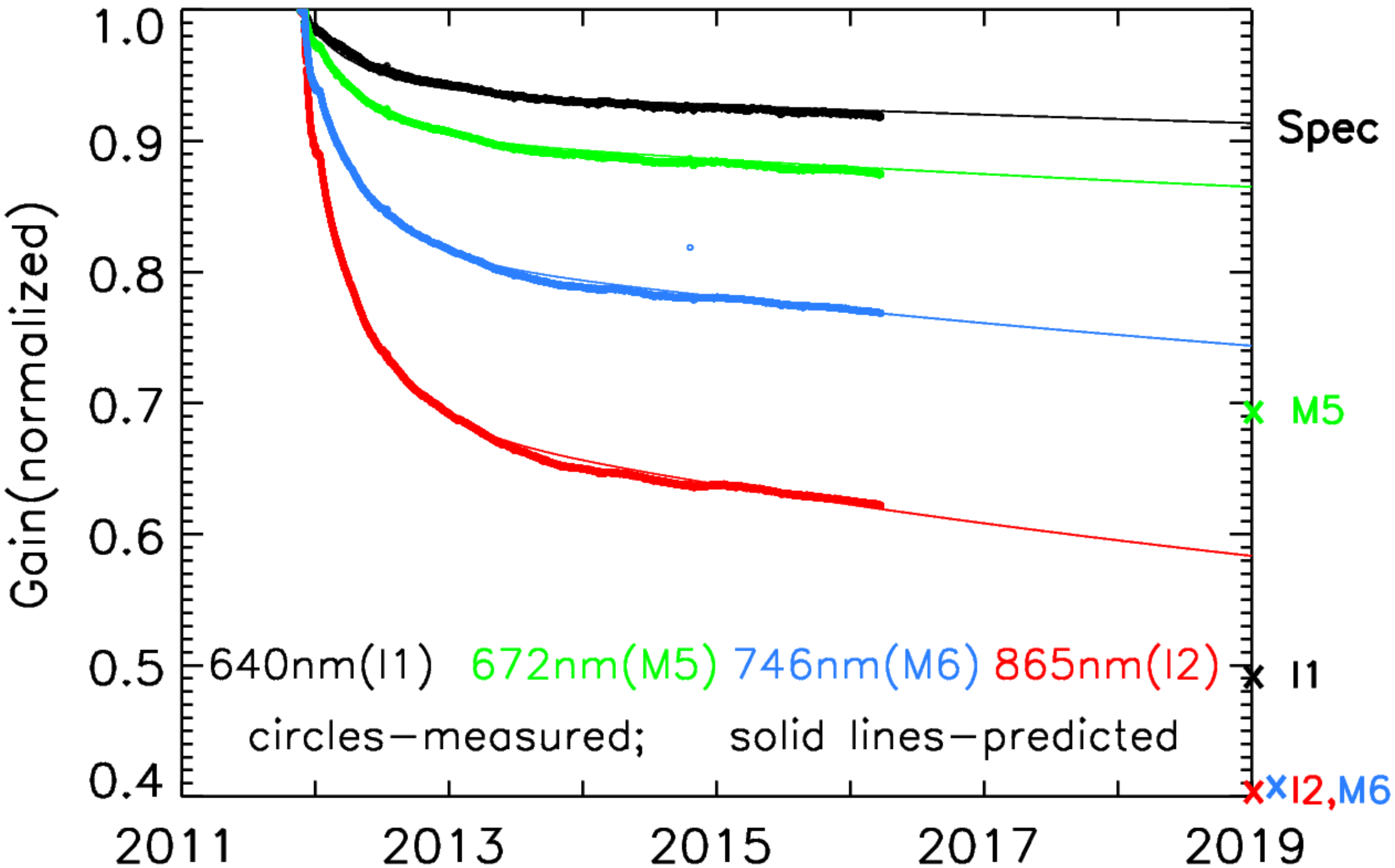

F Determination

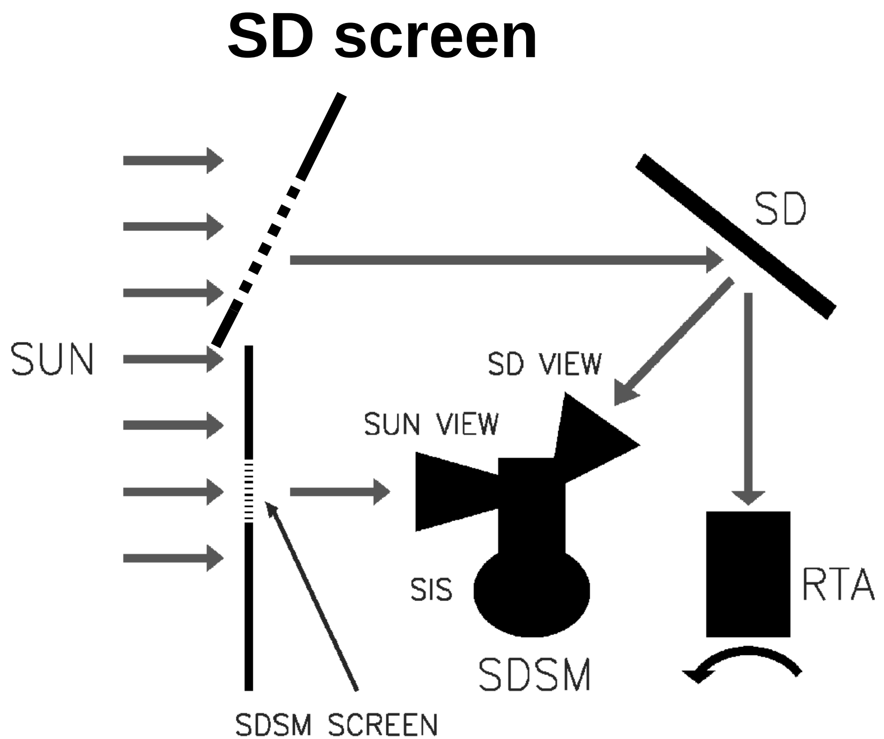

J. McIntire, D. Moyer, B. Efremova, H. Oudrari, and X. Xiong, “On-orbit Characterization of S-NPP VIIRS Transmission Functions”, *IEEE Trans. Geosci. Remote Sens.*, vol. 53, pp. 2354-2892, 2015.

On-orbit Calibration: *F*-factor

$$F = \frac{\int \mathrm{RSR}(\lambda, B, t) \times L_{\mathrm{SD}}(\lambda, t, \vec{\phi})}{\left(c_0 + c_1 dn_{\mathrm{SD}} + c_2 dn_{\mathrm{SD}}^2\right) \times \int \mathrm{RSR}(\lambda, B, t) d\lambda} \qquad (2)$$

L_{SD} : spectral radiance from the SD; improved

$\mathrm{RSR}(\lambda, B, t)$: slightly improved

1/F-factors

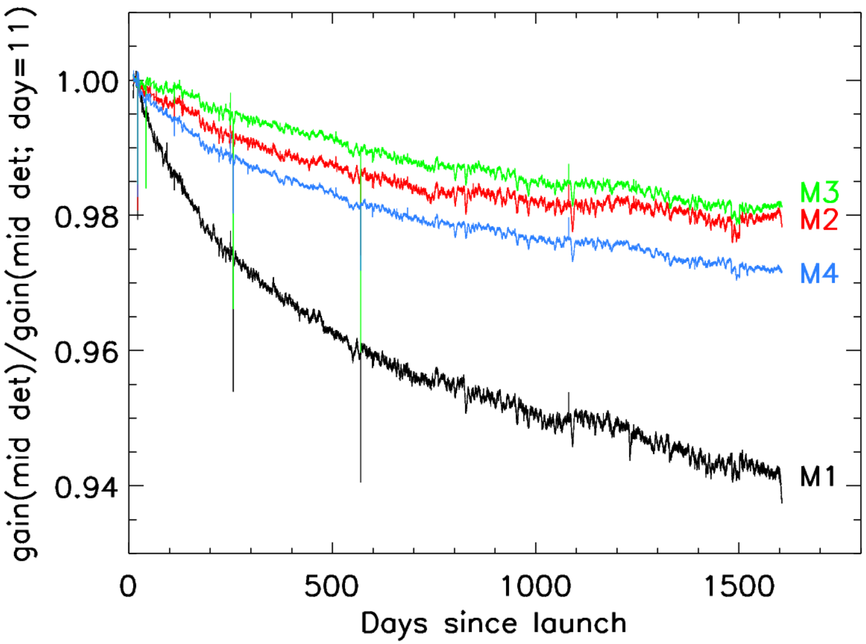

gain(mid det)/gain(mid det; day=11)
1.00
0.98
0.96
0.94
0
500
1000
1500
Days since launch
M3
M2
M4
M1

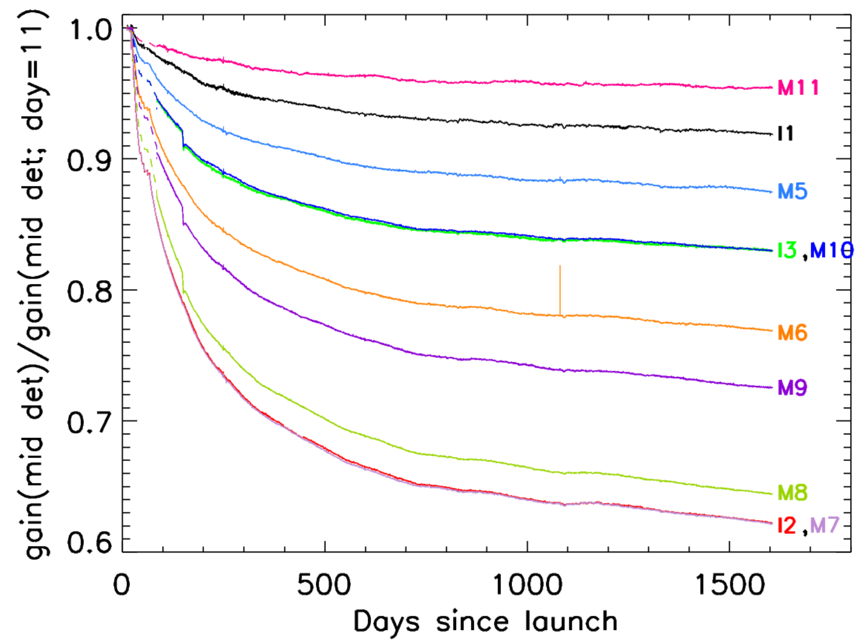

gain(mid det)/gain(mid det; day=11)
1.0
0.9
0.8
0.7
0.6
0
500
1000
1500
Days since launch
M11
I1
M5
I3,M10
M6
M9
M8
I2,M7

F-factors: new vs old

old

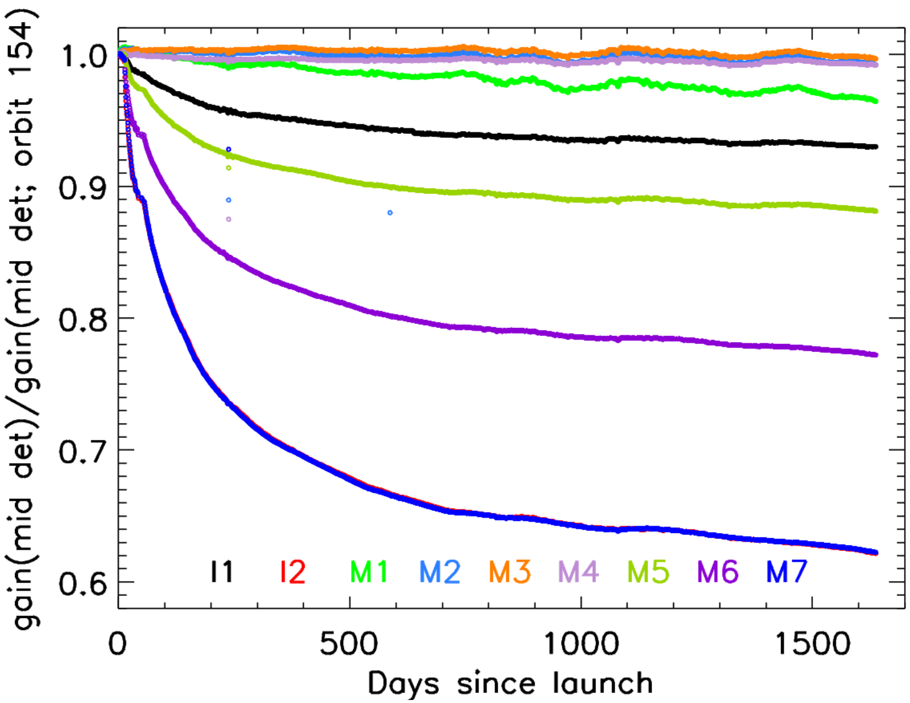

new

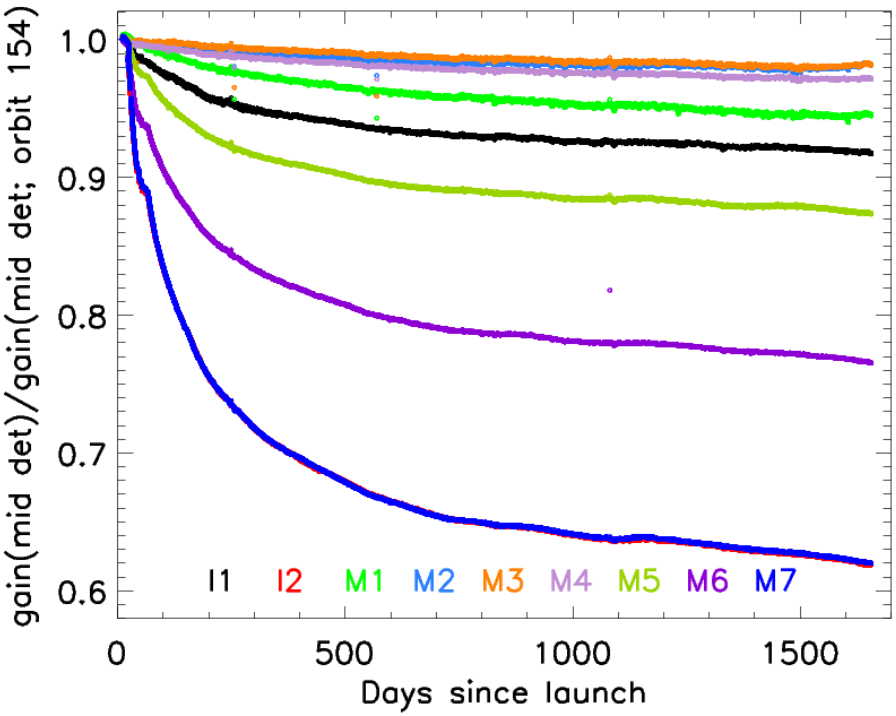

F Precision Estimation

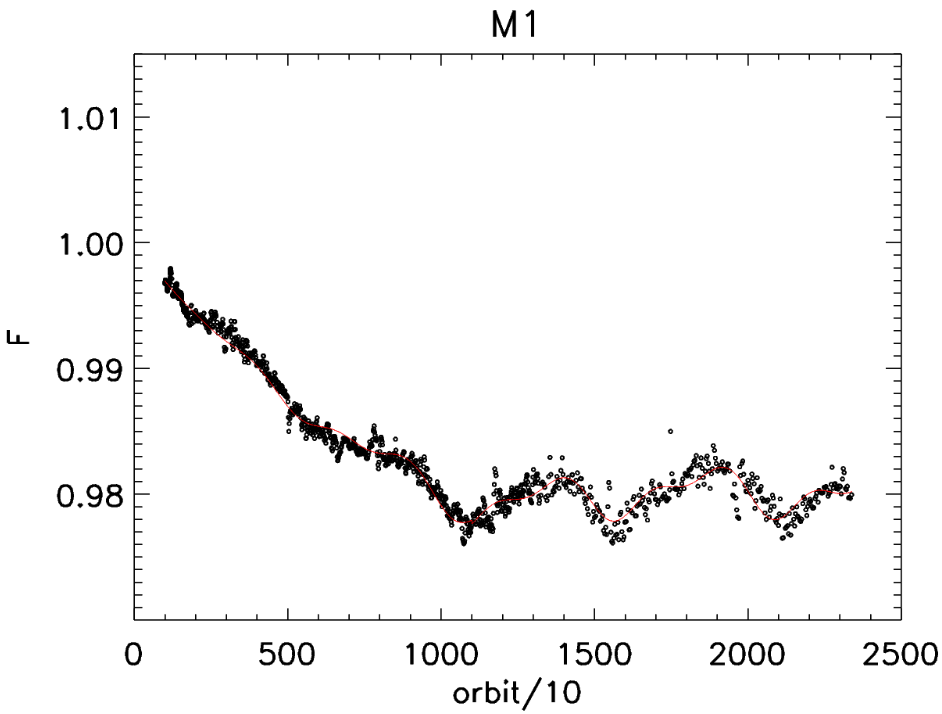

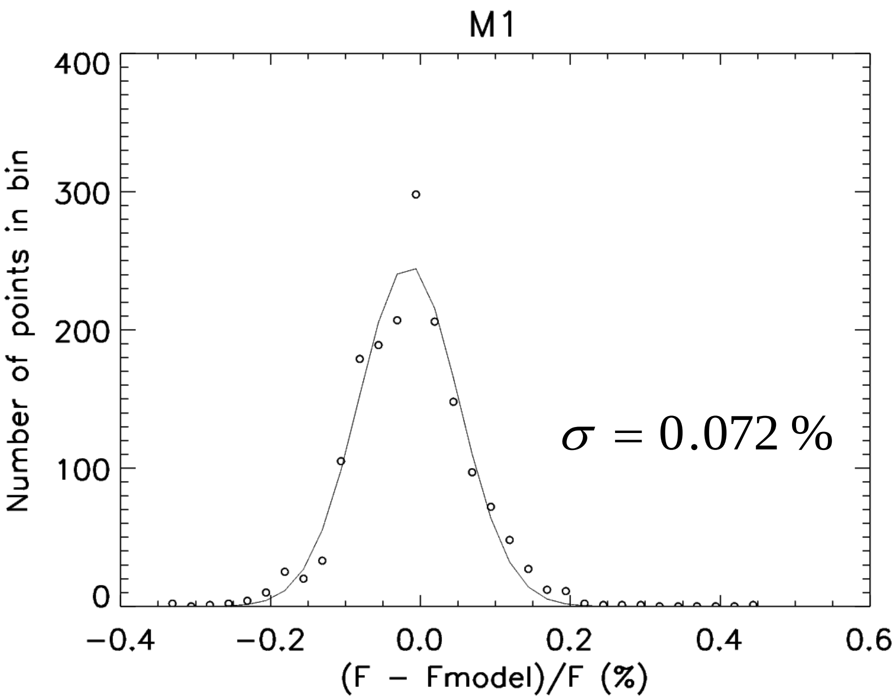

M1:0.07%, M2:0.07%, M3:0.06%, M4:0.04%, I1:0.06%, …, M11:0.05%

Improved Calculated Sunlit SD Spectral Radiance

$$L_{\mathrm{SD}} = E_{\mathrm{sun}}(\lambda)\cos(\theta_{\mathrm{SD-sun}})\underbrace{\tau_{\mathrm{SAS}}\,\mathrm{BRDF}_{\mathrm{RTA}}\left(\lambda, t=0, \vec{\phi}\right)}\underbrace{H_{\mathrm{RTA}}}\left(\lambda, t, \vec{\phi}\right) \quad (3)$$

$H_{\mathrm{RTA}}\left(\lambda, t, \vec{\phi}\right)$: SD BRDF degradation factor, biases removed and screen transmittances are more accurate

$\tau_{\mathrm{SAS}}\left(\lambda, \vec{\phi}\right)\mathrm{BRDF}_{\mathrm{RTA}}\left(\lambda, t=0; \vec{\phi}\right)$: bias removed, 0.05% along solar azimuth direction)

Improvements on H_{SDSM} : part 1

(1) Improved SDSM screen transmittance

use both yaw maneuver and a small portion of regular data (same as last year)

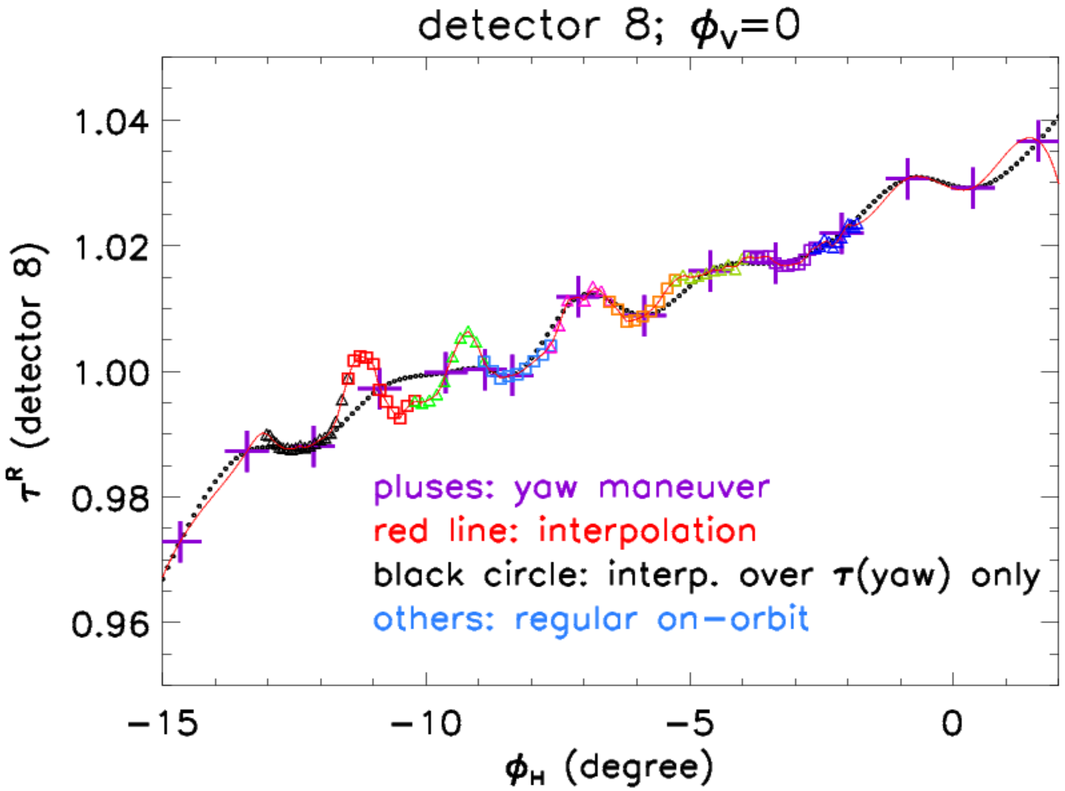

SDSM screen coord.

Improvements on H_{SDSM} : part 2

(2) Improved τ(SD)*BRDF(t=0; SDSM)

use both yaw maneuver and a small portion of regular data

and remove bias from the angular dependence of H_{SDSM}

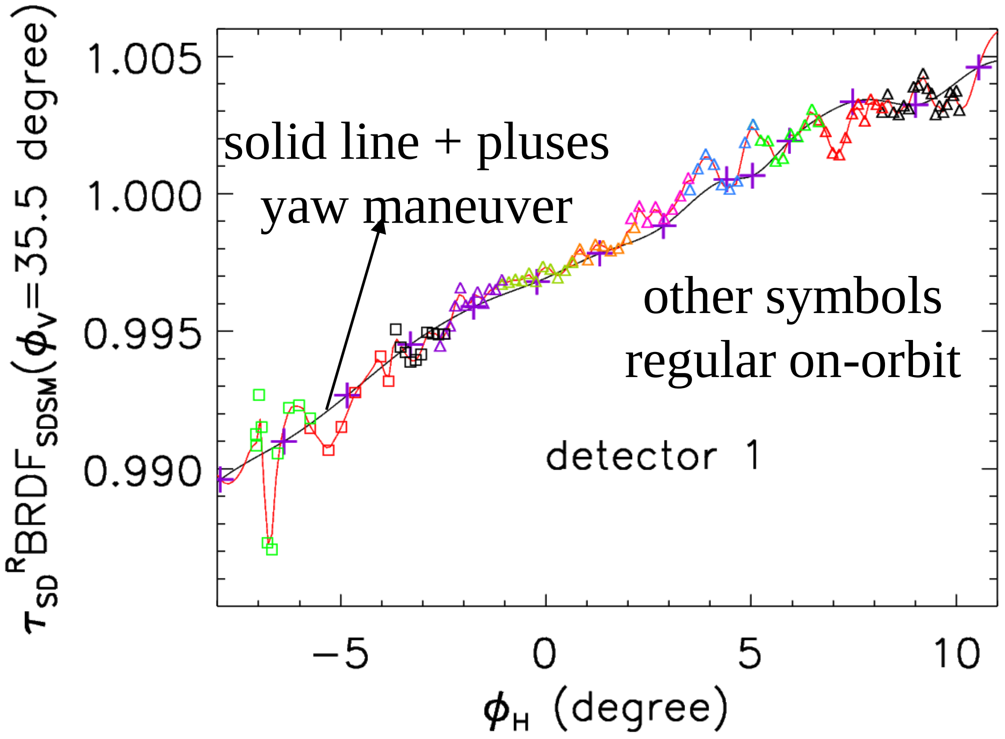

SD coord.

Solar angular dependence of SD BRDF degradation factor

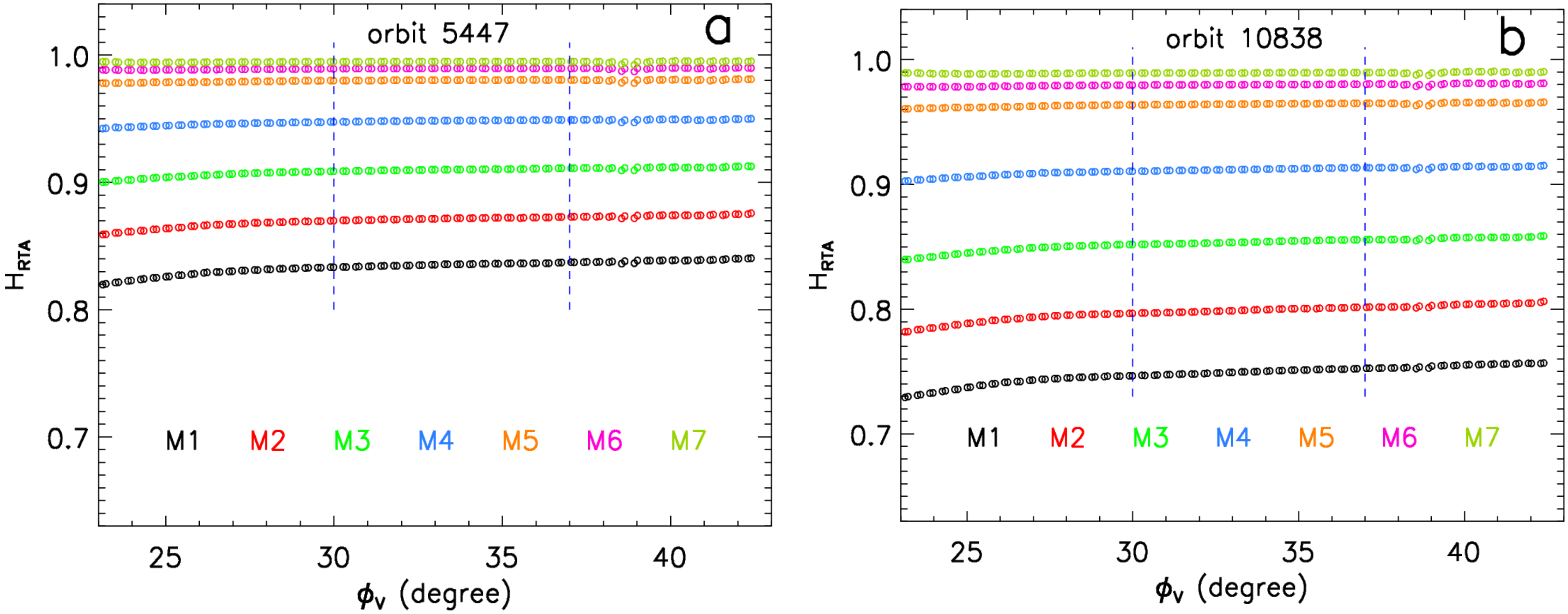

Improvements on H_{SDSM} : part 3

(3) Rescale H_{SDSM}

effectively move up H_{SDSM} at the wavelength of 412 nm (M1) by about 1.0%

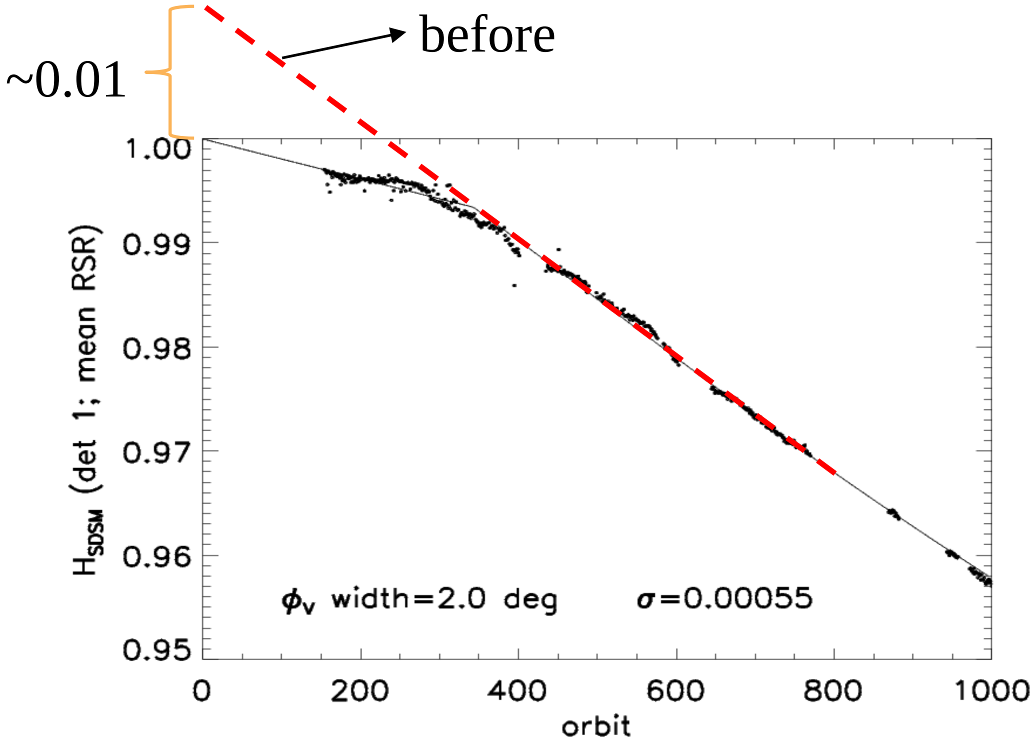

Improvements on H_{SDSM} : part 4

(4) Model H_{SDSM} at SWIR band wavelengths

originally H_{SDSM}(SWIR wavelength)=1

$$1 - H(\lambda, t) = \frac{\alpha(t)}{\lambda^{4.07}} \qquad \alpha(t) = \left\langle (1 - H(\lambda, t)) \times \lambda^{4.07} \right\rangle_{\lambda = (\lambda_{\det 5}, \lambda_{\det 6}, \lambda_{\det 7}, \lambda_{\det 8})}$$

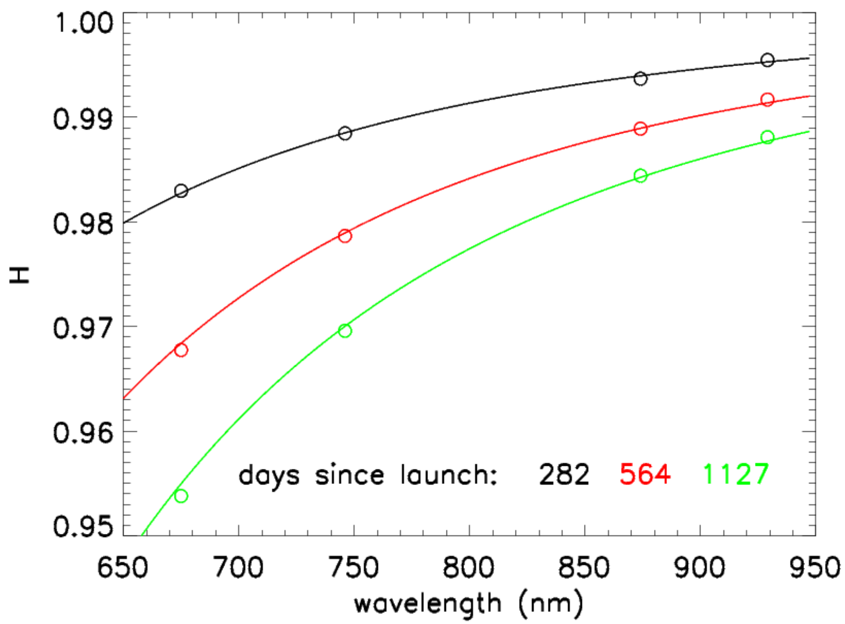

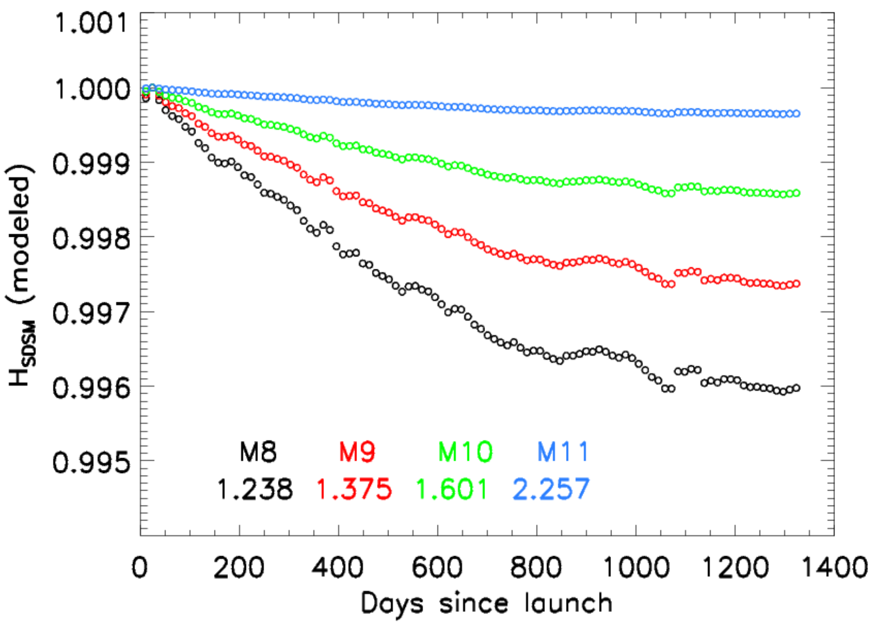

Improved H_{SDSM} (SDSM SD view)

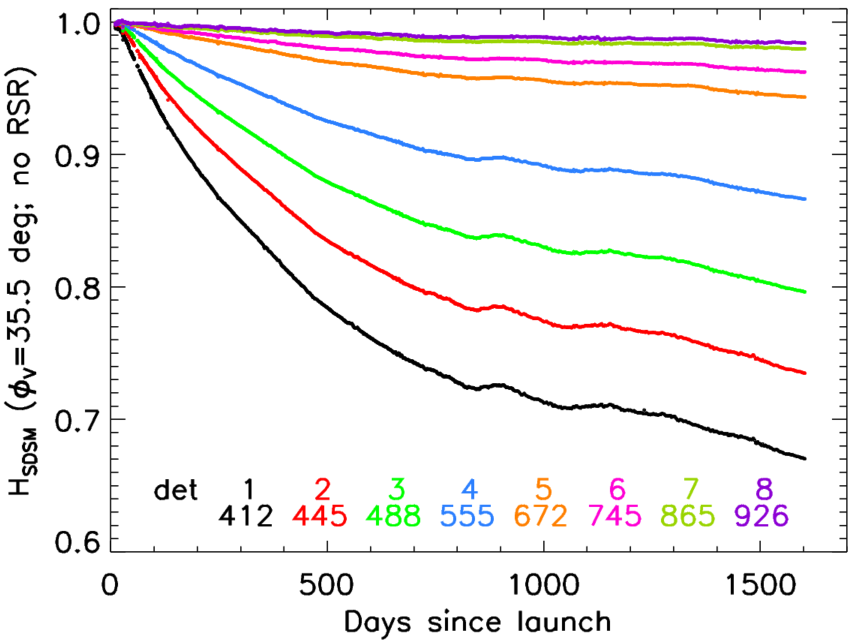

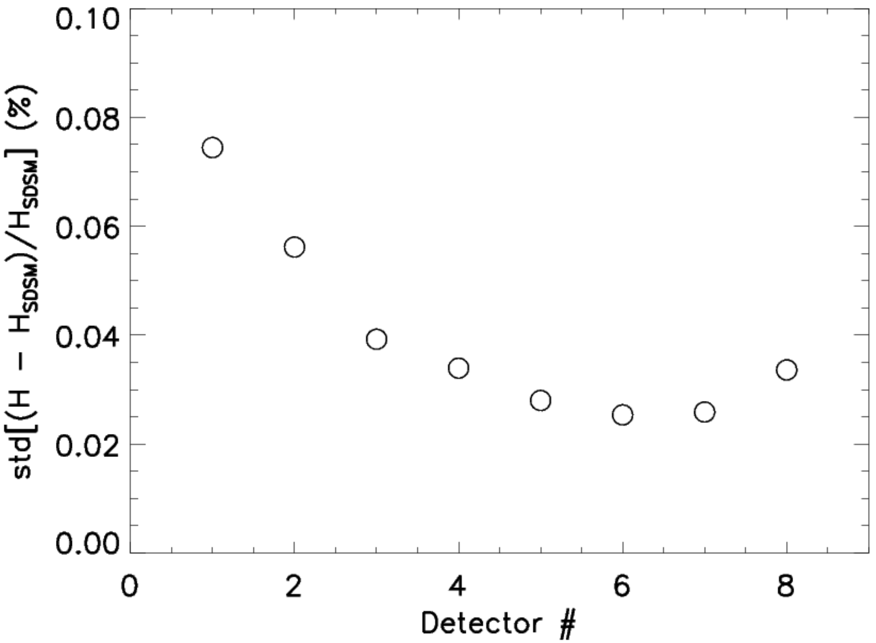

H_{SDSM} can be precisely measured with a relative error from high to low 0.0001

Improvements on H_{RTA} : part 1

(1) H_{RTA} dependence on solar azimuth angle ϕ_H

non-observable dependence on φ_H

F calculated with H_{SDSM}

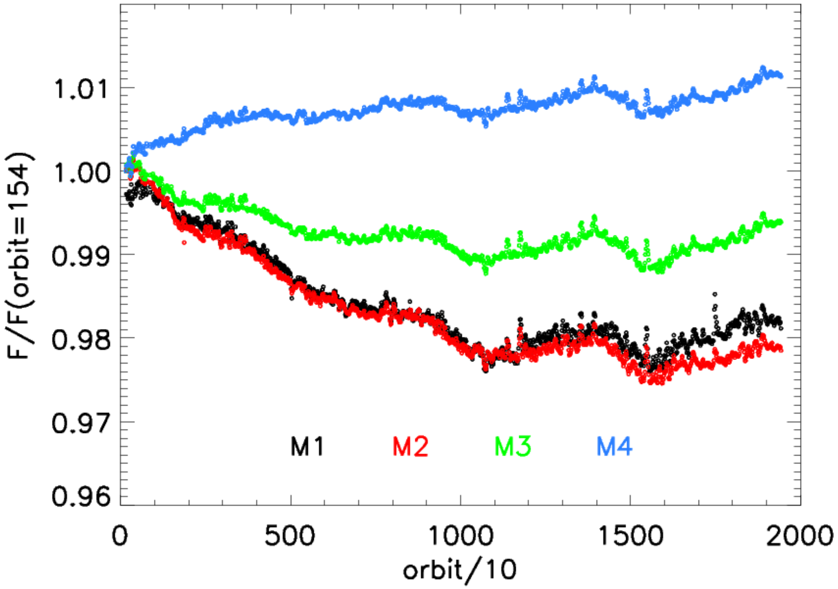

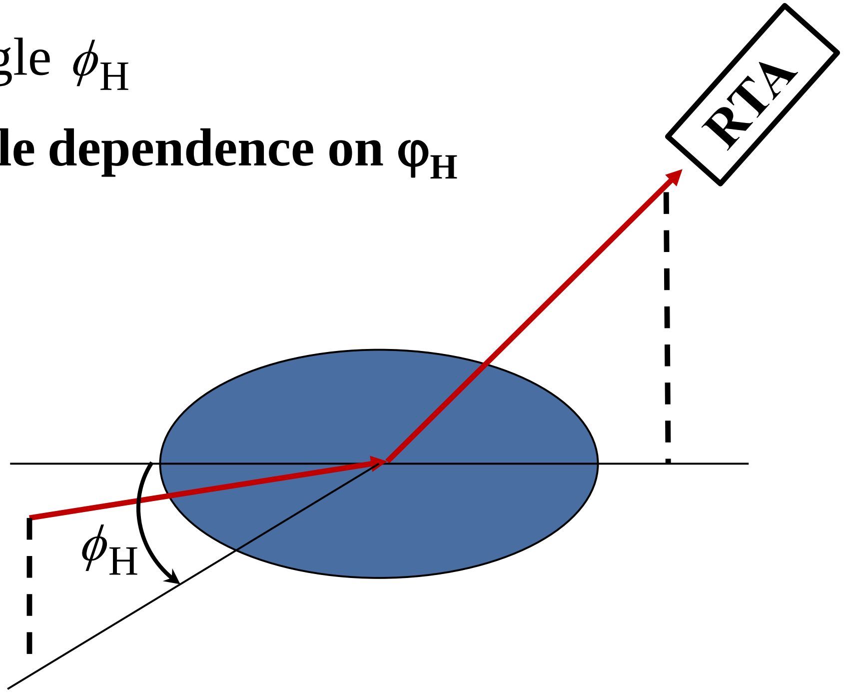

Improvements on H_{RTA} : part 1

(1) H_{RTA} dependence on solar azimuth angle ϕ_{H}

$$F_1 = F / \left[1 + \beta(\lambda) * \left(H_{\mathrm{SDSM,\ mean\ RSR}}(t_{\mathrm{mid}}) - H_{\mathrm{SDSM,\ mean\ RSR}}\right) * (\phi_{\mathrm{H}} - 48.0°)\right]$$

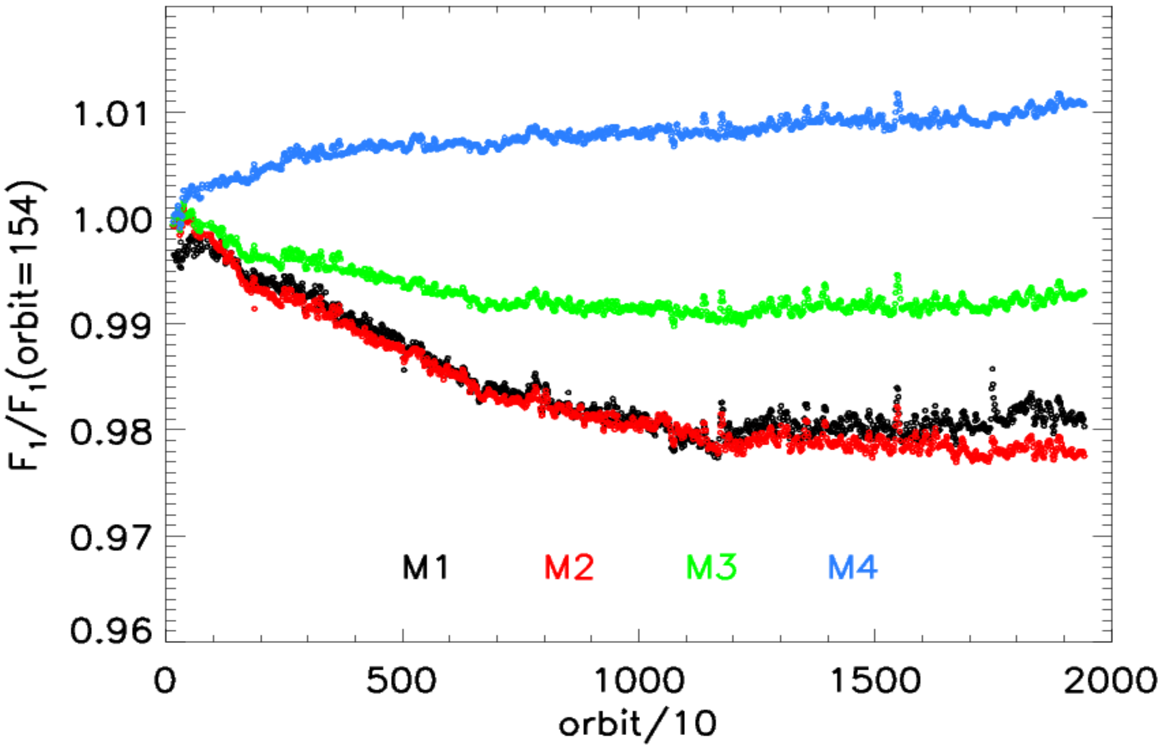

Improvements on H_{RTA} : part 2

(2) H_{RTA} from H_{SDSM}: match scaled lunar results through least square fitting

(2.1) $F_2 = F_1 \times [1 + \gamma(\lambda) * (1 - H_{SDSM})] \times H_{SDSM}$ ➡ update RSR

$$H_{RTA} = H_{SDSM} \times \frac{[1 + \gamma(\lambda) * (1 - H_{SDSM})] \times H_{SDSM}}{1 + \beta(\lambda) * (1 - H_{SDSM}) * (\phi_H - 48.0°)}$$

F

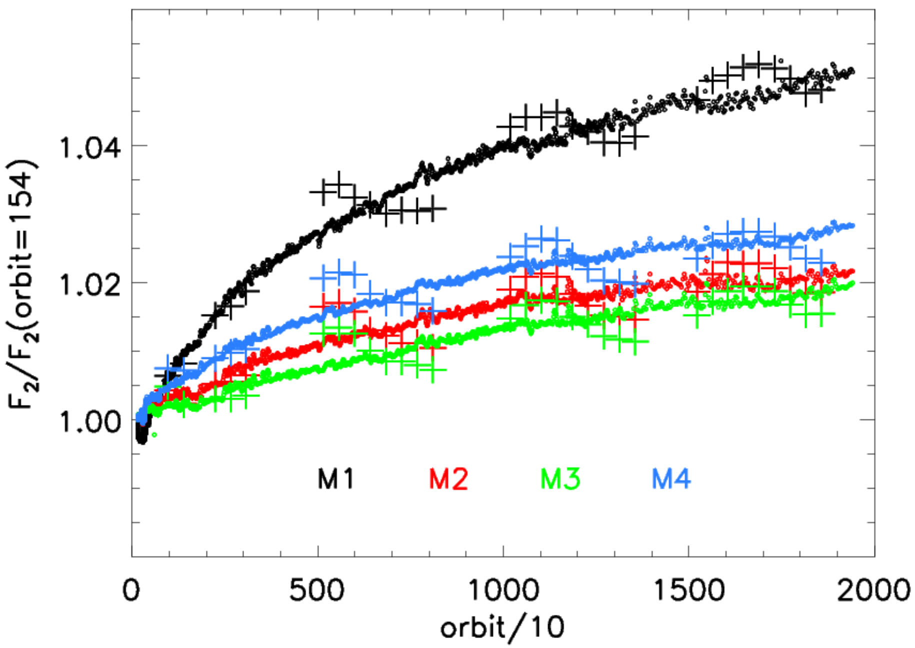

Fit $F[1 + \Delta\gamma(\lambda) * (1 - H_{SDSM})] \times H_{SDSM}$
match scaled lunar results again
-> update RSR; iterate until stable

Summary

- **SNRs are better than specifications and are projected to be better in the near future**
- ***F*-factor precisions are better than 0.1% on a per satellite orbit basis** (M1:0.07%, M2:0.07%, M3:0.06%, M4:0.04%, I1:0.06%, …, M11:0.05%)
  - New algorithms have been applied to improve the calculation accuracy of the SNPP VIIRS RSB throughput
    (1) removed yearly detector gain undulations (as large as 0.5% for M1)
    (2) removed biases (originally observed as large as 1.5% for M1) relative to lunar observations
    (3) removed bias due to incorrect H_{SDSM} normalization at t=0 (~1% for M1)
    (4) removed bias in the original $\tau_{SD}\,\mathrm{BRDF}_{RTA}(t=0)$ (0.05%; yaw)
    (5) removed bias for the calculated SWIR band throughput (0.4% for M8)
    (6) improved accuracies in $\tau_{SD}^{R}\,\mathrm{BRDF}_{SDSM}(t=0)$ and τ_{SDSM}^{R} (yaw+non-yaw) -> H_{SDSM} precision of 0.0003 to 0.0007
  - Correct solar vectors, removing a bias as large as 0.5% for all RSBs

BACKUP

Improvements on H_{SDSM} : part 4

$$1 - H(\lambda, t) = \frac{\alpha(t)}{\lambda^{\eta}} \qquad (4)$$

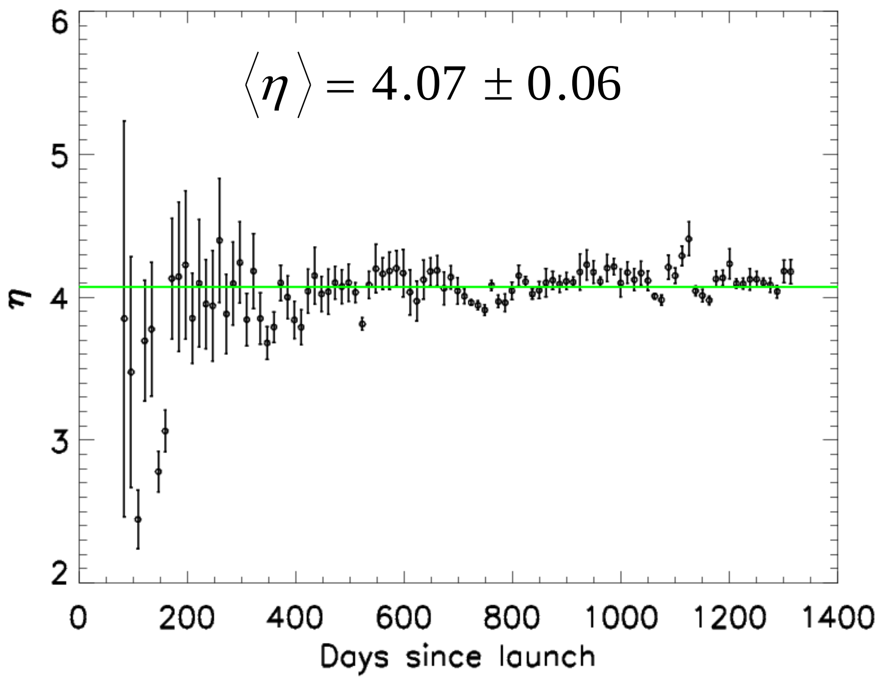

Improvements on H_{RTA} : part 2

(2) H_{RTA} from H_{SDSM}: match scaled lunar results through least square fitting

$$H_{\mathrm{RTA}} = H_{\mathrm{SDSM}} \times \frac{[1+\gamma(\lambda)*(1-H_{\mathrm{SDSM}})]\times H_{\mathrm{SDSM}}}{1+\beta(\lambda)*(1-H_{\mathrm{SDSM}})*(\phi_H-48.0°)}$$

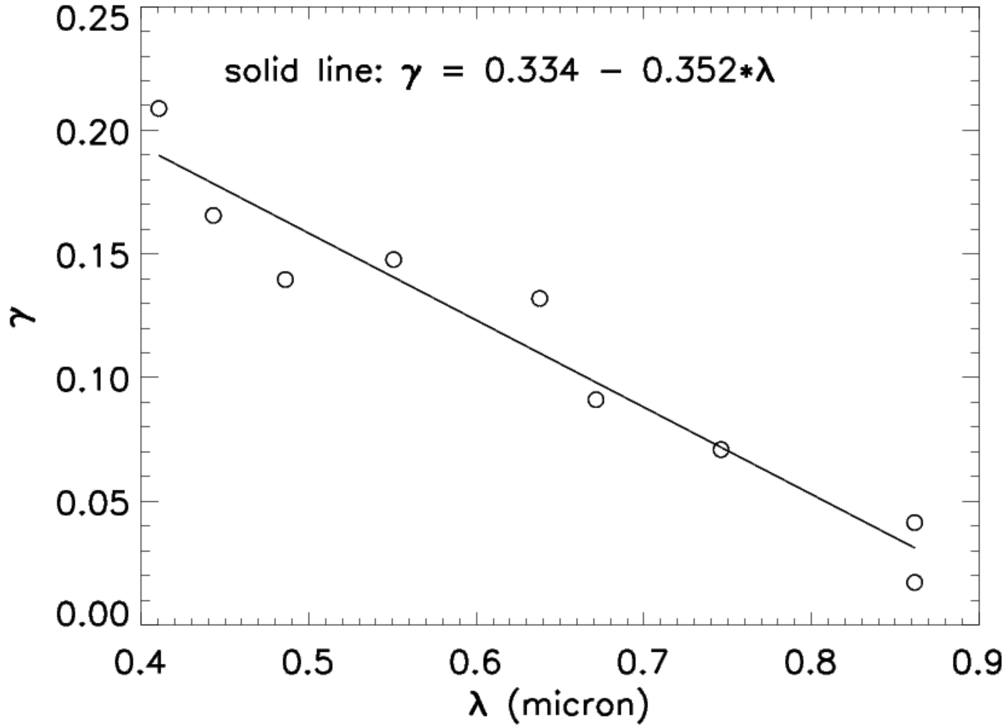

S-NPP VIIRS DNB On-orbit Performance with Stray-light Estimation and Predication

VIIRS Characterization Support Team

June 6, 2016

Outline

- DNB RSR and Degradation Behavior
- DNB Calibration and Predication Algorithm
- DNB On-orbit Performance and Trending
- Stray-light Estimation and Predication
- Stray-light Features in Northern/Southern Hemisphere
- Examples of Data Fusion for Stray-light LUTs
- Selected Results
- Summary

DNB RSR Behavior

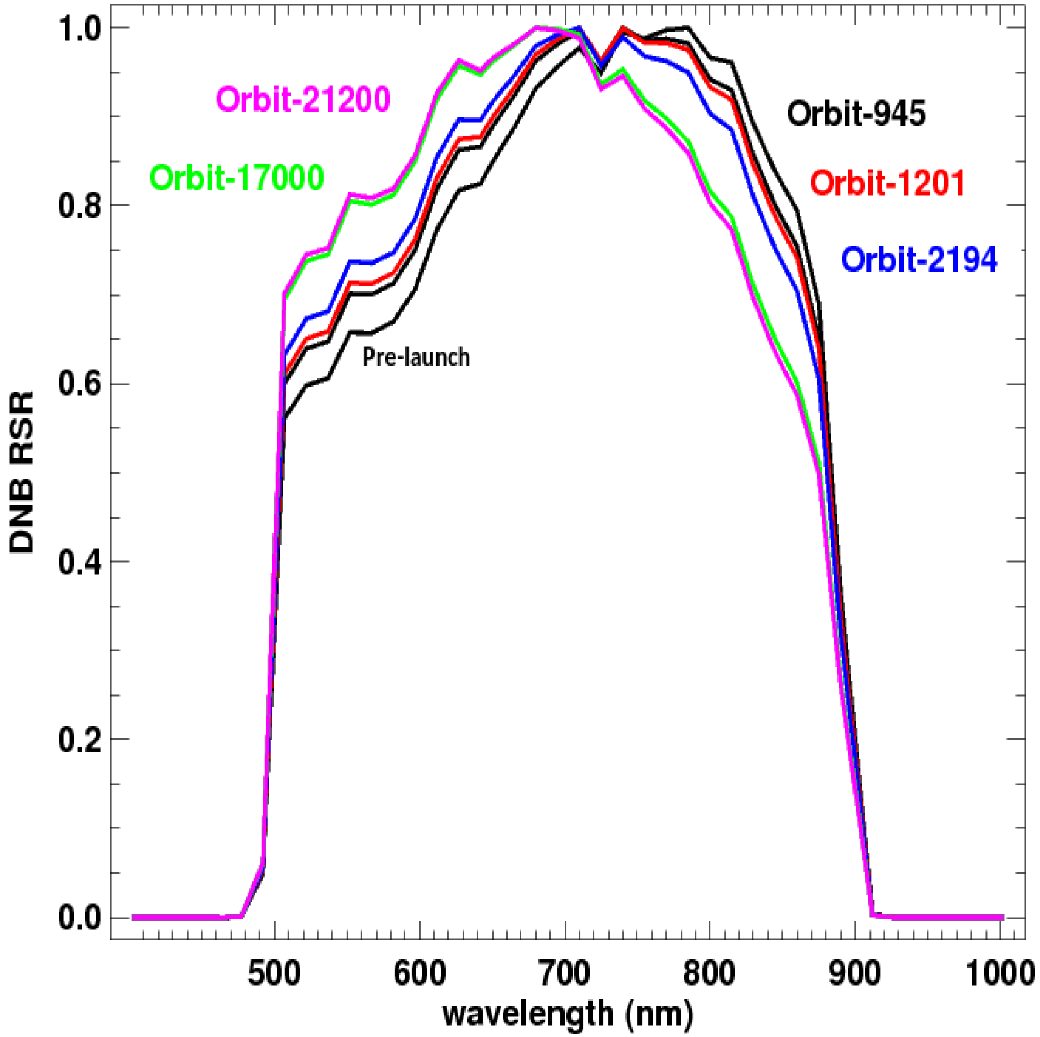

- RSR shows a gradually shifting from right side to left side, as operation goes forward.

- RTA degradation:

$$\frac{\int H'(\lambda) \cdot RSR(\lambda) d\lambda}{\int RSR(\lambda) d\lambda}$$

NOTE: $H'(\lambda)$ is interpolated degradation from SDSM 8 bands.

VIIRS RSB and DNB Degradation

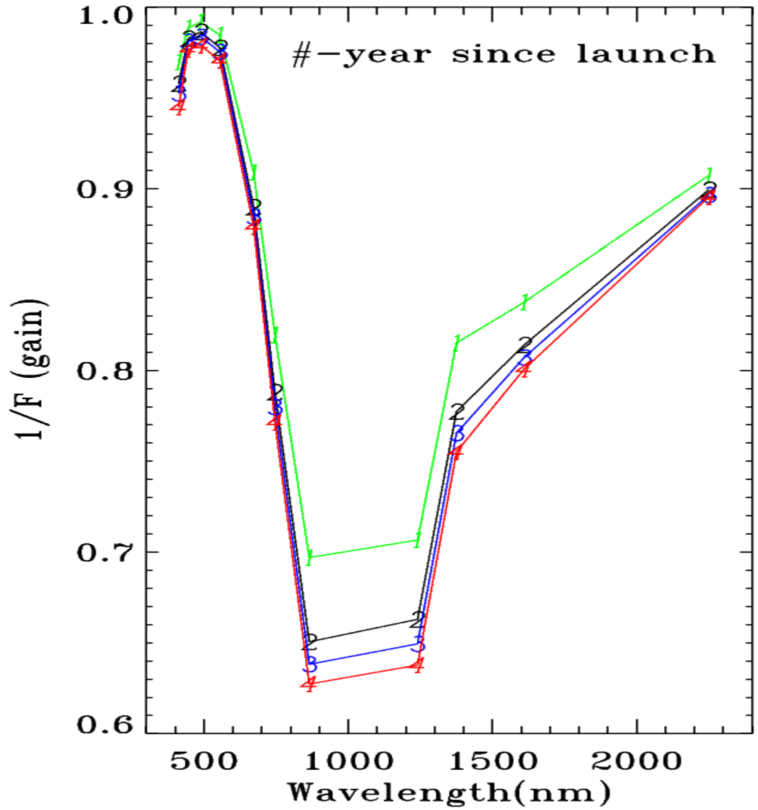

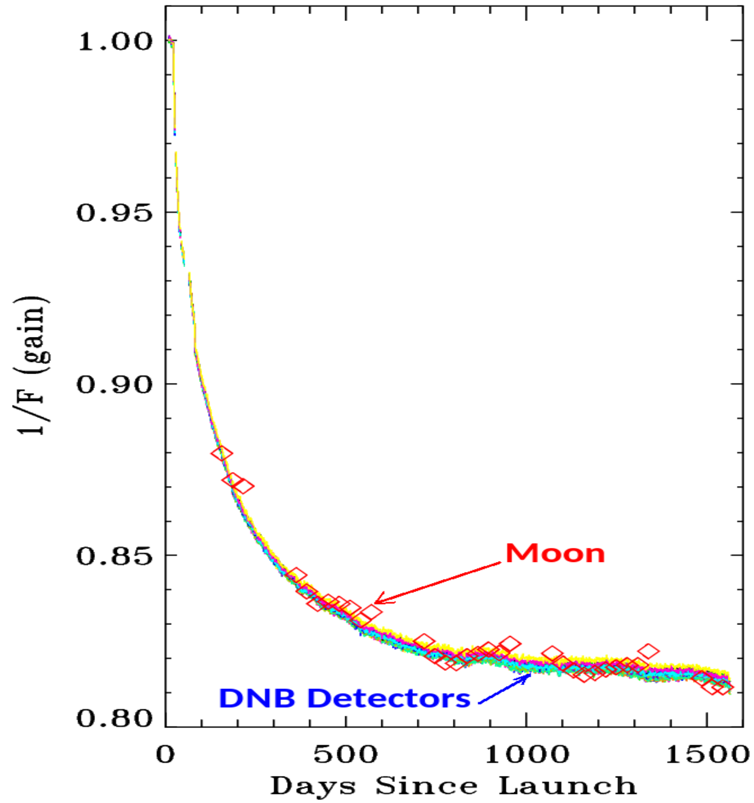

- ❑ **RSB have experienced the largest degradation in the first year.**
- ❑ **DNB has about 18.5% degradation entire mission.**
- ❑ **DNB Moon irradiance trending matches well with SD gain trending.**

DNB Calibration and L1B Algorithm

LGS Gain Calculation:

- SD radiance: $L_{SD} = \cos\theta_{sd} \cdot RVS_{sd} \int BRF(\lambda)\tau_{sd} H(\lambda,t) RSR(\lambda) \frac{\Phi(\lambda)}{4\pi d^2} d\lambda$

  SD-SUN angle, HAM relative response at SD AOI, transmittance of pinhole screen, SD degradation index, relative spectral response, solar spectral power distribution.

- Calculate LGS gain coefficient: $L_{SD} = c_1 \cdot dn$

Dark Offset:

- Select dark data as sun declination angles in 40º~140º.
- Use the minimum of fitted values in SV/BB/SD as dark signal

Cross-stage Gain Ratios:

- Compute daily average gain ratio: MGS/LGS, HGS/MGS

MGS and HGS Gain Coefficients:

- MGS gain = LGS gain * MGS/LGS
- HGS gain = MGS gain * (HGA/MGS +HGB/MGS)/2

Gains/Offsets Use Recent 1-year Data with a Linear-fit for L1B

DNB Gain Ratio (HGS/MGS and MGS/LGS)

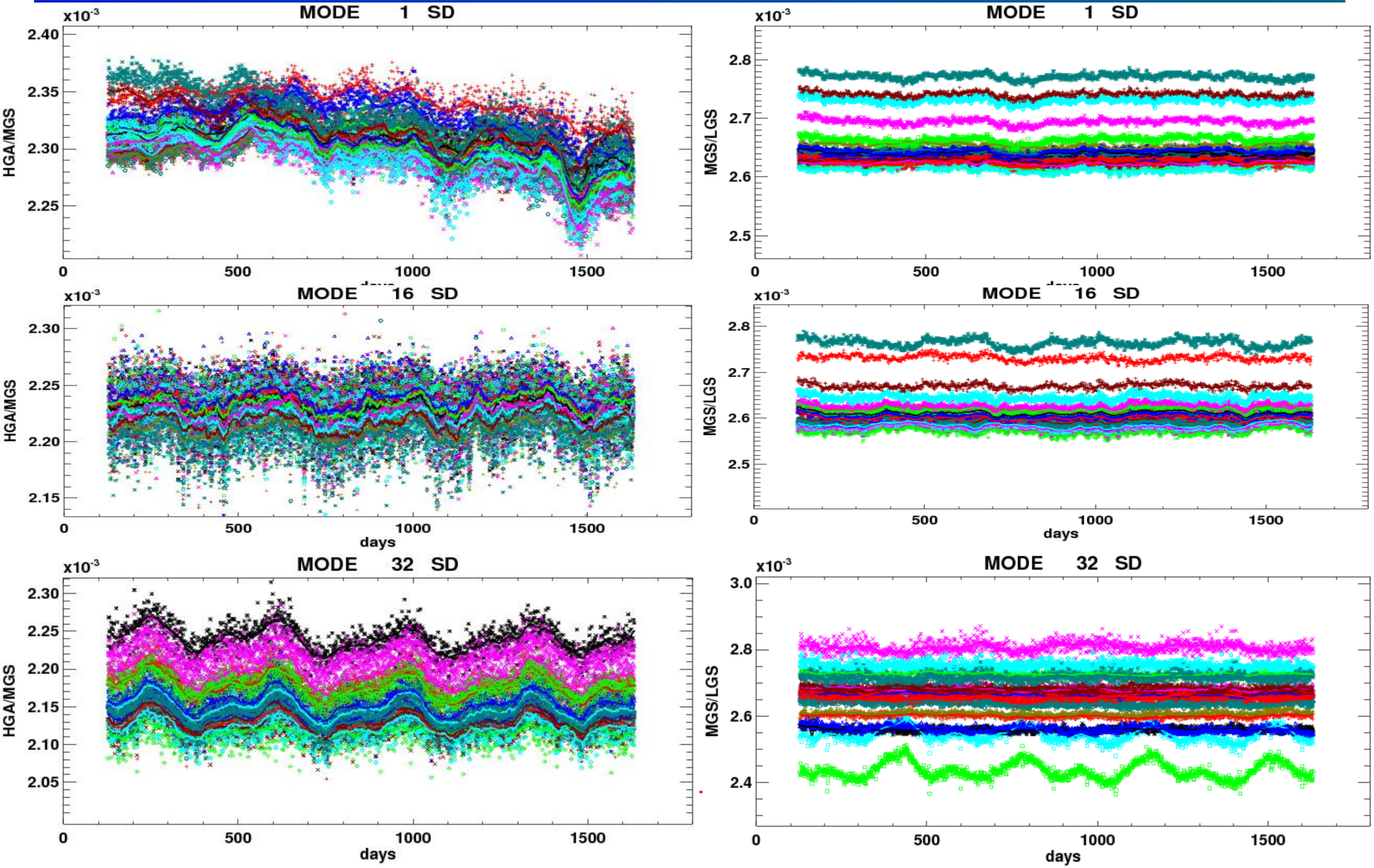

DNB Gain/Offset Trending and Predication

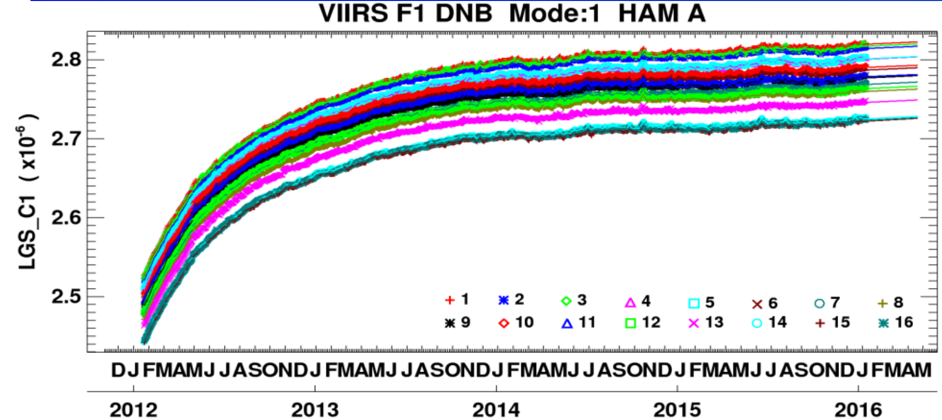

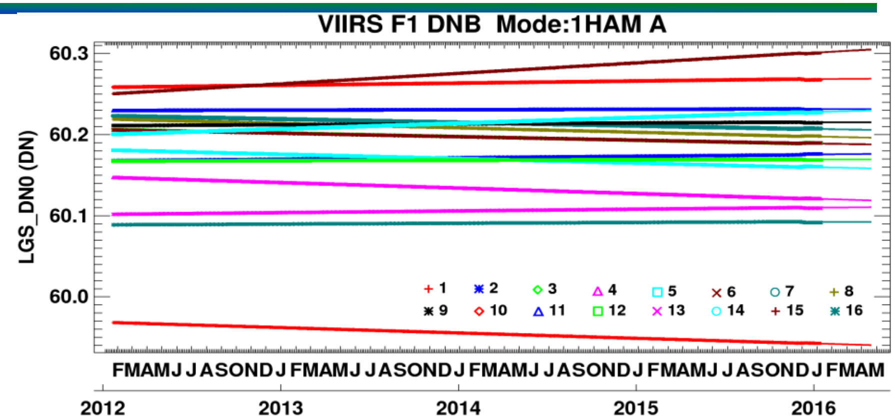

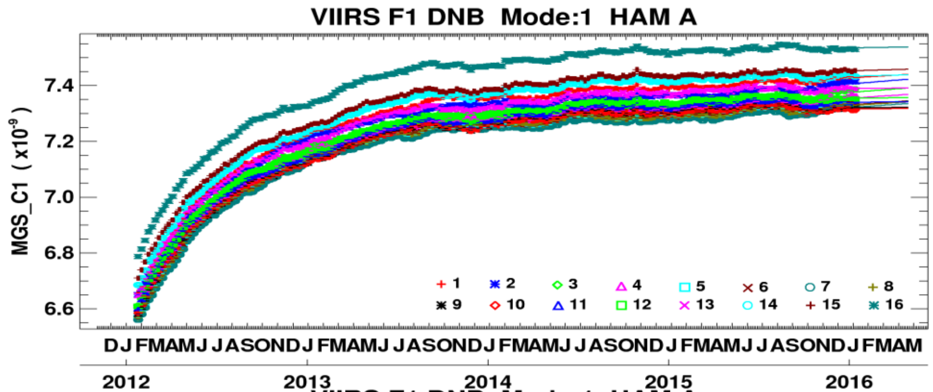

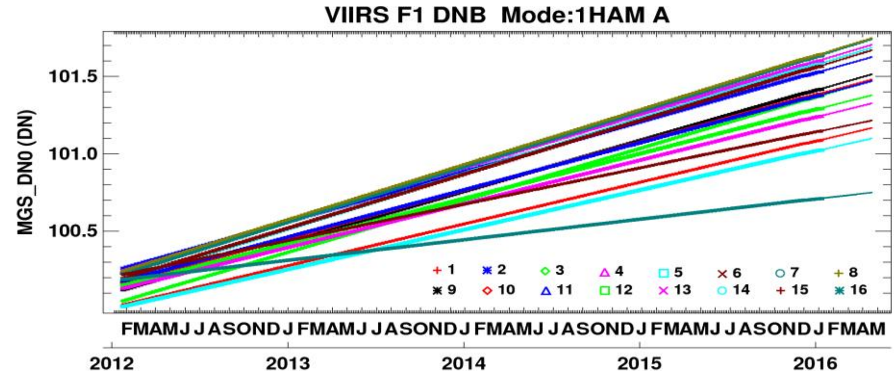

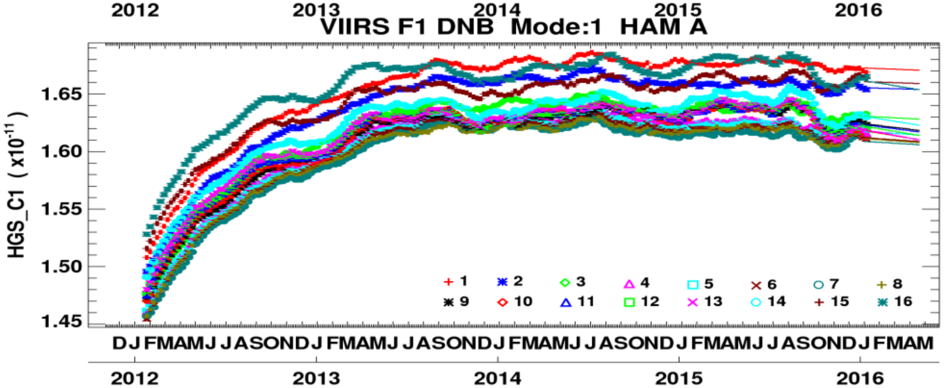

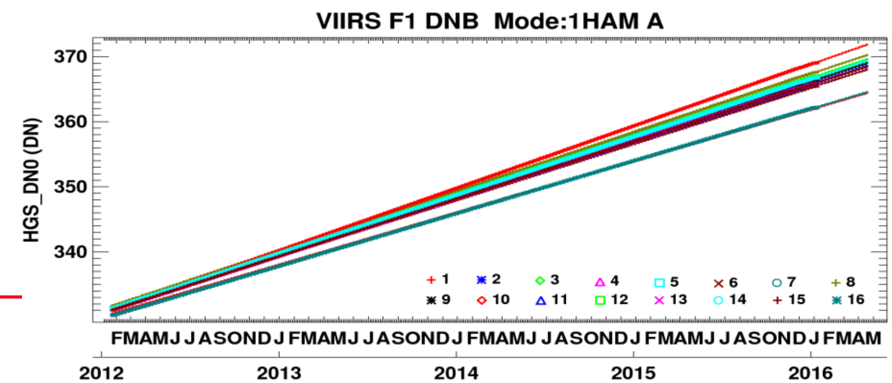

DNB Stray-light Estimation and Predication

- **EV Signals Considered**
  - Use EV data from terminator crossing area during new moon.
  - Separate EV samples into 127 bins of 32 pixels each (4064=127x32).
- **Stray Light Estimation**
  - In twilight regions (SZA < 105°), stray light is assumed the same to the last known value.
  - Produce correction LUT hemisphere, detector, HAM, sample and SZA.
  - Update correction LUT per month (every new moon)
- **Stray Light Predication**
  - Stray-light pattern follows yearly Earth-Sun spacecraft geometry cycle.
  - IDPS uses the same month one-year-ago LUT.
  - VCST uses all previous LUTs via a data fusion mechanism.

NH/SH Stray-light Features

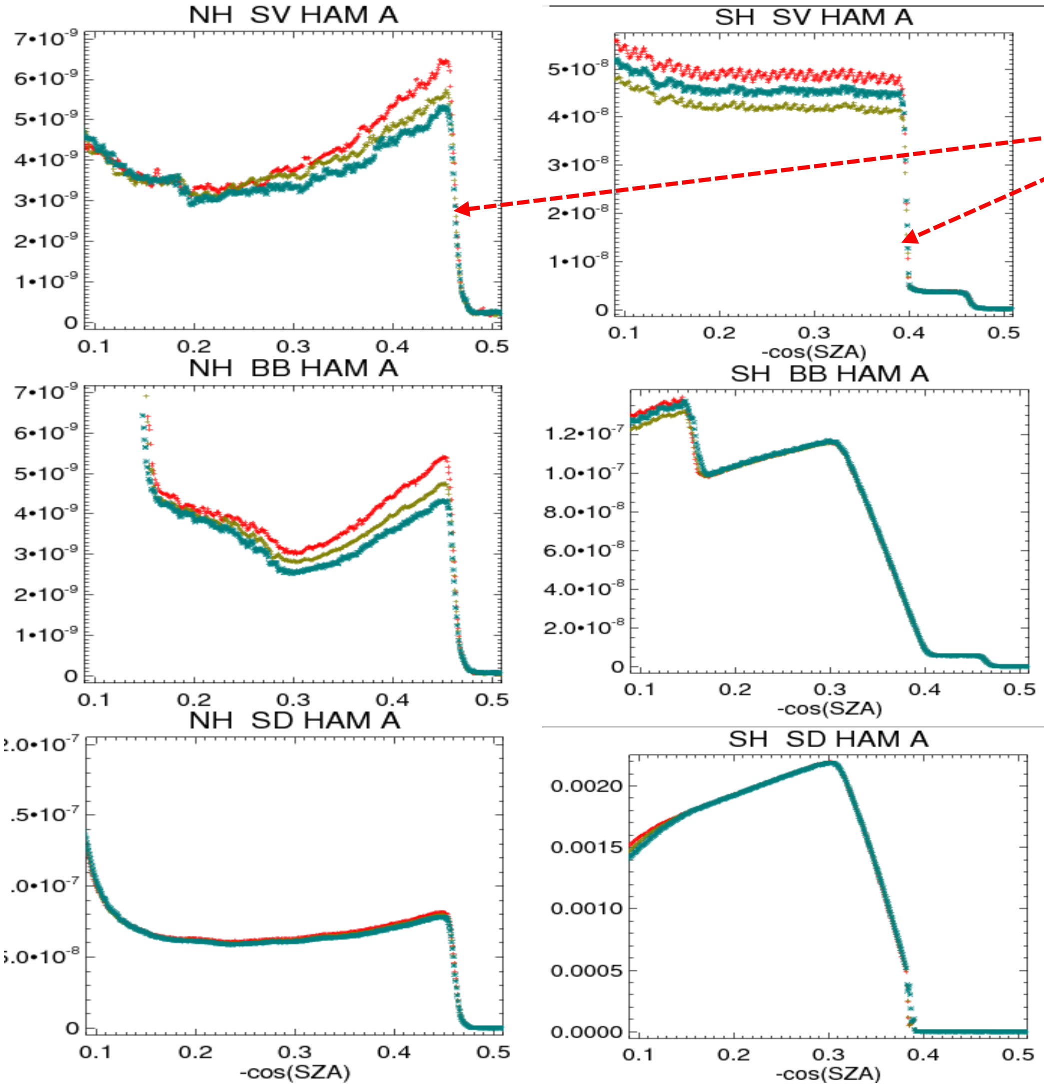

Penumbra Region

- New moon 03/20/2015
  - Northern, Southern hemisphere: SV, BB, SD view
  - Three detectors, d1/d8/d16
  - Radiance vs solar zenith angle
- NH/SH shows different stray-light features.
- Edge (big slop) makes hard for correction.

NH/SH Penumbra Angle Estimates

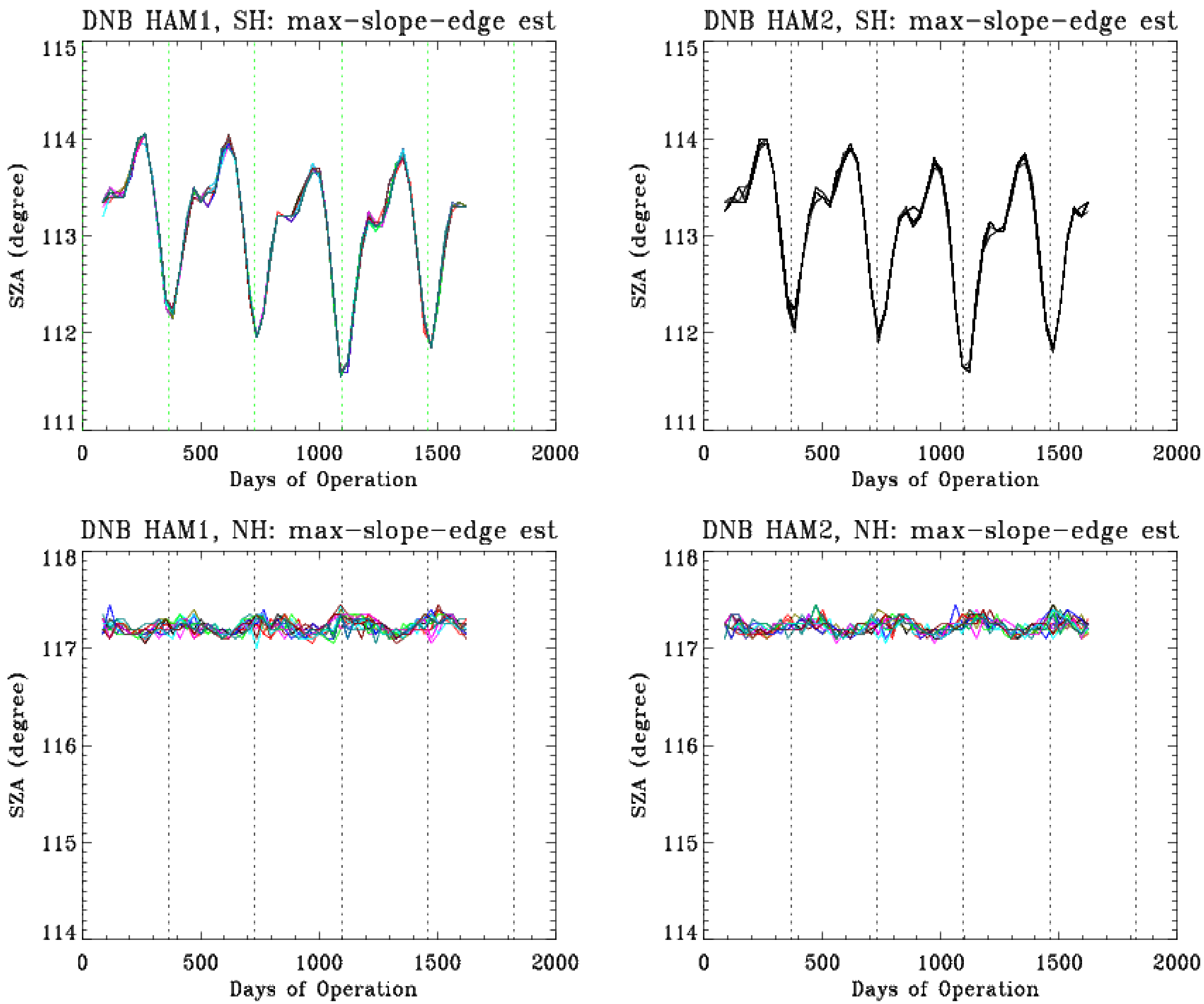

- SV data is used to estimate the penumbra angle.
- NH/SH shows different penumbra angle features.
  - SH has large yearly fluctuations, SZA is in the range of 2 degrees.
  - NH is in the range of 0.3 degree.

Multiple-years Data Consideration

- **Stray-light Estimation LUTs**
  - Each year has 12 LUTs (12 new moon events).
  - LUT size: 469x127 (solar zenith 95º-118.5º, 4064 pixels)
- **Multiple-year Stray-light Historic Data**
  - Simply average introduces additional estimation error.
    - DNB degradation impact.
    - Onset SD angle shift (penumbra region).
    - Hard to be normalized by fitting (limited data each year).
- **Data Fusion**
  - Use all possible historic data and truncate them into yearly groups such that each group has 12 points (months).
  - Introduce a similarity metric to find the best degradation adjustment in each group to make all groups as similar as possible (smallest value of the similarity metric)
  - Adjust the best degradation in each group, and then combine the group together.

Example: Straylight Predication using Historic-data

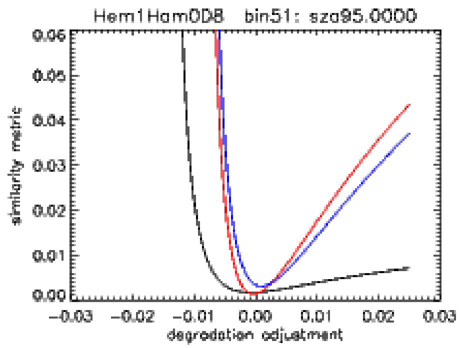

- Relative entropy is used as the similarity metric.
- Similarity versus degradation adjustment.

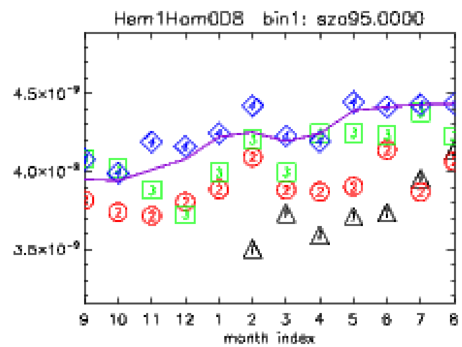

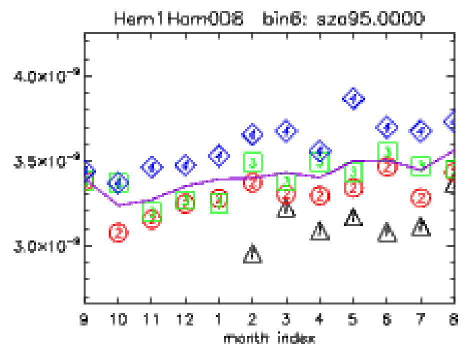

- Historic data (up-to 08/2015).
- Each group is with different color.
- Line denotes the fusion results.
- Results of two bins with SZA=95 are shown.

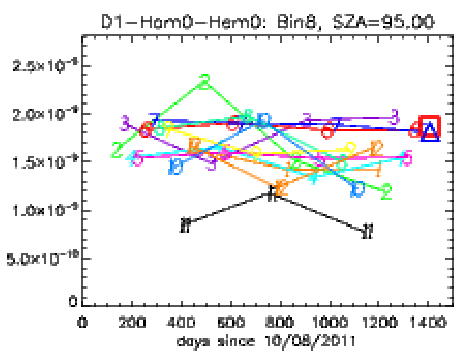

- Each month has its own trending.
- Red-square denotes the actually calculated result using the new moon of 09/2015
- Blue-triangle denotes the predicated result using data up-to 08/2015.

Day20160408: gT08:24:21 original/corrected images

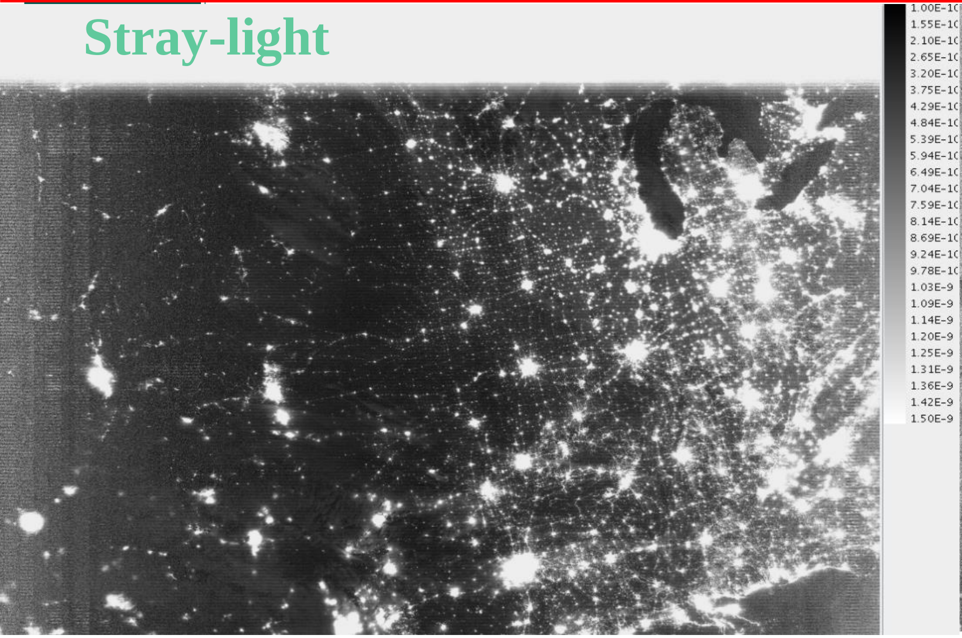

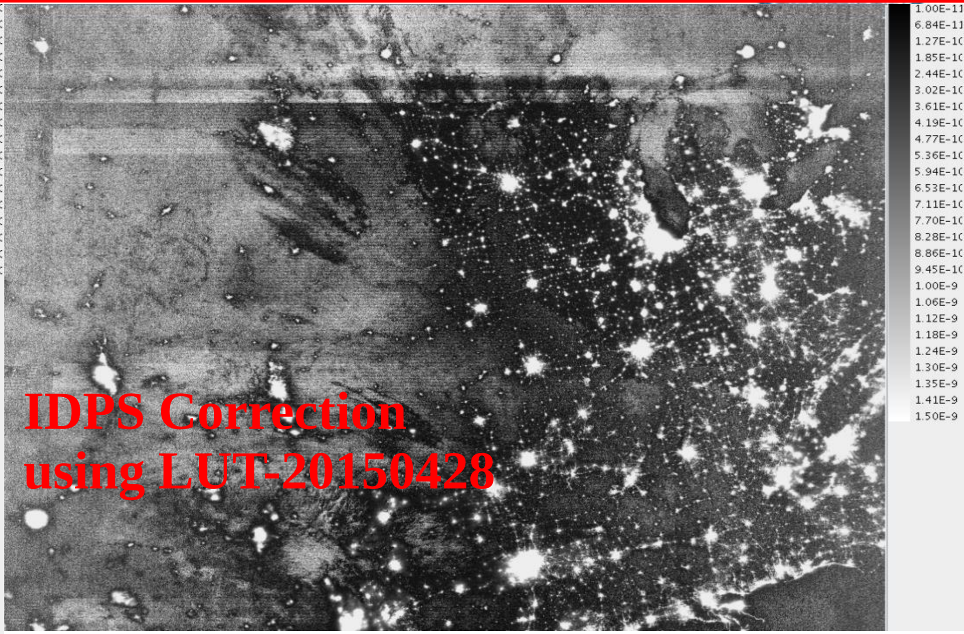

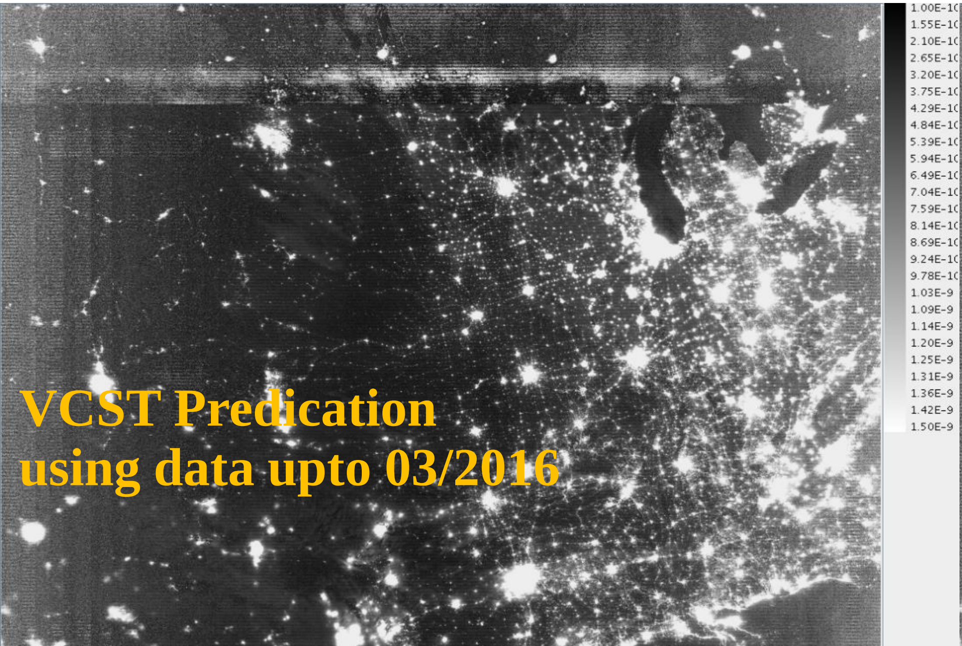

Summary

- DNB calibration and stray-light estimation/predication have been presented.
  1. Gain and offset use the most recent 1-year data via a linear-fit to generate L1B LUT.
  2. Real-time stray-light correction is possible by using the predicted correction LUT.
  3. L1B forward calibration delivery (gain/stray-light LUTs) can be effectively performed.
- DNB on-orbit performance and trending have been illustrated.
  1. RSB degradation behavior is normal. DNB SD and Moon F-factors are matched well.
  2. LGS gain/offset are stable trending, and gain coefficients gradually increase over time.
  3. HGS gain coefficients have large fluctuations convolving gain ratios of H/M and M/L.
- Stray-light correction results show the effectiveness of estimation/predication.
  1. Fuse historic data (straylight correction LUT) with degradation and/or SZA adjustments.
  2. Example (2015-08): Stray-light predication matches the actual estimation very well.
  3. Example (2016-04): Original/corrected night images show results of using IDPS, VCST and VCST predication LUTs. In the operational point view, VCST predication provides better straylight removal results than IDPS.

S-NPP VIIRS Thermal Emissive Bands On-Orbit Performance and Calibration

Jeff McIntire, Chengbo Sun, Sergey Gusev, and Vincent Chiang

VCST, NASA/GSFC

Acknowledgements: **VIIRS SDR Team Members**
VCST Members

June 6, 2016

Outline

- **TEB Calibration**
- **On-orbit Performance**
  - BB performance
  - Detector short-term stability and long-term response (F-factors)
  - Detector noise characterization (NEdT)
  - Trending during WUCD
- **Improvements**
  - Improvements already implemented
  - Future improvements
- **Conclusions**

Thermal Emissive Bands (TEB)

5 M-bands and 2 I-bands, covering wavelengths from 3.7 to 12 μm

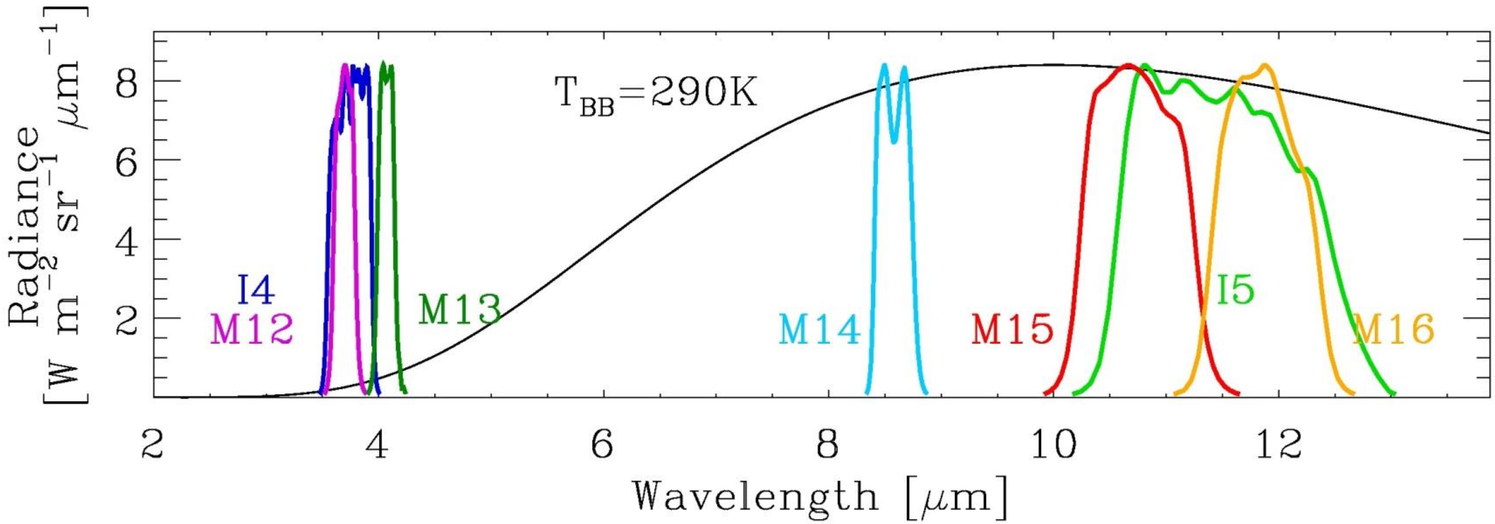

Band	I4	I5	M12	M13	M14	M15	M16
Wavelength [μm]	3.74	11.45	3.70	4.05	8.55	10.76	12.01

Calibrated using an on-board blackbody (BB):

- Scaling factor "F-factor" is derived and applied each scan.
- Warm-up and cool-down (WUCD) cycles are performed quarterly to fully characterize TEB detector response, including offset and nonlinear terms.

TEB Calibration Methodology

VIIRS Earth View radiance is retrieved following ATBD Eq. (116)

$$L_{EV}(B,\theta) = \frac{F(B)\sum_{i=0}^{2} c_i(B)dn^i(B) - \Delta L_{bg}(B,\theta)}{RVS(B,\theta)},$$

dn: detector response
c_i: calibration coefficients
RVS: response versus scan-angle

where the $\Delta L_{bg}(B,\theta)$ is the background difference between the EV and SV path:

$$\Delta L_{bg}(B,\theta) = (RVS(B,\theta) - RVS_{SV}(B))\left[\frac{(1-\rho_{RTA}(B))}{\rho_{RTA}(B)} L_{RTA} - \frac{1.}{\rho_{RTA}(B)} L_{HAM}\right],$$

The F-factor is derived each scan for each band, detector, and HAM side:

$$F(B) = \frac{RVS_{BB}(B)L_{ap}(B) + \Delta L_{bg}(B,\theta_{BB})}{\sum_{i=0}^{2} c_i dn_{BB}^{i}},$$

Estimated BB radiance

Retrieved BB radiance

and the aperture radiance from the BB is:

$$L_{ap}(B) = \varepsilon L_{BB} + (1-\varepsilon)(F_{RTA}L_{RTA} + F_{SH}L_{SH} + F_{CAV}L_{CAV})$$

BB Performance

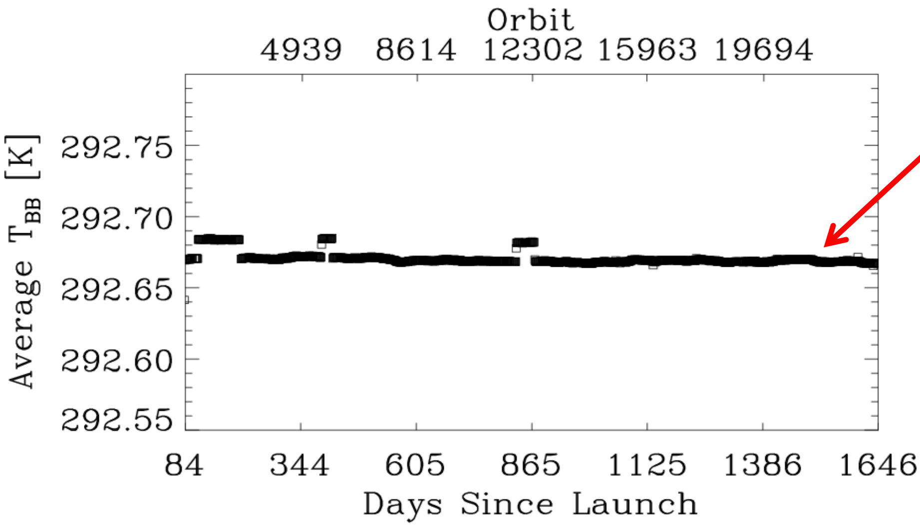

Long-term trend of daily-averaged T_{BB}

- Stable to within a few mK.
- ~15 mK offsets were due to the use of two different T_{BB} settings.

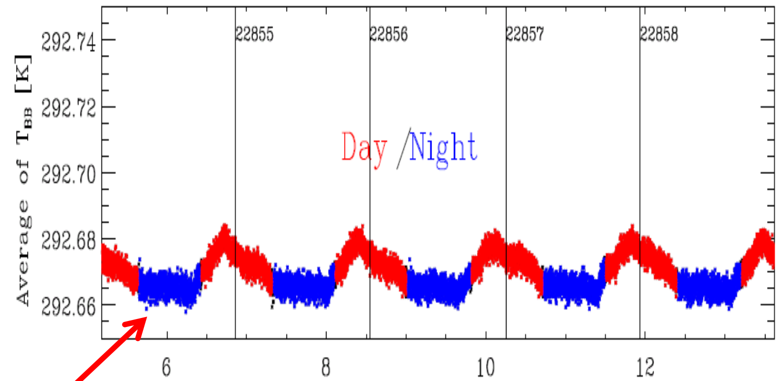

Short-term stability (scan-by-scan T_{BB}):

- Orbital variations of individual thermistors up to 40 mK
- Variations in average temperature ~ 20 mK
- Temperature difference between individual thermistors up to 60 mK
- **BB uniformity meets the requirement with standard deviation less than 30mK**

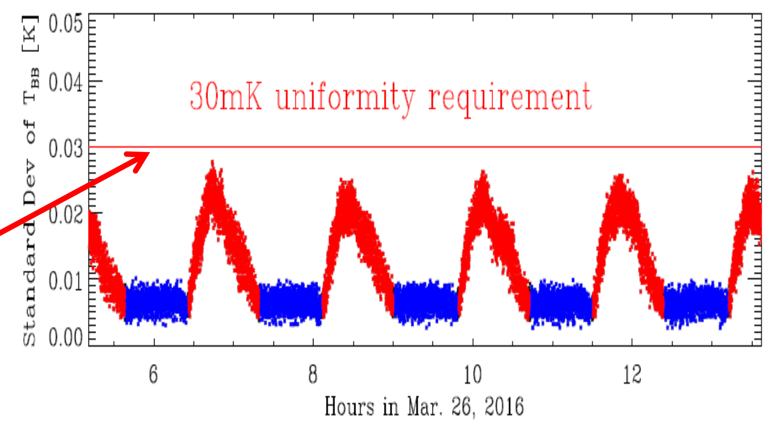

Detector Short-term Stability

Detector responses (F-factors) show small orbital variations:

- ±0.2 % or less on a per scan basis
- ±0.1 % or less on a per granule basis

Would using averaged F-factors improve SDR product?

F-factor orbital variations correlate with T_{BB} variations and instrument temperatures variations.

F-factor shown for orbits 22854 – 22858 for HAM side A.

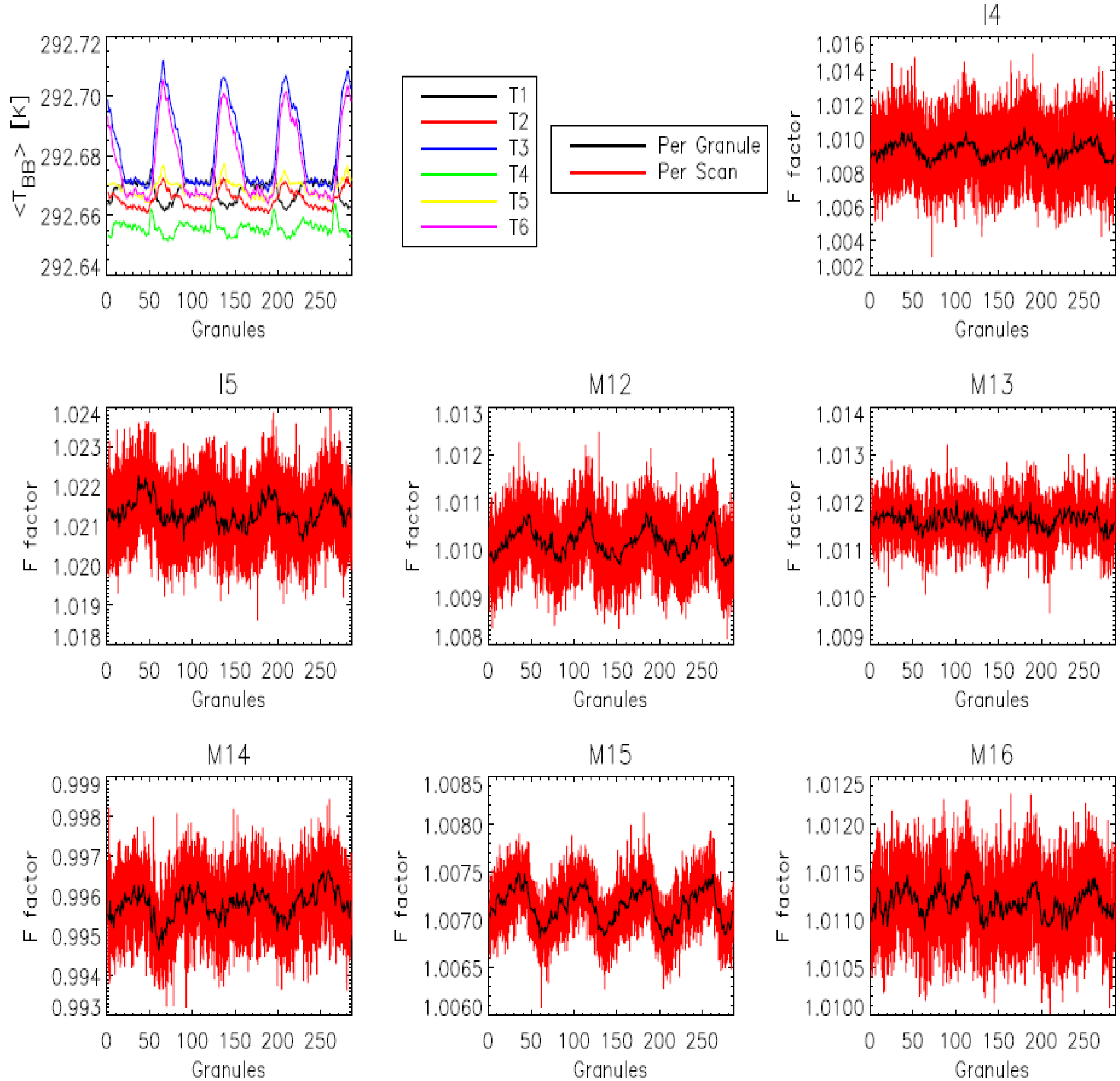

Detector Long-term Response

Daily average F-factor trend:

- From January 20, 2012 (orbit 1200) to May 1, 2016 (orbit 23361)
- I5 shows the most noticeable trend of ~1.4 %, while the rest of the bands are within 0.47 % (I4).
- Discontinuities in the trend are coincident with anomalies during which the cold FPA and/or instrument temperatures changed.
- Features in LWIR bands F-trend appear to coincide with the passage of the Earth through perihelion.

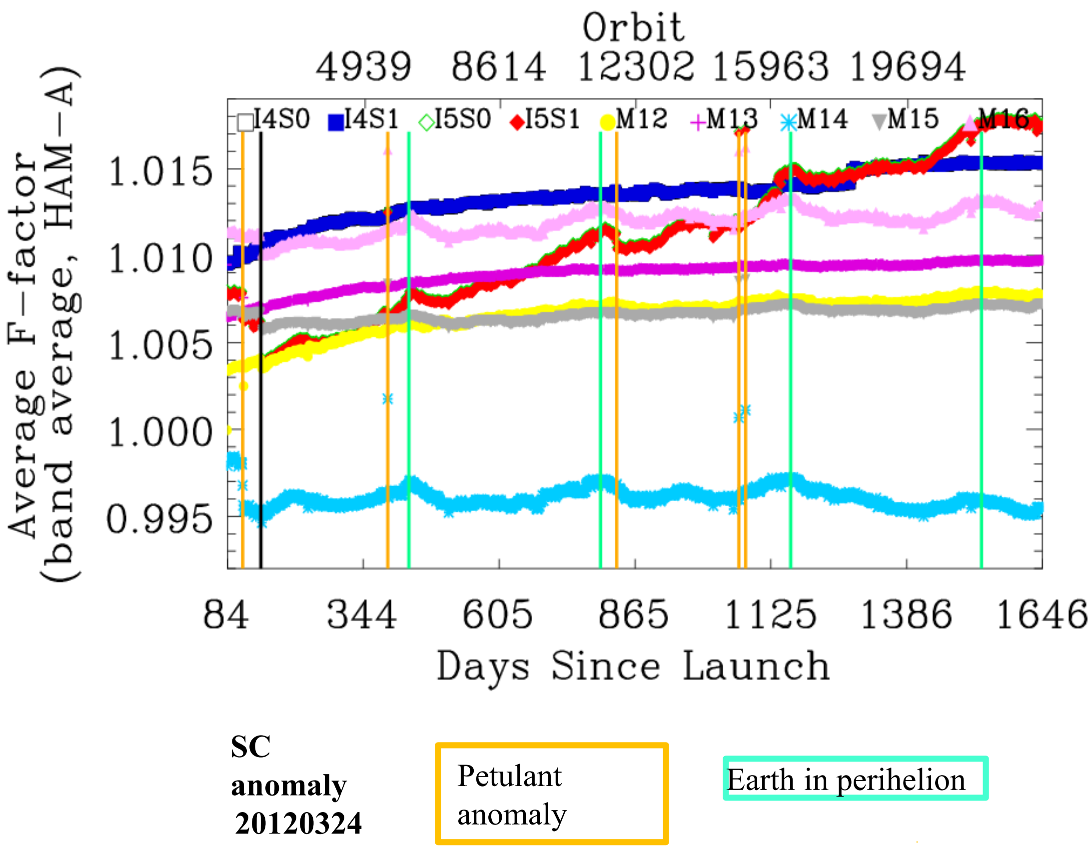

Band	I4	I5	M12	M13	M14	M15	M16
Average F-factor: 03 26 2012	1.0105	1.0040	1.0035	1.0070	0.9946	1.0056	1.0101
Average F-factor: 03 26 2016	1.0153	1.0177	1.0077	1.0097	0.9952	1.0070	1.0126
Trend [%]	0.47	1.36	0.42	0.26	0.06	0.14	0.24

Instrument Temperatures Trend

- Discontinuities in the instrument temperatures trends coincident with discontinuities in the F-factor trends shown on previous slide.
- Features in instrument temperature trends appears to coincide with the passage of the Earth through perihelion. The F-factor for LWIR bands shows features at the same time.
- There is a small increasing trend of SMWIR focal plane temperature, which can explain the trend observed in MWIR bands (I4, M12, M13).

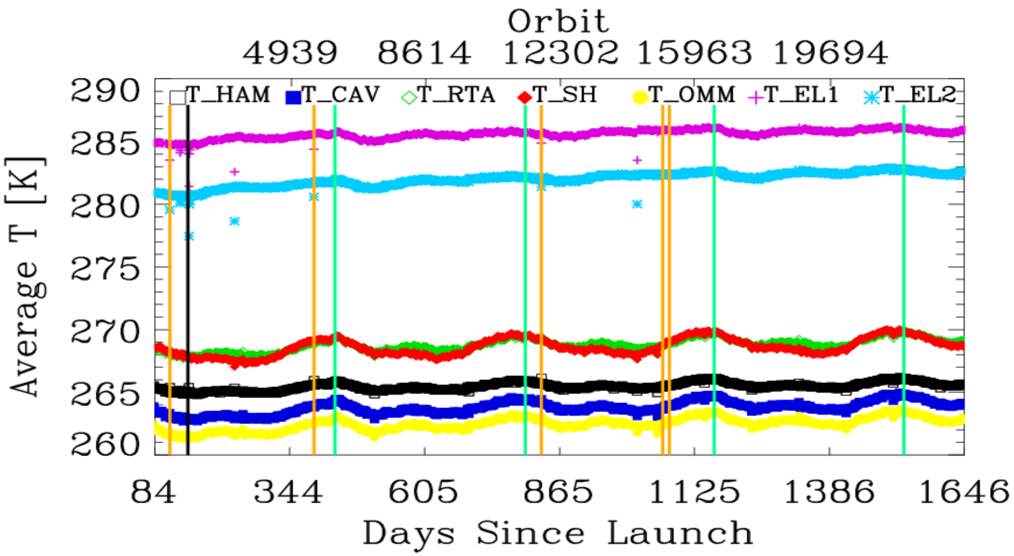

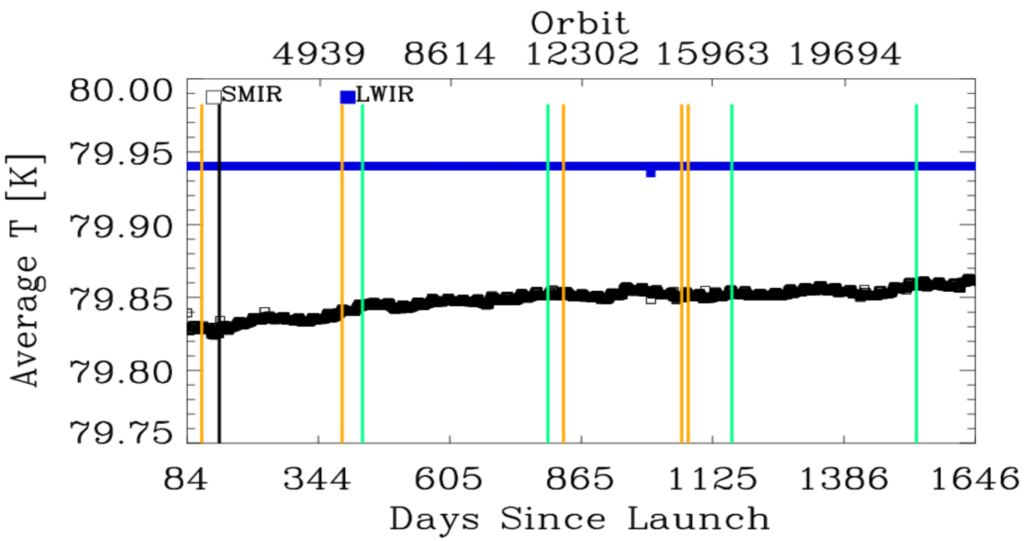

Detector Noise Characterization (NEdT)

$$NEdT = \frac{NEdL}{\partial L/\partial T} = \frac{L}{SNR\ \partial L/\partial T}$$

- NEdT routinely trended at 292.5 K: stable since the CFPA temperatures reached ~80 K (orbit 1200). Band averaged values are within 0.2 K for I bands and 0.07 K for M bands

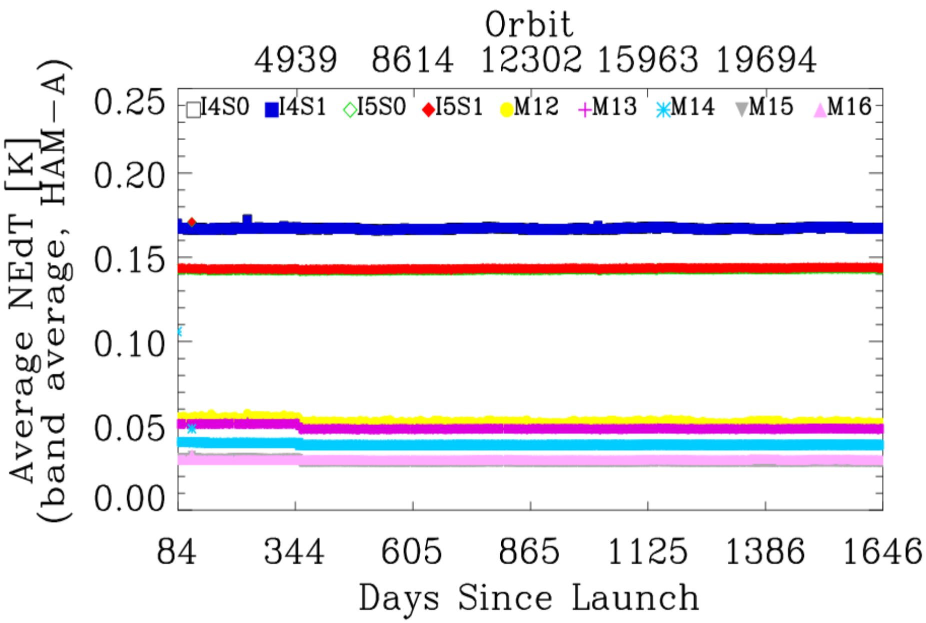

- NEdT at T_{TYP} derived periodically from BB WUCD data: stable and meeting the sensor design requirements by a wide margin:

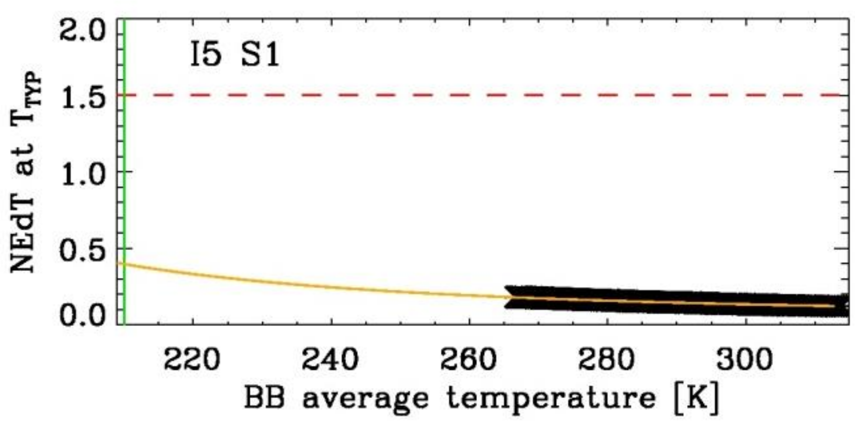

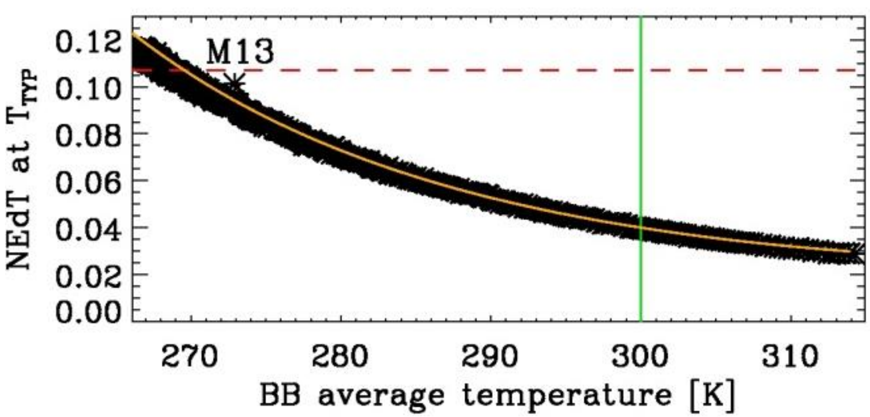

Detector Noise Characterization (NEdT)

Band	T_{TYP} [K]	NEdT at T_{TYP} [K]					
		Requirement	02/12	03/13	03/14	03/15	03/16
I4	270	2.5	0.4	0.4	0.4	0.4	0.4
I5	210	1.5	0.4	0.4	0.4	0.4	0.4
M12	270	0.396	0.13	0.12	0.12	0.12	0.12
M13	300	0.107	0.04	0.04	0.04	0.04	0.04
M14	270	0.091	0.05	0.06	0.06	0.06	0.06
M15	300	0.070	0.03	0.03	0.03	0.03	0.03
M16	300	0.072	0.03	0.03	0.03	0.03	0.03

NEdT at T_{TYP} (derived from BB cool-down data)
Only February / March cool-down measurements listed
TEB bands continue to meet the sensor design requirements

Calibration Coefficients – Band-average c_1

- Band-average c_1 coefficients, as derived from the thirteen WUCD until March 2016, are shown in red (WU data), and blue (CD data) and compared to pre-launch (green). I5 c_1 starts to show noticeable trend, consistent with results from F-factor trending.
- Band-average c_1 coefficients derived during WUCD cycles are within 1.9 % on average (at M16 CD) from pre-launch values.
- An offset between WU and CD results is present through the thirteen WUCDs, most prominent for LWIR bands.

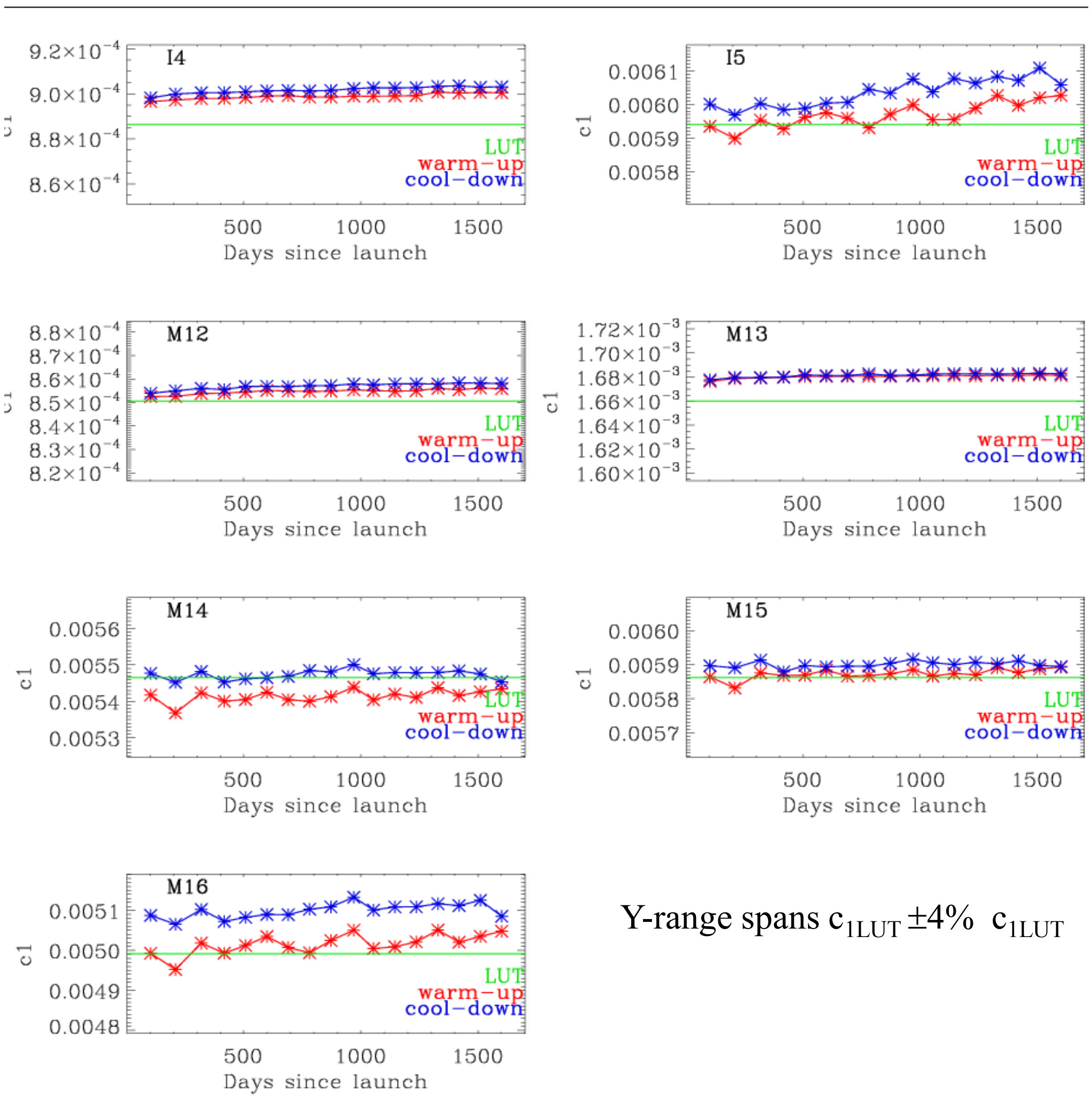

Y-range spans c_{1LUT} ±4% c_{1LUT}

c_0 and c_2 Coefficients

Band average c_0

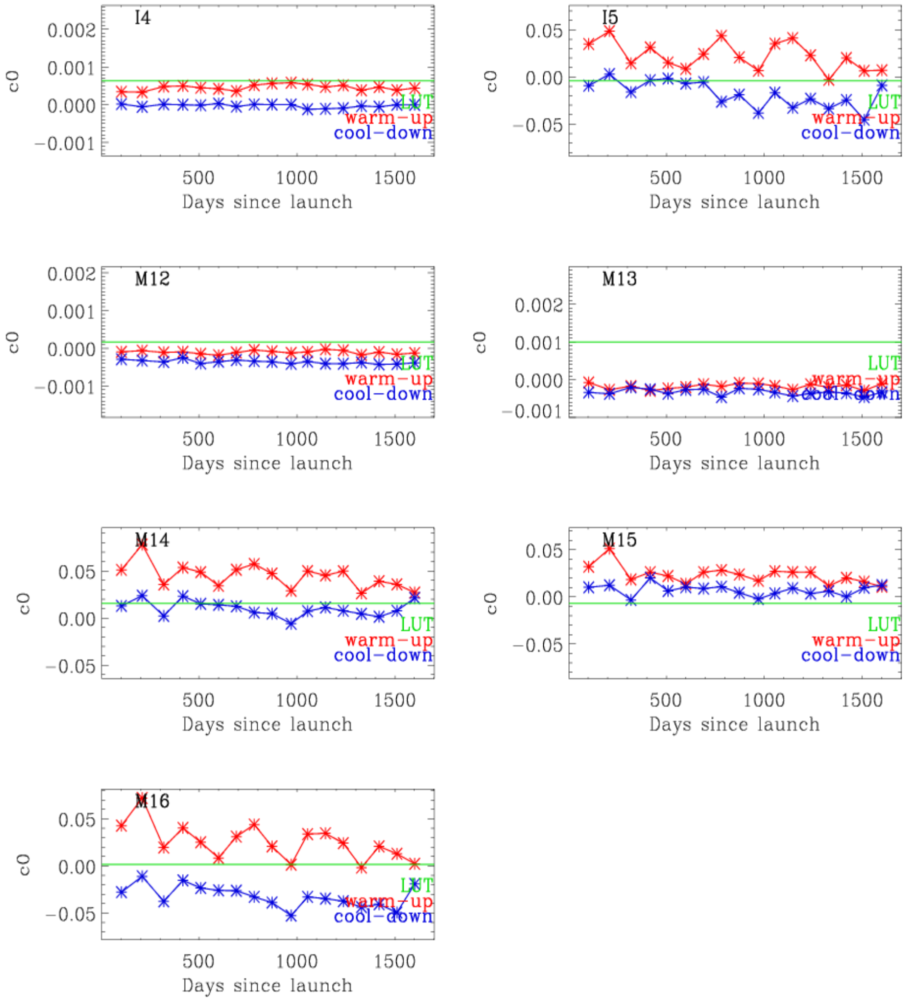

Y-range spans: $c_{0LUT} \pm 0.002$ (MWIR),
$c_{0LUT} \pm 0.1$ (LWIR)

Band average c_2

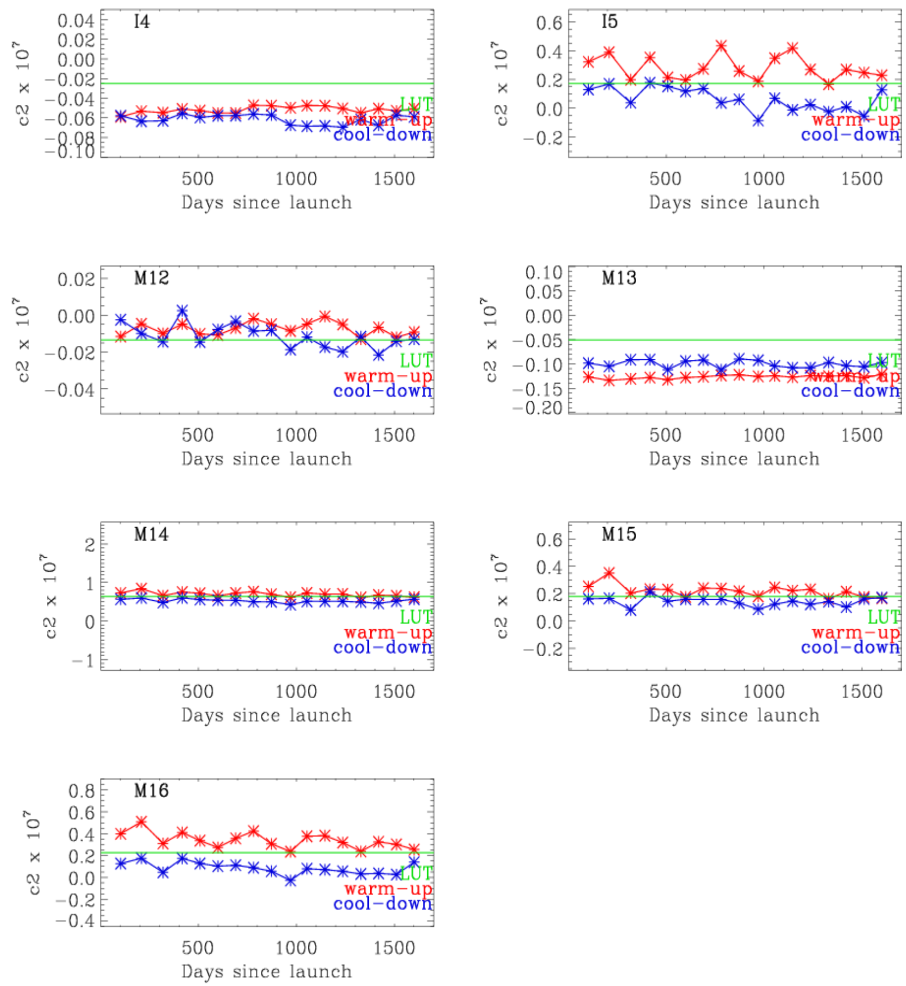

Y-range spans: $c_{2LUT} \pm 3 \times c_{2LUT}$

F-factors Orbital Variation Reduction

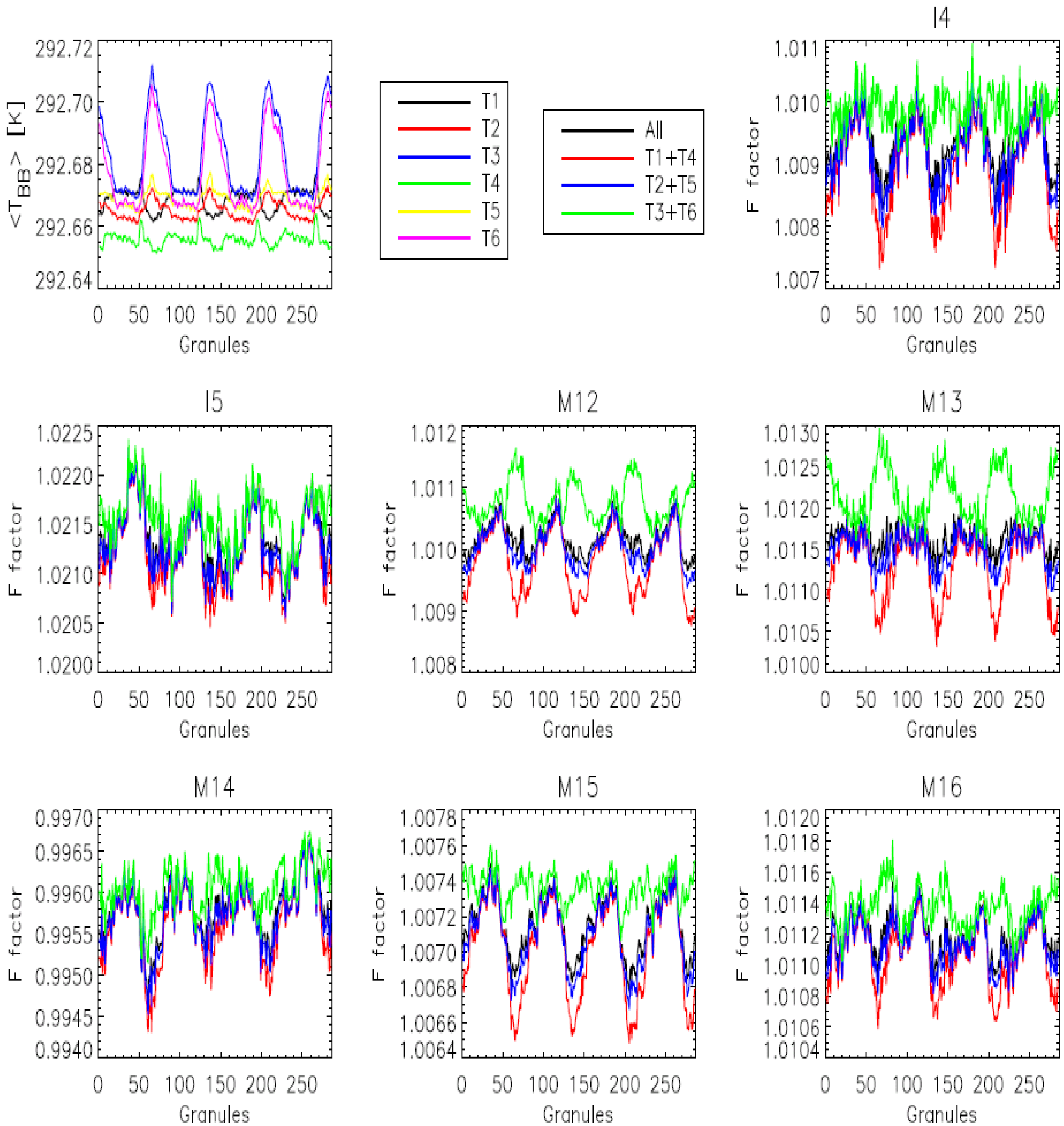

- F-factor orbital variations are present, on the order of ±0.05 – 0.1 %.
- Changing the BB thermistor weighting can reduce the F-factor orbital variations. Using T3 and T6 yield less variation for most bands (except M12 and M13).

- Improving the background model which would also reduce the F-factor orbital variations.

- F-factor shown for orbits 22854 – 22858 for HAM side A.

NASA L1B TEB Improvements

- NASA L1B TEB improvements not in IDPS
  - Moon in SV update
  - Unaggregated M13 output in separate products
  - All radiance now reported as scaled integer
- NASA L1B TEB improvements in progress
  - Update to M13 low gain calibration coefficients
  - Update BB thermistor weighting
  - Uncertainty index added to products
  - Flagging of spurious fires in band I4

Conclusions

- **S-NPP VIIRS on-orbit BB long-term (4+ years) performance is very stable. Short-term (orbital) temperature variations are present but within the uniformity requirement of 30 mK.**
- **Detector response (F-factor) trending is stable, with I5 showing maximum band-average trend of 1.4 % followed by M12 and I4. Small orbital variations are present (±0.0.5 – 0.1 %).**
- **No change is observed for TEB detector noise characteristics. NEdT at T_{TYP} is in compliance with the requirements.**
- **Improvements: Moon in SV, scaled integer, and unaggregated M13; uncertainty index, BB thermistor weighting, spurious I4 fire flagging, and M13 low gain calibration.**

Back Up

M13 LG Calibration

M13 low gain: No scan by scan F-factor correction

Prelaunch analysis differs between Government team (Aerospace and VCST) and sensor subcontractor – current LUT. Government team results are:

- $\mathbf{c_1 = 0.142}$ - 7 % higher than LUT value $\mathbf{c_{1LUT} = 0.132}$;
- $\mathbf{c_0 = 0}$ - inconsistent with $\mathbf{c_{0LUT} = 1.15}$

Proposal:

Update M13 low gain coefficients based on Government team pre-launch analysis, which is consistent with results from on-orbit calibration

On-orbit comparison of lunar images in M13 LG and M13 HG - supports Government team pre-launch results:

- $\mathbf{c_1 = 0.142}$; 7 % higher than c_{1LUT} - consistent with Gov. team pre-launch
- $\mathbf{c_0 = 0}$ consistent with Gov. team pre-launch

M13 LG c_{1LUT}, c_{0LUT}

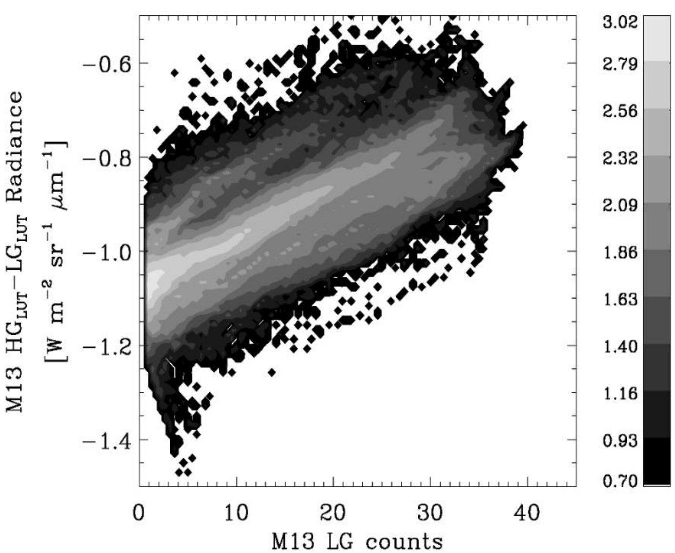

M13 LG c_1=0.142, c_0=0

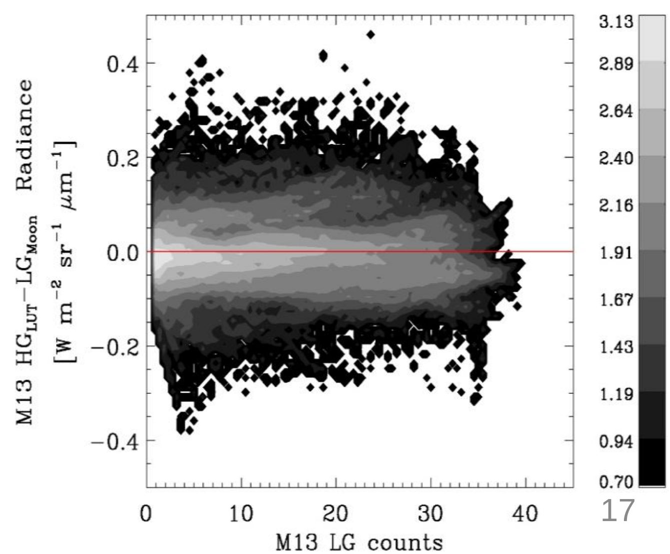

Effect of F-factor Noise

Evaluating the effect of using average F-factors

- The VCST VIIRS SDR code was modified to apply average F-factors instead of per-scan F-factors for TEB calibration.
- The F-factors for each band, detector, HAM side are averaged over 24 scans.
- Using average F-factors does not significantly impact the SDR product.
- Striping on the noise level affects SST products based on M15 and M16 brightness temperatures.

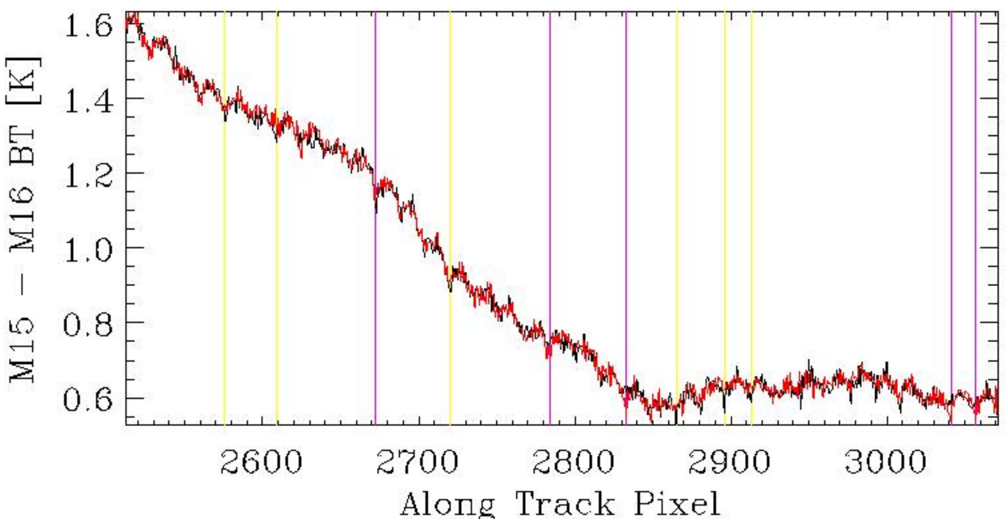

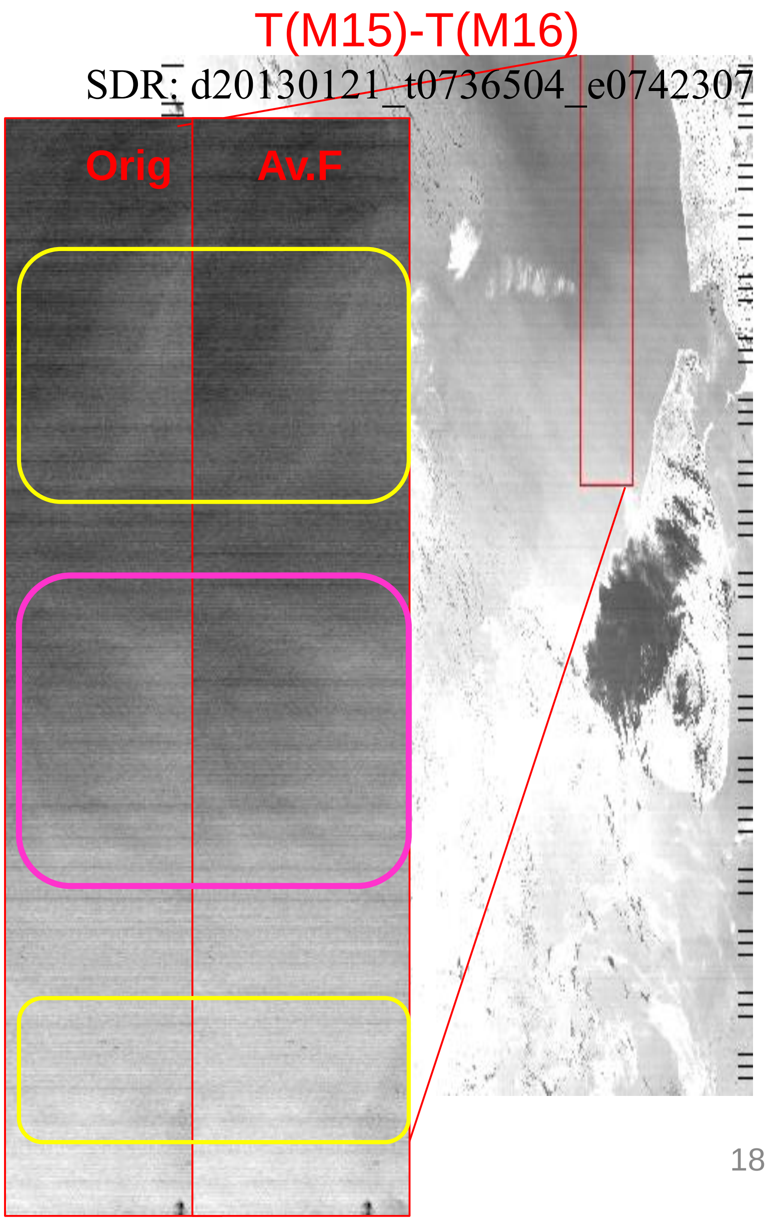

Short-term Stability- Individual Detectors

Orbits: 17553, 17554, 17555

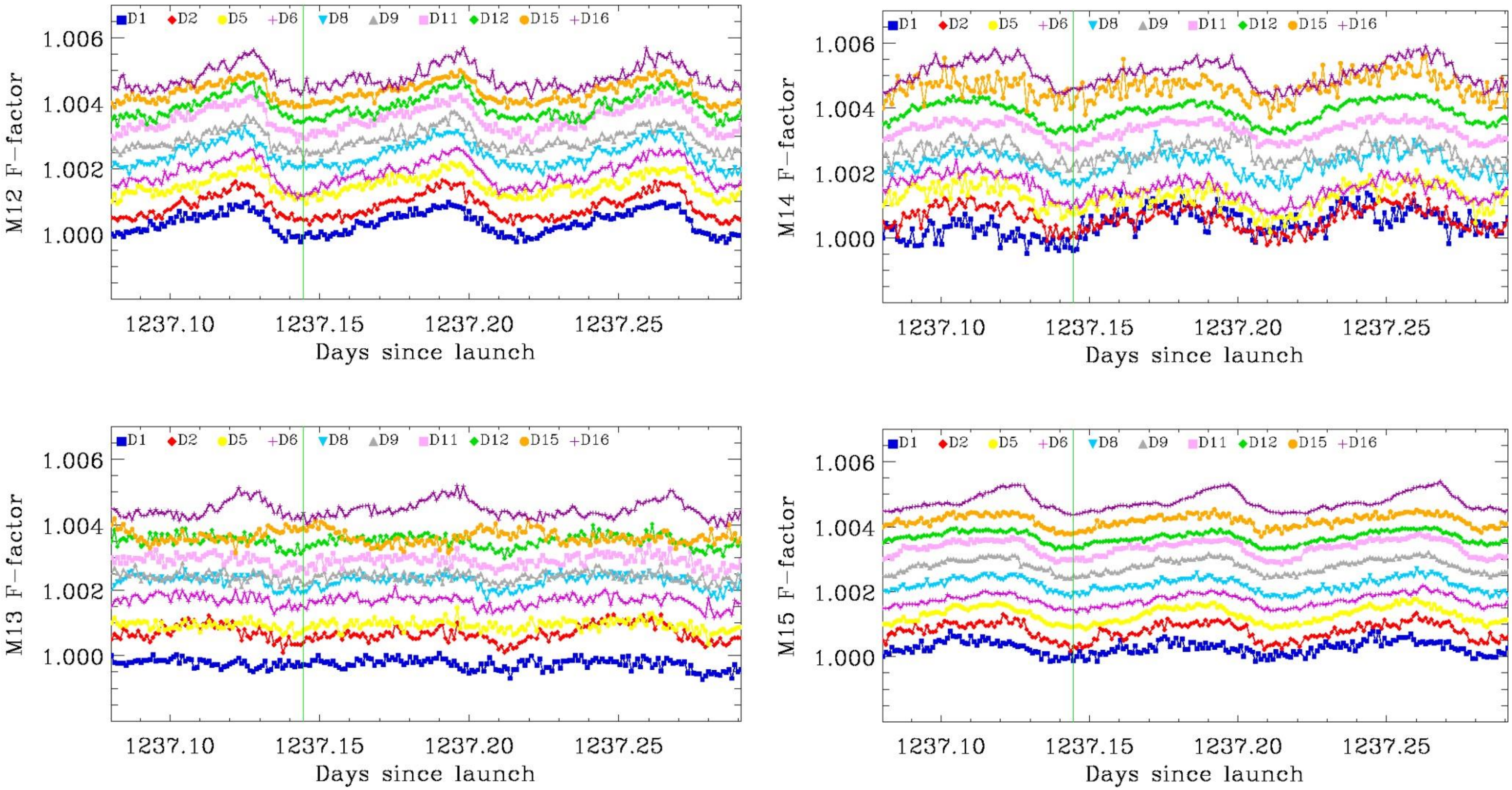

Granule average (HAM A)

M16 (not shown) similar to M15; same D16 our of family behavior

* For clarity the F-factors are shifted.

Dynamic Range Verification

Dynamic range verified using scheduled Lunar observations

- All detectors of all TEB bands meet the T_{MIN} (marginal non-compliance at I4) and T_{MAX} requirements
- For some detectors of some bands the radiance limits in the Radiance-to-Temperature LUT do not extend to the largest possible unsaturated radiance

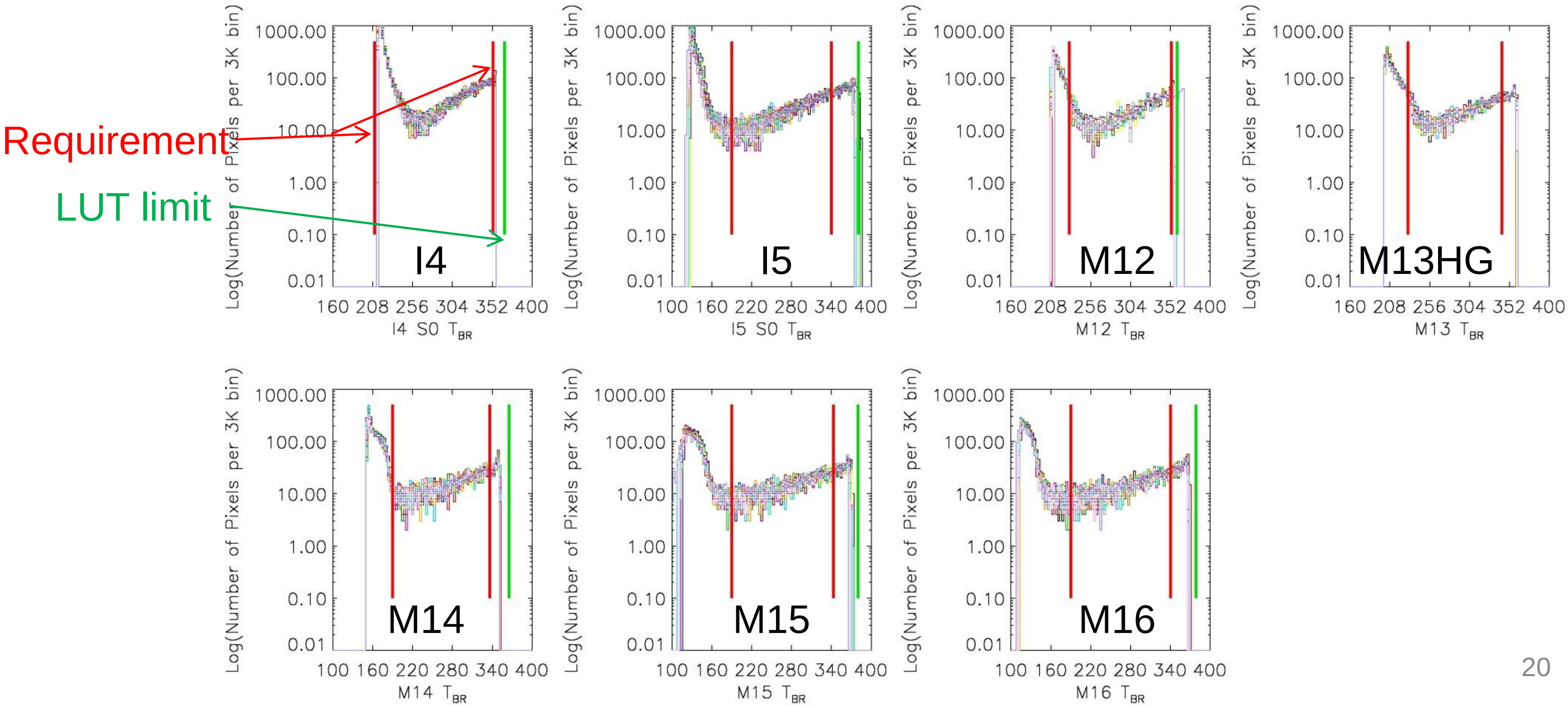

Detector Specific NEdT

- Detector specific NEdT is stable throughout the mission.

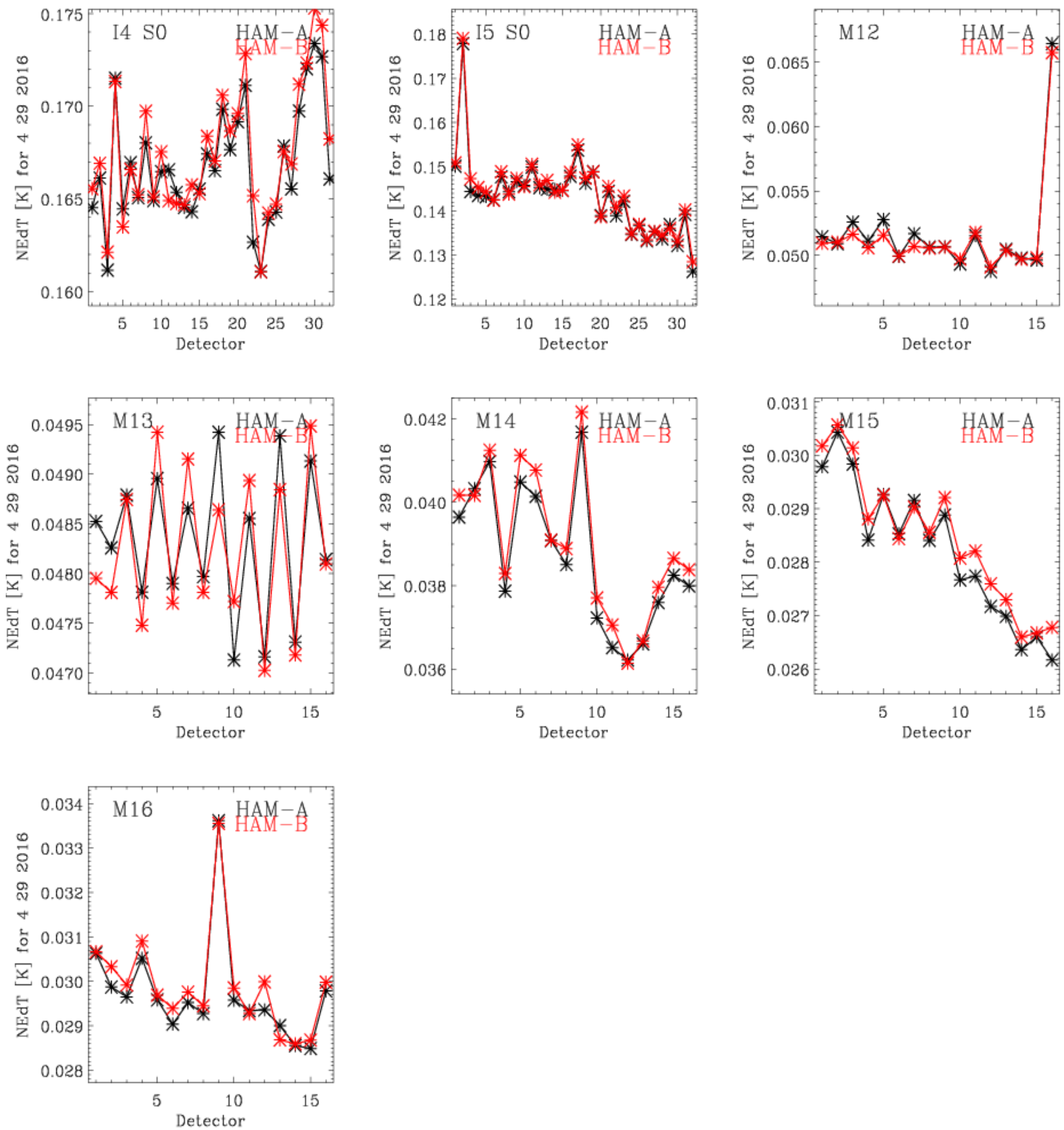

Warm-up Cool-down (WUCD) Cycles

WUCD cycles performed: Feb, May, Sep, Dec 2012; Mar, Jun, Sep, Dec 2013, Mar 2014

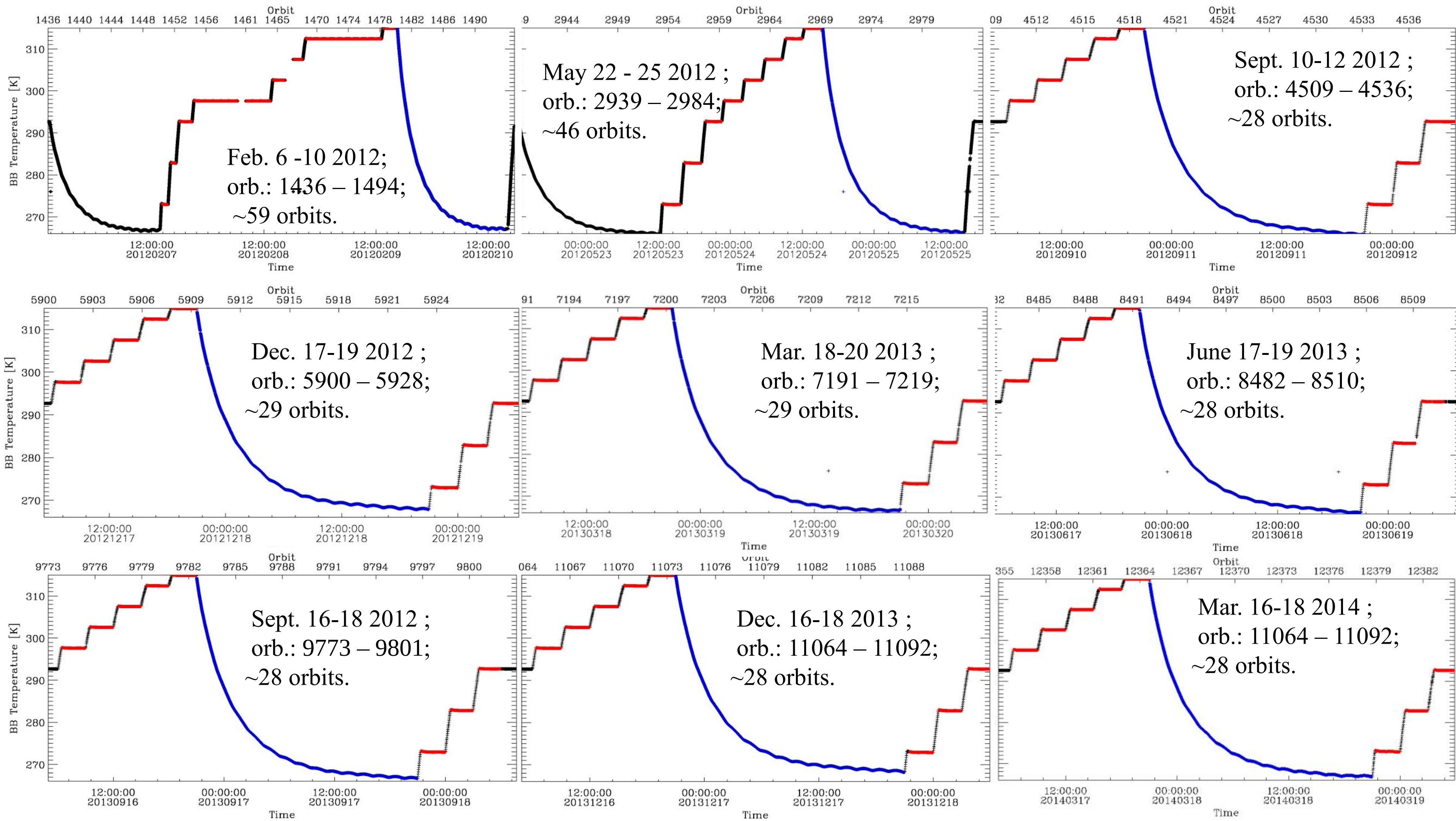

Warm-up Cool-down (WUCD) Cycles

WUCD cycles performed previously: Jun - Dec 2014, Mar - Dec 2015

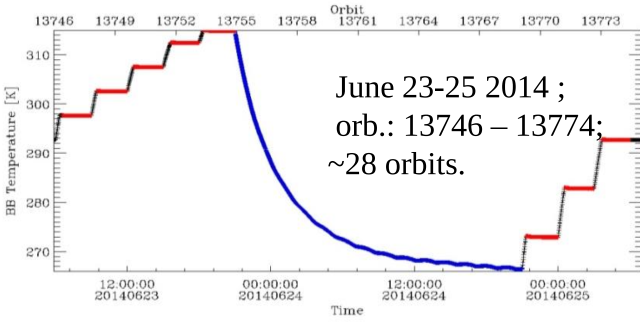

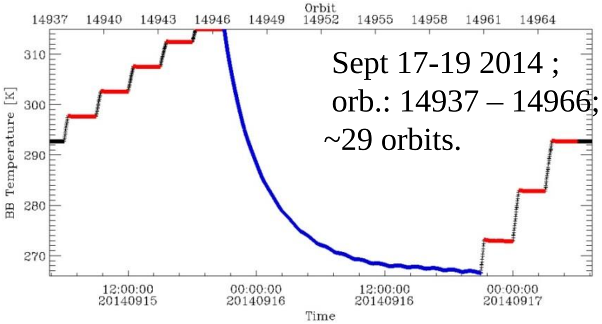

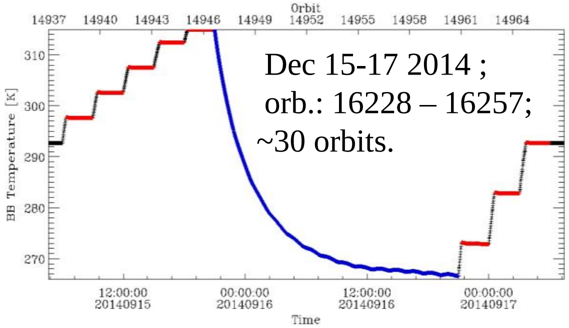

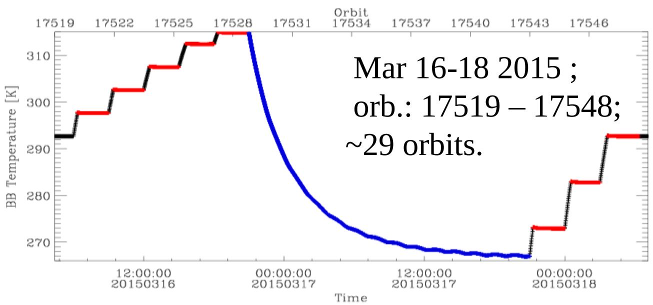

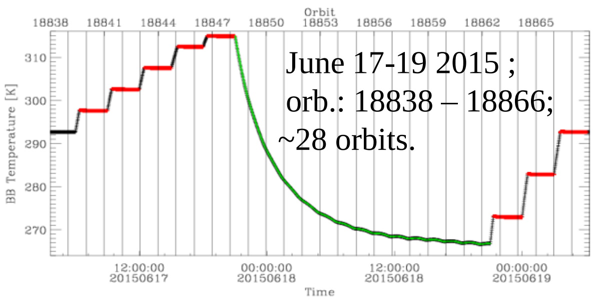

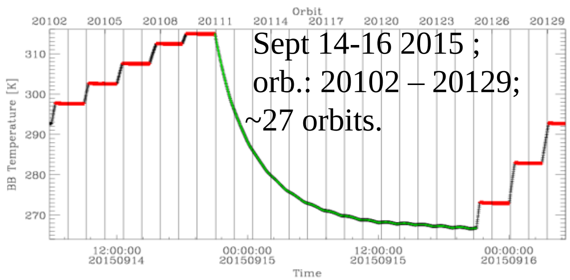

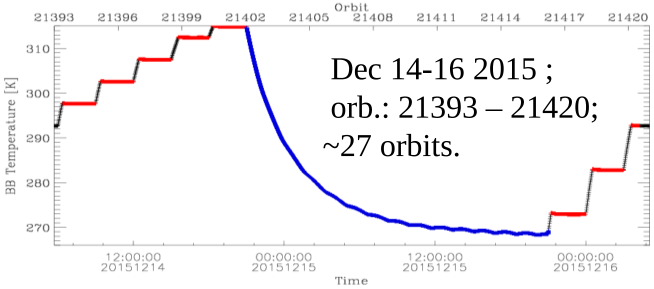

WUCD 14-16 Mar 2016 Data Selection

Warm-up:

- Orbits: 22684 – 22693; 22708 – 22711
- T_{BB} set to: 297.5K, 302.5K, 307.5K, 312.5K, 315.0K and 272.5K, 282.5K, 292.5K,
- The scans used are highlighted in red.

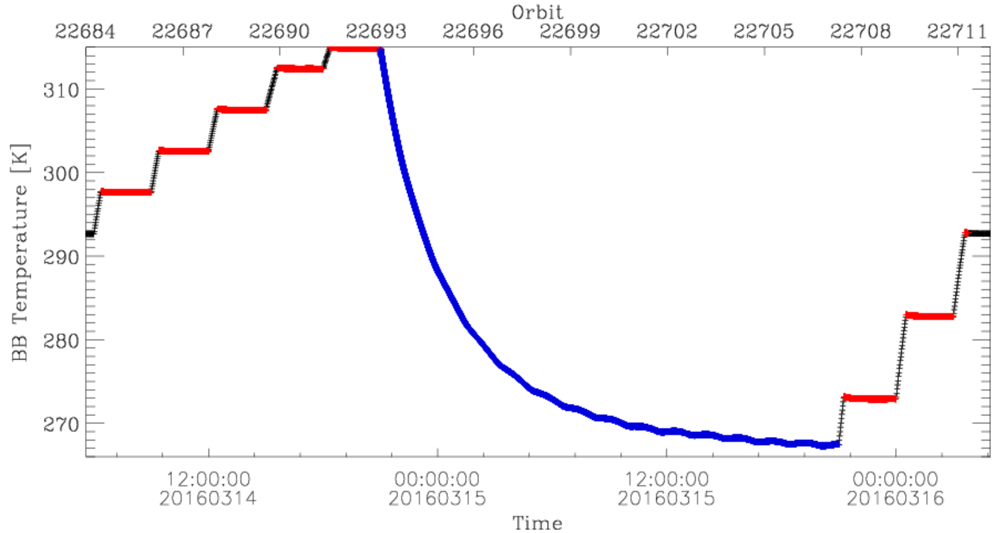

Cool-down:

- Orbits: 22693 – 22708.
- T_{BB} range: 266.9 K to 315K;
- The scans used are shown in blue.

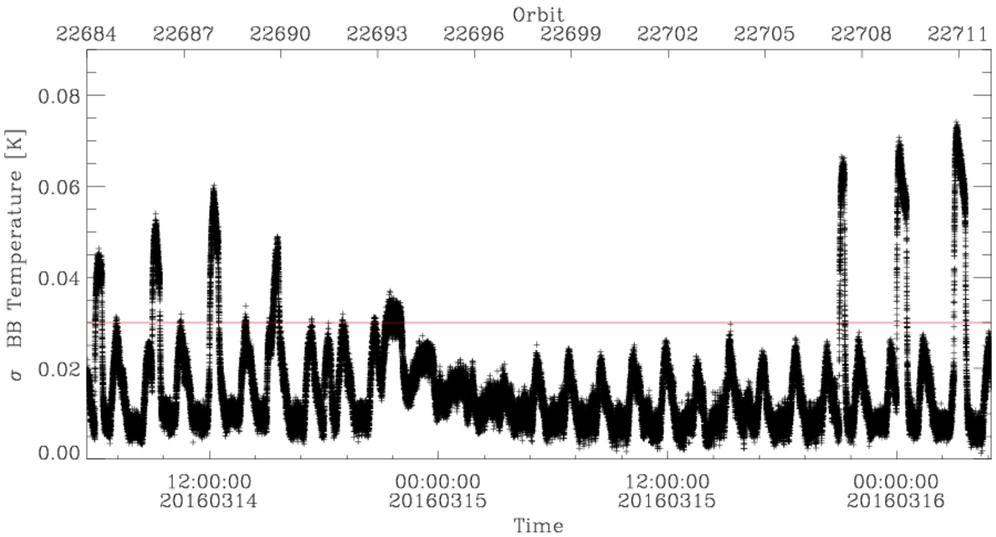

C_0 Coefficients

Band average c_0

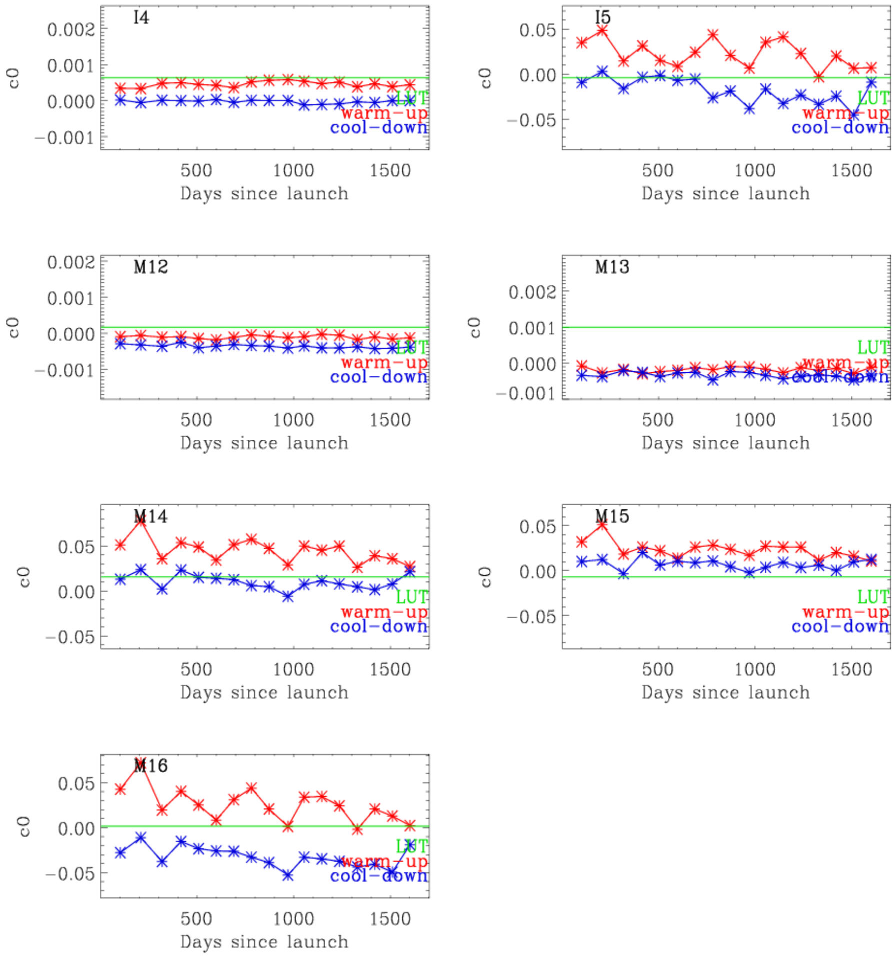

Detector specific c_0/c_{0LUT}

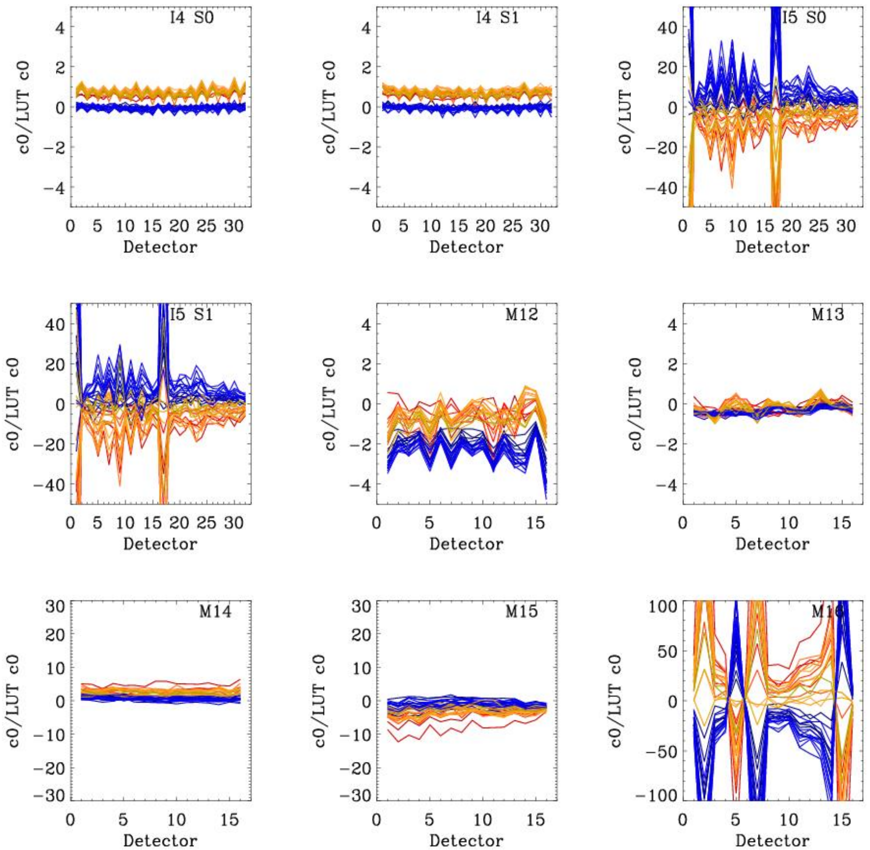

Y-range spans: $c_{0LUT} \pm 0.002$ (MWIR),
$c_{0LUT} \pm 0.1$ (LWIR)

C2 Coefficients

Band average c_2

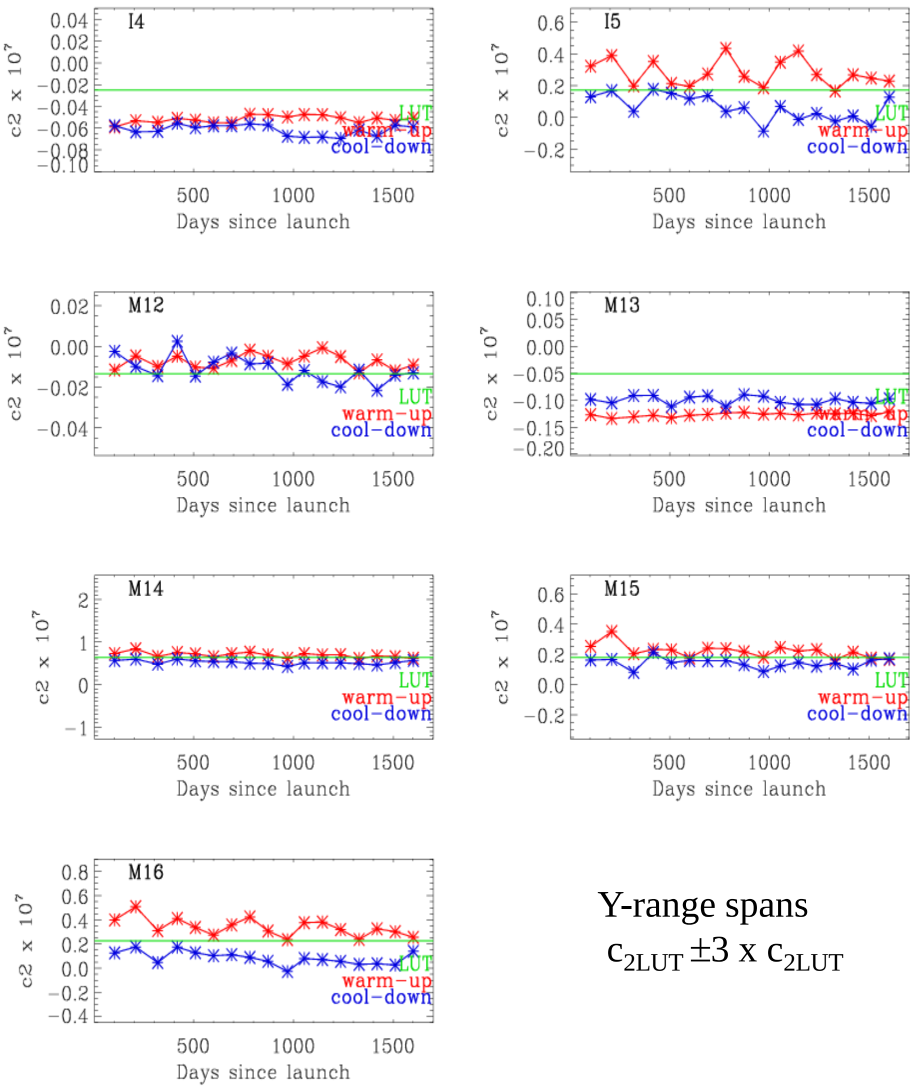

Y-range spans

$c_{2LUT} \pm 3 \times c_{2LUT}$

Detector specific c_2/c_{2LUT}

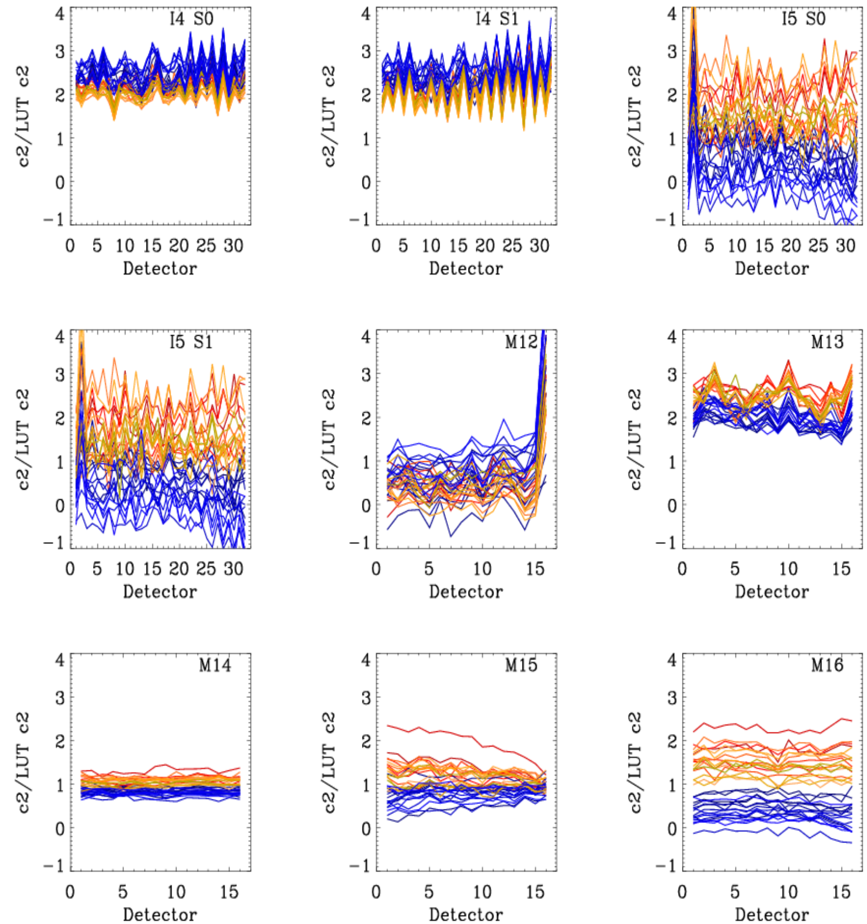

Calibration Coefficients – c1/LUT

Band average:$100^{*}\ (c1_{on\text{-}orbit} - c1_{LUT})/c1_{LUT}$:

	I4	I5	M12	M13	M14	M15	M16
WU 02/12 [%]	1.2	-0.8	0.4	1	-1.1	-0.2	-0.3
WU 05/12 [%]	1.2	-0.6	0.4	0.9	-1.7	-0.6	-0.8
WU 09/12 [%]	1.3	0.2	0.6	1.2	-0.8	0.2	0.5
WU 12/12 [%]	1.3	-0.2	0.6	1.2	-1.2	0.1	0.03
WU 03/13 [%]	1.4	0.4	0.6	1.2	-1.1	0.1	0.4
WU 06/13 [%]	1.4	0.6	0.7	1.2	-0.7	0.4	0.9
WU 09/13 [%]	1.5	0.3	0.7	1.2	-1.1	0.1	0.3
WU 12/13 [%]	1.4	-0.18	0.7	1.2	-1.2	0.1	0.05
WU 03/14 [%]	1.4	0.5	0.7	1.2	-1.0	0.2	0.7
WU 06/14 [%]	1.4	1.0	0.7	1.3	-0.5	0.4	1.2
WU 09/14 [%]	1.4	0.2	0.7	1.3	-1.1	0.1	0.3
WU 12/14 [%]	1.4	0.2	0.7	1.3	-0.8	0.2	0.4
WU 03/15 [%]	1.5	0.8	0.7	1.3	-1.0	0.1	0.6
WU 06/15 [%]	1.6	1.7	0.8	1.3	-0.3	0.6	1.5
WU 09/15 [%]	1.6	1.3	0.8	1.3	-0.5	0.6	1.2
WU 12/15 [%]	1.6	1.4	0.8	1.3	-0.7	0.4	0.9
WU 03/16 [%]	1.6	1.5	0.8	1.3	-0.6	0.5	1.1

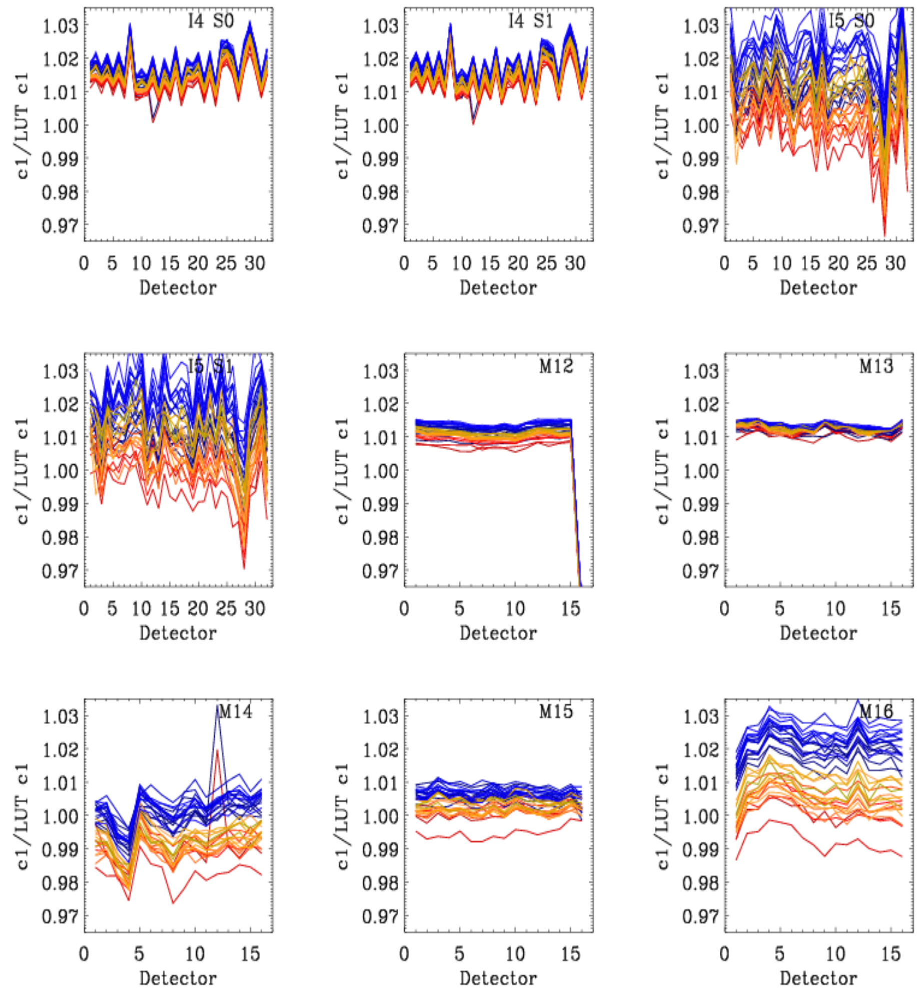

Calibration Coefficients – c1/LUT

Band average: $100^{*}\,(c1_{on\text{-}orbit} - c1_{LUT})/c1_{LUT}$:

	I4	I5	M12	M13	M14	M15	M16
CD 02/12 [%]	1.5	0.6	0.6	1.2	0.2	0.4	1.6
CD 05/12 [%]	1.6	0.5	0.7	1.3	-0.6	0.3	1.1
CD 09/12 [%]	1.6	1	0.8	1.7	0.3	0.9	2.2
CD 12/12 [%]	1.6	0.7	0.8	1.2	-0.2	0.3	1.6
CD 03/13 [%]	1.7	0.8	0.9	1.3	-0.1	0.6	1.8
CD 06/13 [%]	1.7	1.1	0.9	1.3	-0.01	0.5	2
CD 09/13 [%]	1.7	1.1	0.9	1.3	0.05	0.6	2
CD 12/13 [%]	1.7	1.7	0.9	1.4	0.4	0.6	2.2
CD 03/14 [%]	1.7	1.6	0.9	1.3	0.3	0.7	2.4
CD 06/14 [%]	1.8	2.3	1.0	1.3	0.6	0.9	2.8
CD 09/14 [%]	1.8	1.6	1.0	1.4	0.2	0.7	2.2
CD 12/14 [%]	1.8	2.3	1.0	1.4	0.3	0.7	2.4
CD 03/15 [%]	1.9	2.1	1.0	1.4	0.2	0.8	2.4
CD 06/15 [%]	1.9	2.4	1.0	1.3	0.3	0.7	2.5
CD 09/15 [%]	2.0	2.2	1.0	1.4	0.3	0.8	2.4
CD 12/15 [%]	1.9	2.8	1.1	1.4	0.2	0.6	2.4
CD 03/16 [%]	1.9	2.0	1.0	1.4	-0.2	0.5	1.9

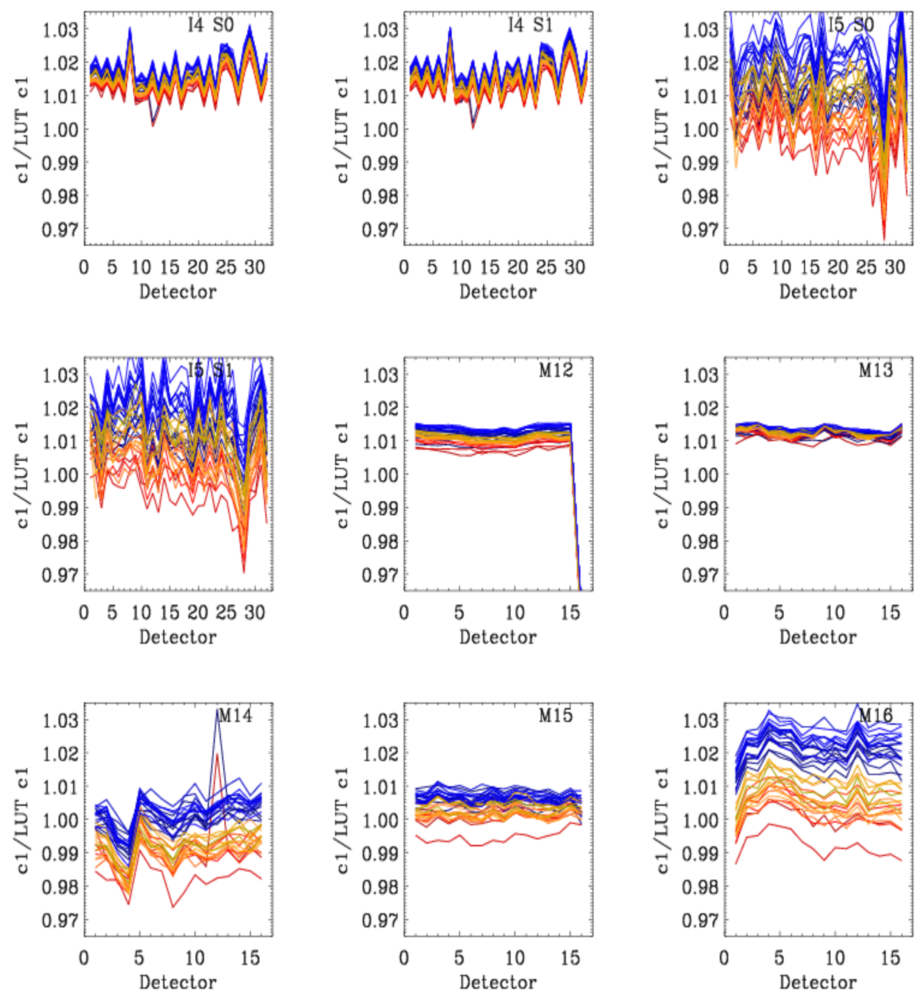

Uncertainty Estimates

- EV retrieved radiance uncertainty propagated using standard NIST formulation (k=1)

- Some uncertainty contributors determined pre-launch by the instrument vendor: RTA reflectance BB emissivity

- Radiometric coefficient and RVS uncertainties determined from NASA pre-launch analysis

- Uncertainties investigated for a range of input signal levels and scan angles

Total Uncertainty
- Radiometric coefficients
- Response
- RVS
- RTA reflectance
- BB emissivity
- Radiance (BB, SH, CAV, HAM, RTA)
- Reflectance factors off BB

Comparison to Requirement [K]

Uncertainty specifications

Defined in terms of %, at particular uniform scene temperatures, converted to K

Estimates exceed the specification at lower scene temperatures for bands M12 and M13

Band	267 K
I4 spec	0.91
I4 estimate	0.468
I5 spec	1.4
I5 estimate	0.226

Band	190 K	230 K	270 K	310 K	340 K
M12 spec	---	0.92	0.13	0.17	0.21
M12 estimate	---	1.11	0.13	0.07	0.09
M13 spec	---	0.85	0.14	0.19	0.23
M13 estimate	---	1.01	0.14	0.07	0.10
M14 spec	2.60	0.75	0.26	0.23	0.34
M14 estimate	0.95	0.26	0.12	0.12	0.20
M15 spec	0.56	0.24	0.22	0.28	0.34
M15 estimate	0.42	0.18	0.12	0.13	0.19
M16 spec	0.48	0.26	0.24	0.31	0.37
M16 estimate	0.35	0.16	0.12	0.14	0.19

Comparison to Requirement [%]

Uncertainty specifications

Defined in terms of %, at particular uniform scene temperatures

Estimates exceed the specification at lower scene temperatures for bands M12 and M13

Band	267 K
I4 spec	5.00
I4 estimate	2.55
I5 spec	2.50
I5 estimate	0.41

Band	190 K	230 K	270 K	310 K	340 K
M12 spec	---	7.00	0.70	0.70	0.70
M12 estimate	---	8.98	0.71	0.27	0.32
M13 spec	---	5.70	0.70	0.70	0.70
M13 estimate	---	7.50	0.69	0.26	0.31
M14 spec	12.30	2.40	0.60	0.40	0.50
M14 estimate	4.82	0.84	0.28	0.21	0.29
M15 spec	2.10	0.60	0.40	0.40	0.40
M15 estimate	1.59	0.47	0.22	0.19	0.22
M16 spec	1.60	0.60	0.40	0.40	0.40
M16 estimate	1.24	0.37	0.21	0.18	0.20

Uncertainty [K]

Uncertainty contributors:

- **Dominant for MWIR bands are the relative BB radiance uncertainty and the relative EV *dn* uncertainty (increasing rapidly with decreasing scene temperature).**
- **The LWIR bands uncertainties are dominated by the c_0, RVS, and EV *dn* relative uncertainties, which increase with decreasing scene temperatures.**

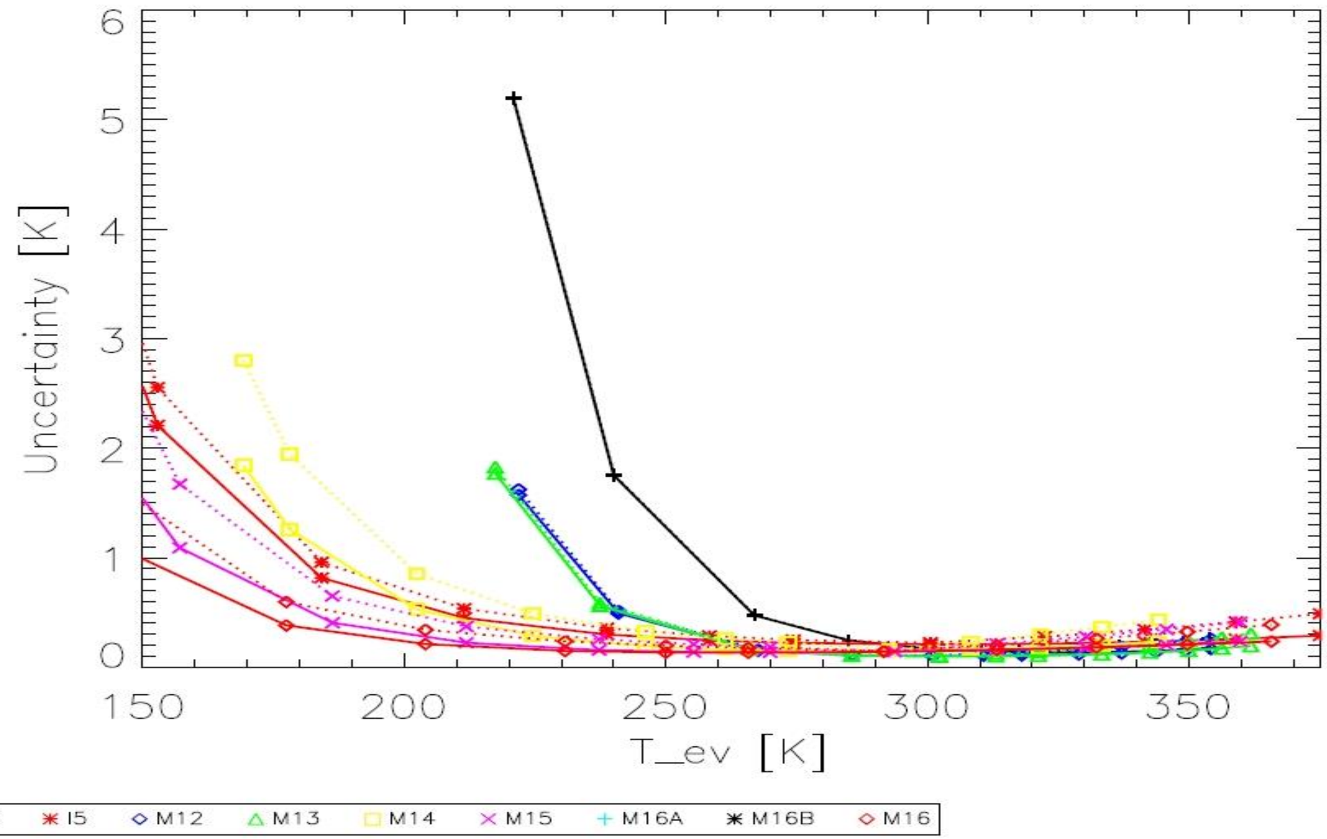

Uncertainty [K]

Uncertainty contributors:

- **Dominant for MWIR bands are the relative BB radiance uncertainty and the relative EV *dn* uncertainty (increasing rapidly with decreasing scene temperature).**
- **The LWIR bands uncertainties are dominated by the c_0, RVS, and EV *dn* relative uncertainties, which increase with decreasing scene temperature.**

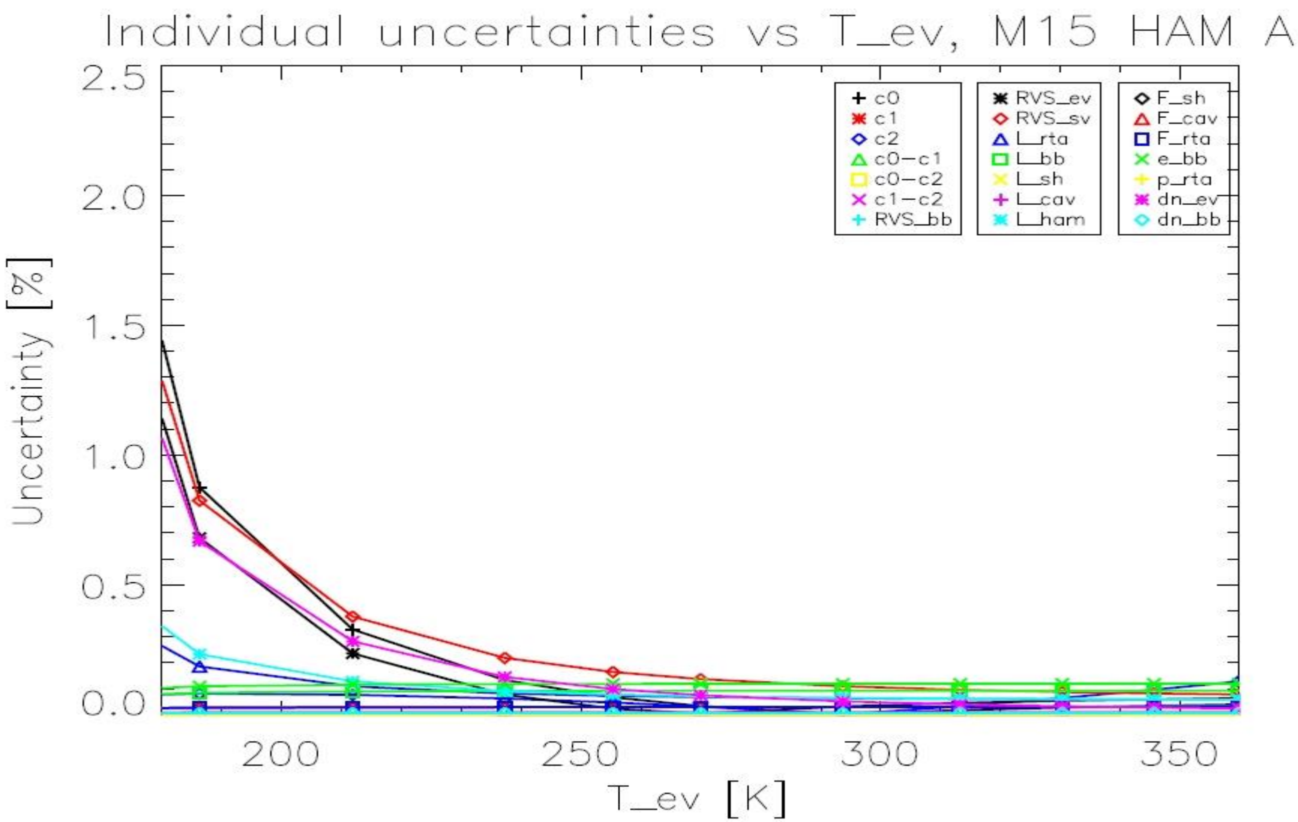

TEB Calibration when Moon in SV

- Currently for TEB, Fill values are assigned in EV SDR when the Moon is in the SV.
- Improved algorithm computes the mean and standard deviation of a 48-frame sample each scan. Then the outlier samples (Moon intrusion) with selected rejection scheme are identified and excluded from the SV average for background subtraction.

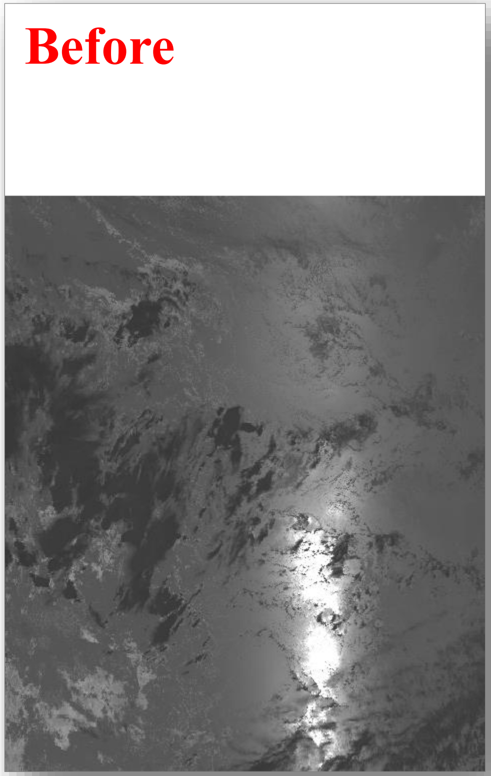

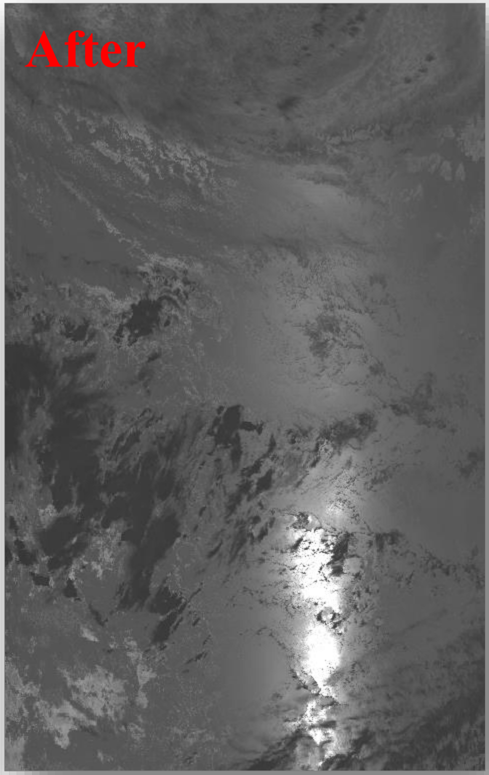

Images of calibrated radiance from 4 consecutive Band **M12** SDRs, generated with current SDR code (left) and modified (right) calibration algorithms (Data: Jan 22, 2013; Time 22:24:02). [Reference SPIE 2013, 8866-72]

VIIRS Special Calibration Topics: Calibration Stability Monitoring using the Moon and EV Sites

2016-06-06

VIIRS Characterization Support Team

Scheduled Lunar Calibration

- VIIRS lunar calibration has been scheduled on a nearly monthly basis.
- Lunar phases are designated within a range of [-51.5º, -50.5º].
- A satellite roll maneuver is usually necessary for VIIRS detectors to view the Moon through the SV port.

Number	M/D/Y	H:M:S	Roll Angle	Phase Angle	SEaVr Angle	Number	M/D/Y	H:M:S	Roll Angle	Phase Angle	SEaVr Angle
1	01/04/2012	08:48:53	-9.490	-55.41	35.9	23	06/09/2014	03:48:42	0.301*	-51.05	329.3
2	02/03/2012	04:21:32	-5.445	-56.19	41.3	24	10/04/2014	17:29:10	0.696	-50.81	302.2
3	02/03/2012	06:03:34	-5.279	-55.38	39.6	25	11/03/2014	01:07:35	-6.089	-50.53	304.8
4	04/02/2012	23:05:11	-3.989	-51.24	23.0	26	12/02/2014	08:41:44	-10.841	-50.83	322.7
5	05/02/2012	10:20:06	-3.228	-50.92	340.2	27	12/31/2014	19:38:07	-8.981	-50.73	24.2
6	05/31/2012	14:47:14	-0.081*	-52.97	53.5	28	01/30/2015	08:22:14	-5.674	-51.16	28.1
7	10/25/2012	06:58:15	-4.048	-51.02	309.0	29	03/01/2015	00:34:22	-4.048	-50.91	30.0
8	11/23/2012	21:18:20	-9.429	-50.74	326.6	30	03/30/2015	16:49:09	-5.236	-51.29	27.2
9	12/23/2012	15:00:50	-7.767	-50.90	24.0	31	04/29/2015	12:29:27	-4.701	-50.43	20.0
10	01/22/2013	12:13:35	-3.383	-50.81	28.1	32	05/29/2015	04:47:10	-2.304	-51.07	336.4
11	02/21/2013	09:31:25	-1.712	-50.71	28.8	33	06/27/2015	14:17:10	0.314	-54.43	322.5
12	03/23/2013	03:29:00	-3.320	-51.15	25.2	34	10/23/2015	19:02:24	-1.669	-51.27	302.4
13	04/21/2013	19:47:54	-3.882	-50.82	18.6	35	11/22/2015	04:20:25	-7.171	-50.77	313.0
14	05/21/2013	08:43:15	-0.809*	-50.67	335.7	36	12/21/2015	13:35:44	-8.176	-50.31	333.5
15	10/14/2013	21:39:19	-1.305	-50.95	305.6	37	01/19/2016	22:54:45	-5.302	-50.41	22.9
16	11/13/2013	06:57:41	-7.981	-50.66	314.9	38	02/18/2016	08:18:15	-3.331	-51.10	28.1
17	12/12/2013	19:35:46	-9.438	-50.39	334.3	39	03/18/2016	21:08:23	-2.860	-50.82	29.1
18	01/11/2014	09:59:45	-6.727	-51.30	25.9	40	04/17/2016	11:43:12	-3.634	-50.62	23.6
19	02/10/2014	05:34:12	-3.714	-51.03	29.0	41	05/17/2016	04:01:05	-2.640	-50.47	342.0
20	03/12/2014	01:11:43	-3.944	-51.05	28.4	42**	06/15/2016	18:36:12	0.230	-51.59	334.2
21	04/10/2014	20:53:17	-4.977	-50.60	22.2	*: No satellite roll maneuver when the predicted angle is within ±1 degree					
22	05/10/2014	13:13:00	-4.177	-50.91	338.6	**: Predicted lunar calibration events					

- Since 04/02/2012 calibration, the lunar images are read-out from the center of EV data sector by applying electric sector rotation.

Lunar Calibration Parameters

• Instrument parameters at the time of lunar calibration show various seasonal oscillation patterns.

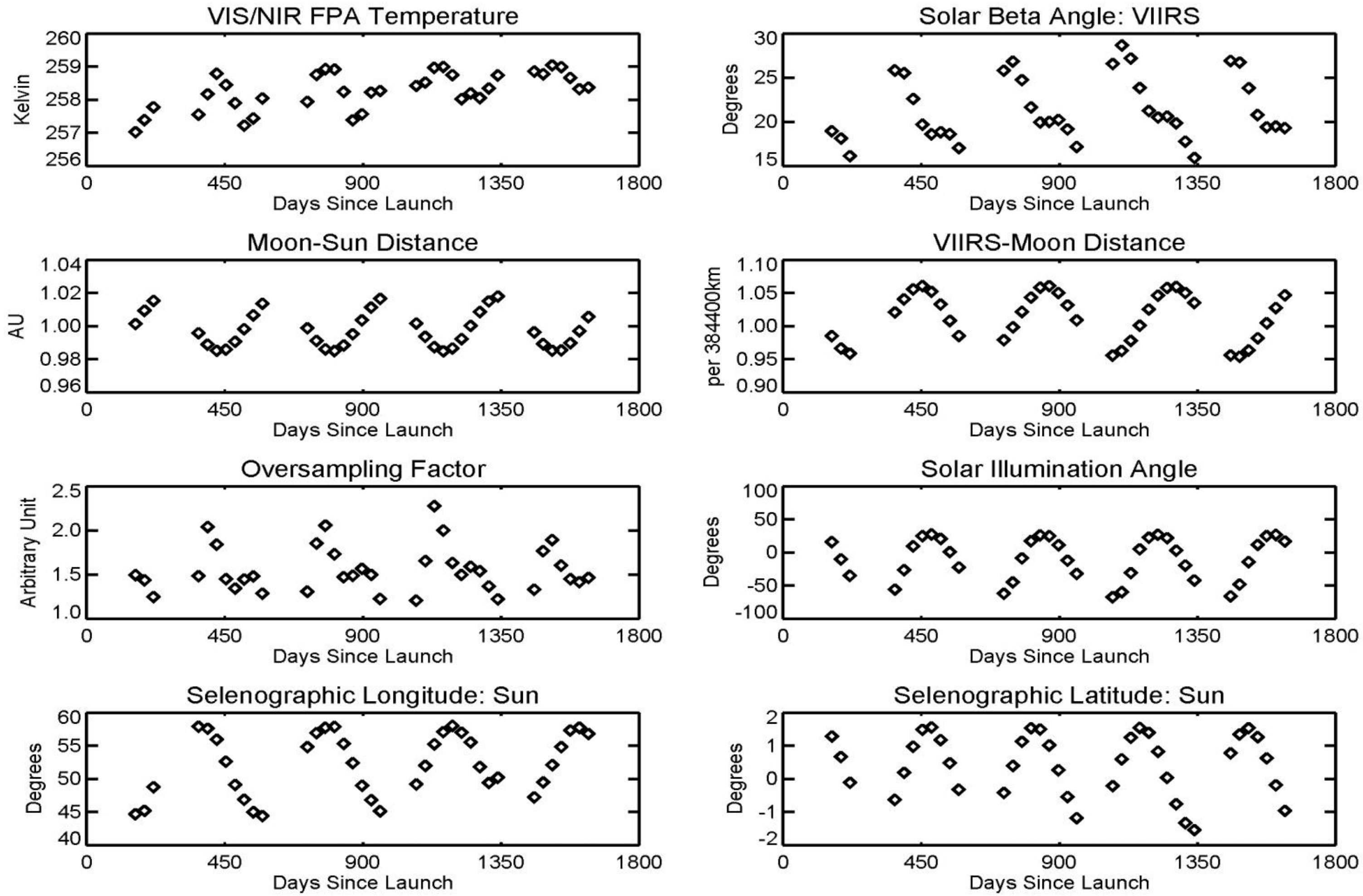

Radiometric Calibration Methodology

- Current lunar calibration methodologies were developed for MODIS and extended to VIIRS with adaptation.
- The Moon and SD are viewed at the same AOI (60.2º) for RTA HAM.
- The lunar F-factor is defined similarly to SD F-factor.

$$F_{MOON} = \frac{I_{ROLO}}{I_{MOON,PL}} = \frac{I_{ROLO}}{\sum L_{MOON,PL} \cdot \Omega_{\mathrm{B}}}$$

- I_{ROLO}: the USGS ROLO model predicted lunar irradiance calculated by Tom Stone*. VCST provides input photometric parameters and the VIIRS detector (prelaunch and RTA degradation modulated) RSRs.

- $I_{MOON,PL}/L_{MOON,PL}$: the lunar irradiance/radiance of individual pixels retrieved with the pre-launch gain coefficient c_0, c_1 and c_2.

$$L_{MOON,PL} = (c_0 + c_1 \cdot dn_{MOON} + c_2 \cdot dn^2_{MOON}) / RVS_{SV}$$

- The $I_{MOON,PL}$ summation is performed over samples and detectors for those center scans (marked in the plot) with “complete” lunar images.

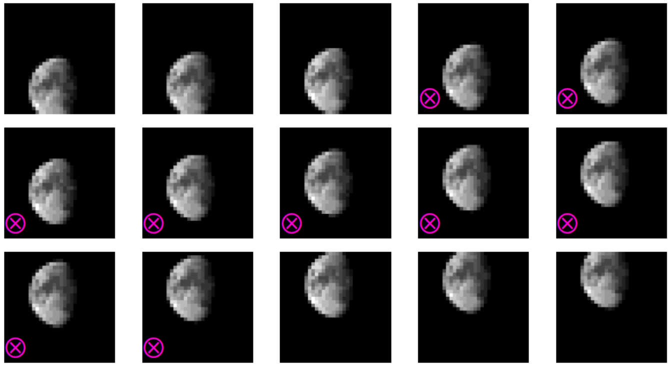

* *H. H. Kieffer and T. C. Stone, “The spectral irradiance of the Moon”, Astronom. J., vol. 129, pp. 2887-2901, 2005.*

Lunar/SD Calibration Comparison

Land PEATE SD F-factor

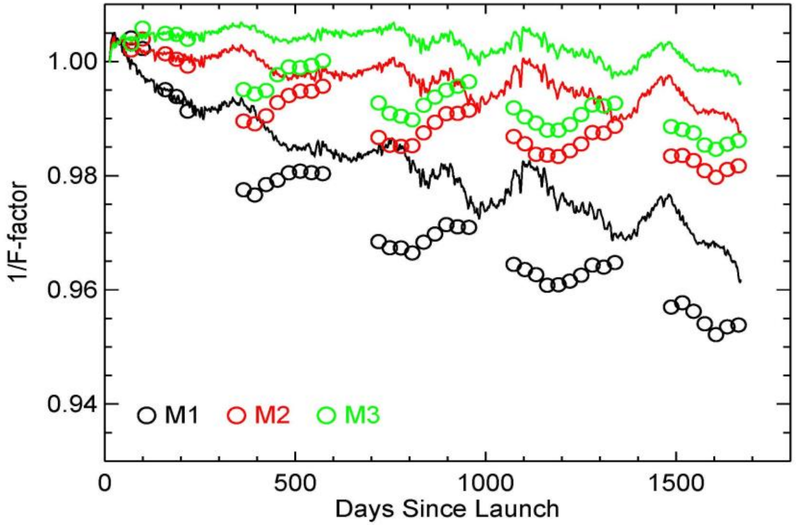

L1B SD F-factor

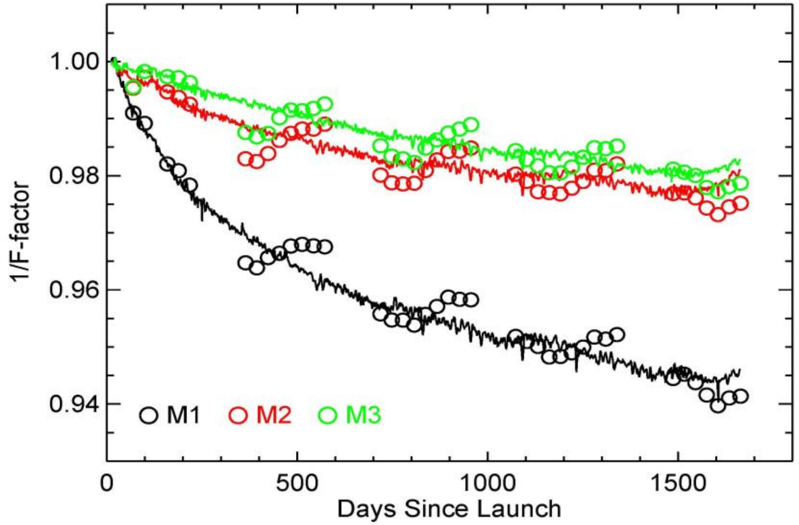

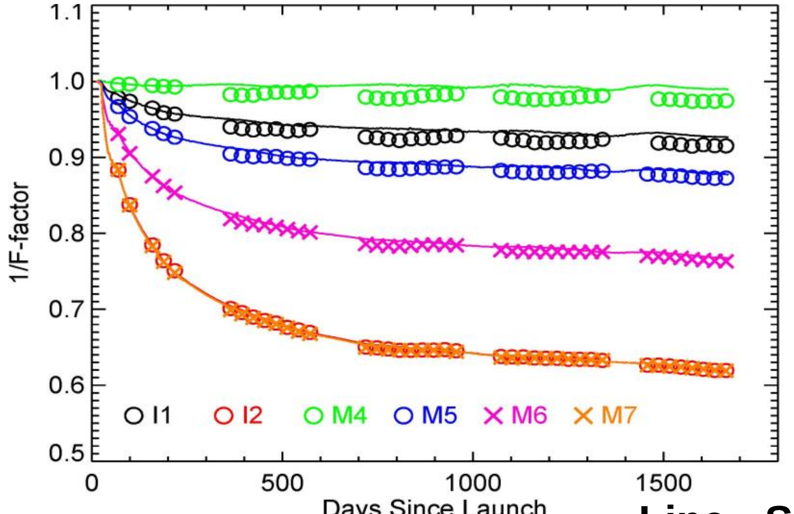

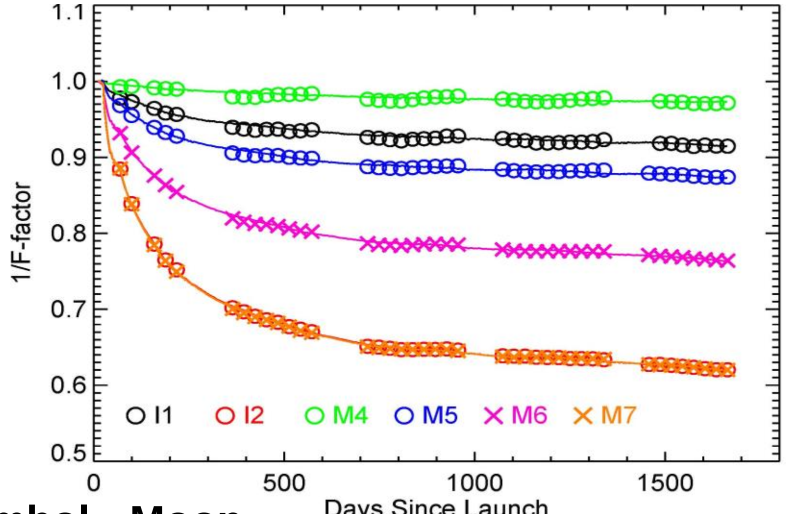

Line - SD Symbol - Moon

Lunar/SD Calibration Comparison

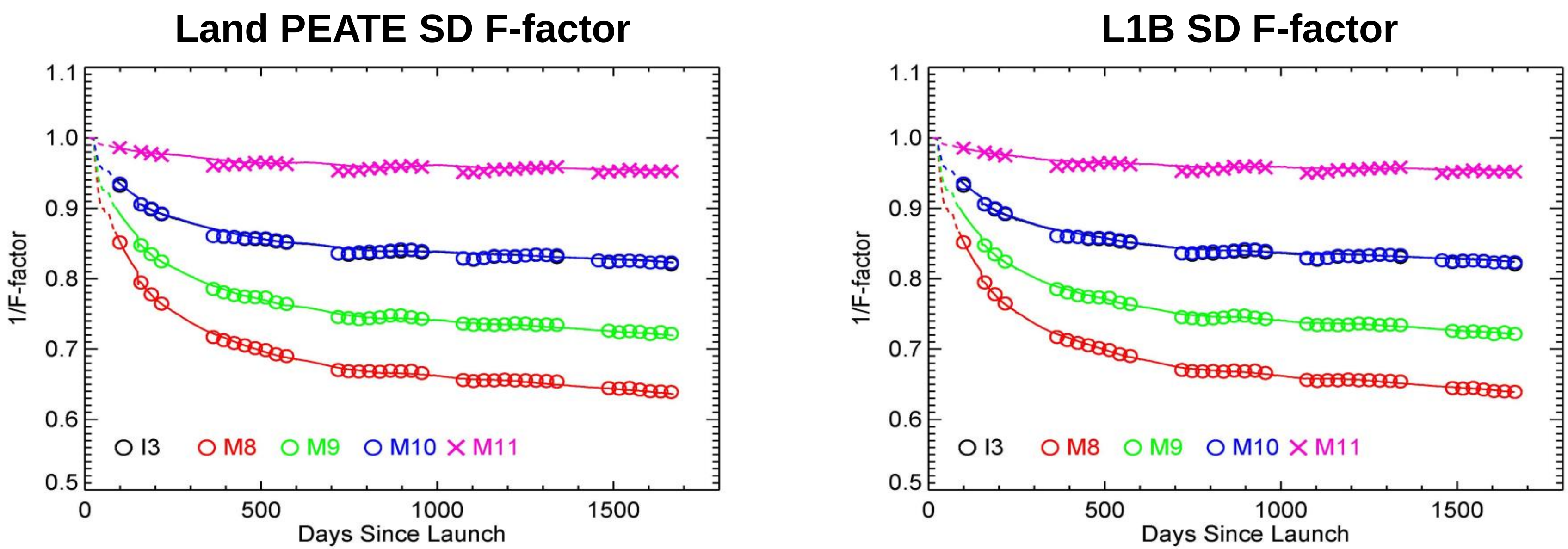

- The detector gain changes tracked by SD and Moon overall agree.
- SD F-factor calibrated per orbit is used for LUT to produce SDR/L1B.
- There are band-dependent drifts between SD and lunar data trends.
- The SD F-factor used for L1B v1 is adjusted based on lunar F-factor.
- The oscillation of lunar data is tied to lunar irradiance reference.
- To accurately determine the drift and apply the adjustment, the oscillation in lunar F-factor trending needs to be mitigated.

Detector Gain Difference

- Lunar F-factors can also be calculated on a detector basis to characterize the detector gain difference within a band.

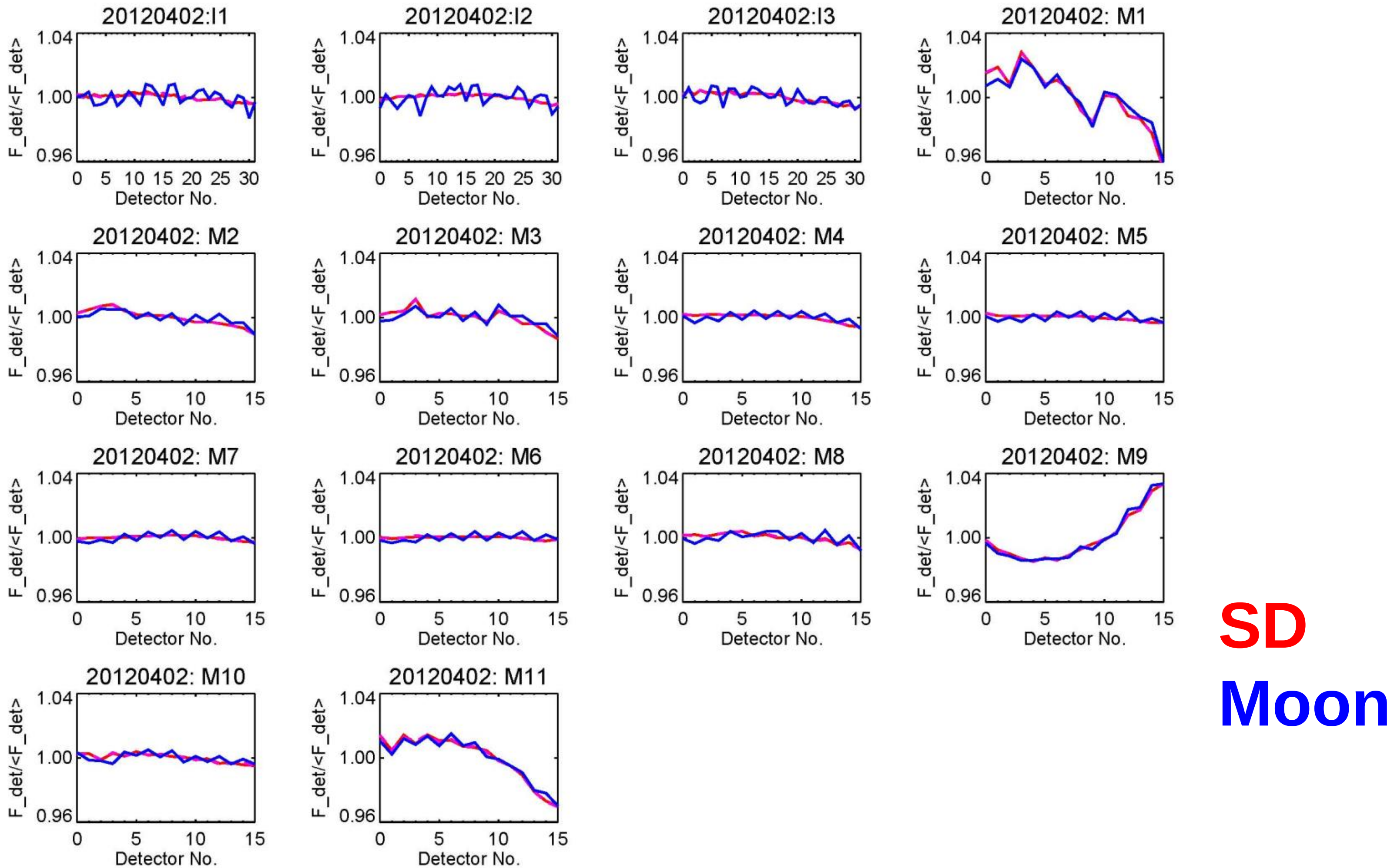

Detector Gain Difference

- The detector gain differences derived from Moon and SD overall agree with noticeable temporal drifts for some bands.

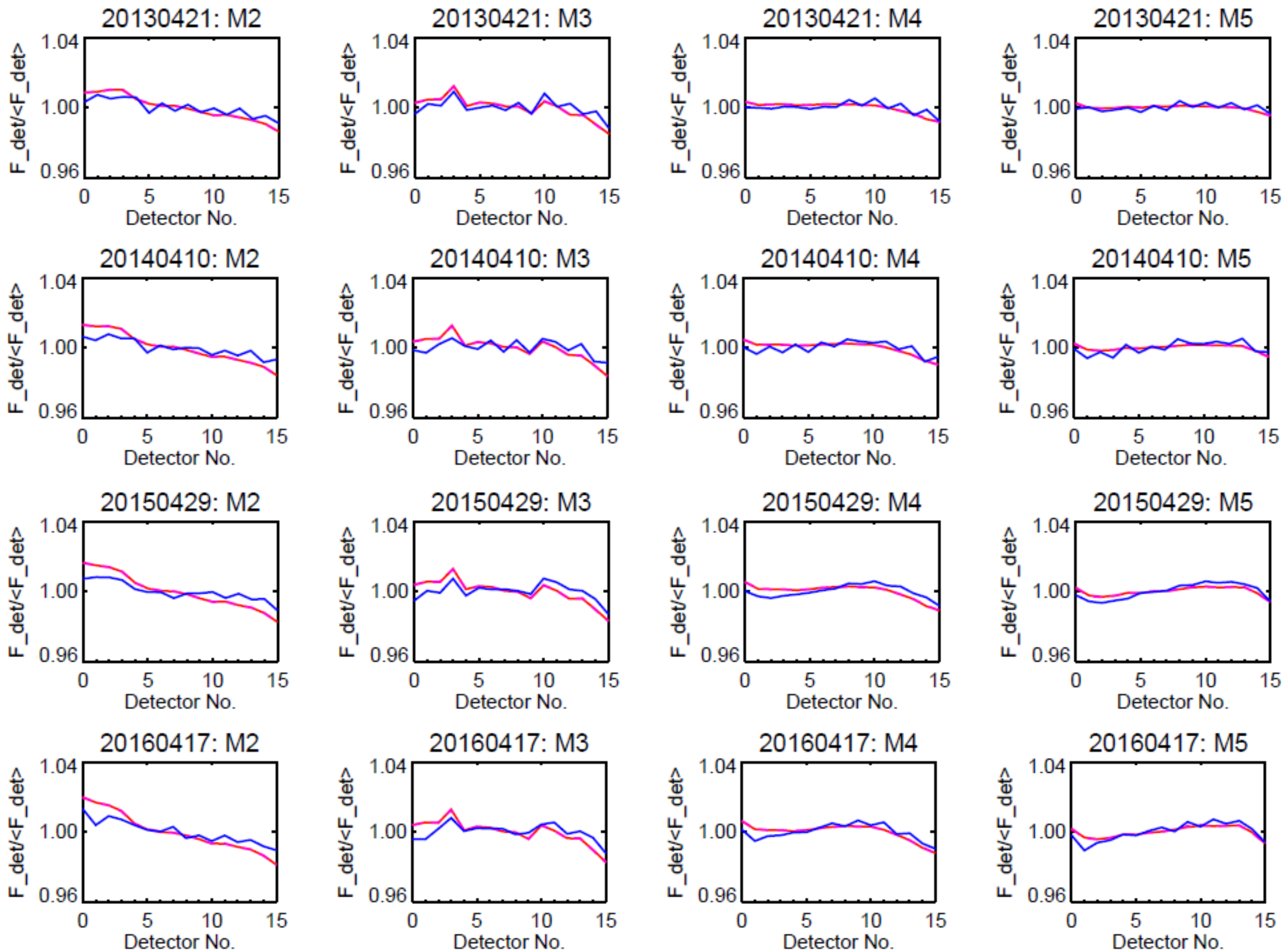

SD

Moon

Lunar DNB LGS Calibration

- The DNB LGS can be calibrated similarly to other RSBs.
- The DNB lunar images are composed of pixels at high-gain stage. (HGS) and mid-gain stage (MGS), and low-gain stage (LGS).
- Gain ratio LUTs are used to convert *dn* among different gain stages.
- Dark offset LUTs are used to correct the background.
- The RSR change has more impact to DNB F-factor than other RSBs.
- The impacts to SD and lunar calibrations are different.

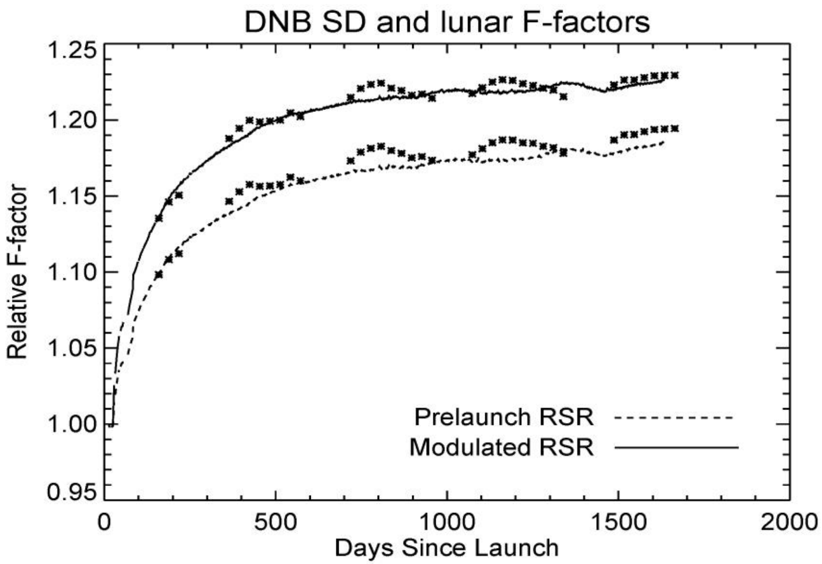

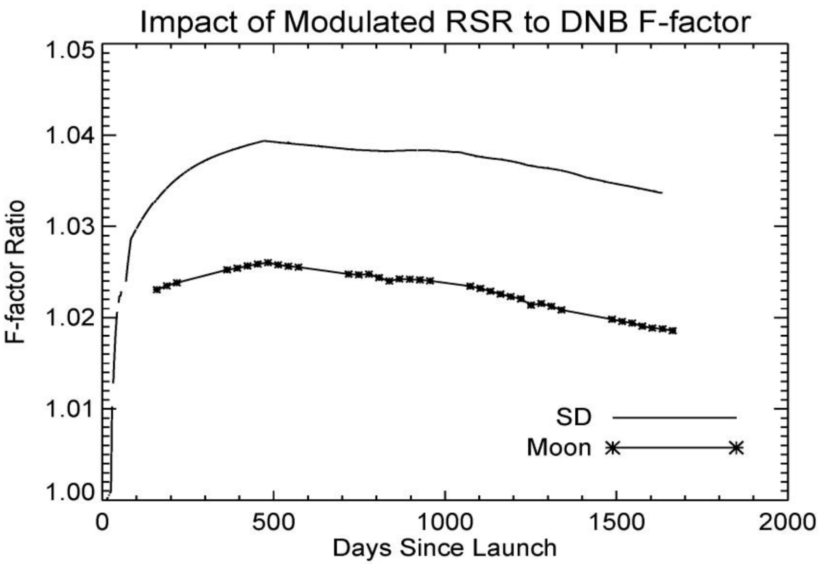

Unscheduled Lunar Observations

- Moon can be viewed without satellite roll maneuver.
- Lunar Images are read-out from SV data sector and are not co-registered in the along-scan direction.
- Till May 2016, 165 lunar observations have been made. 126 of them with 2+ bands capturing unclipped Moon

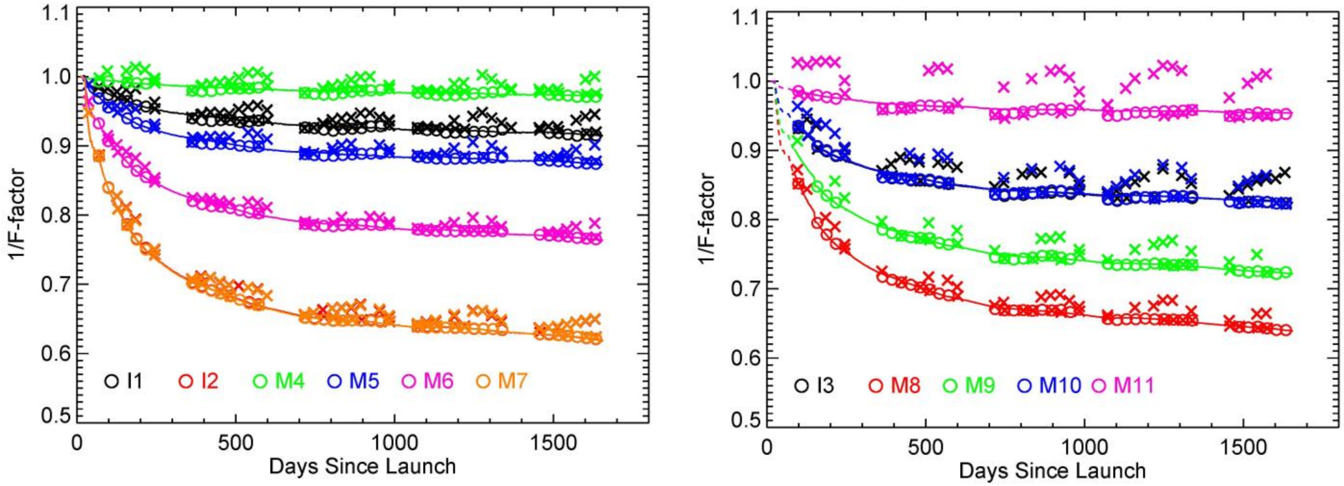

- Lunar phases vary significantly between -95º and -35º.
- Lunar irradiance reference introduces mostly phase and libration angles dependent bias.
- Empirical approach can be used to correct lunar data.

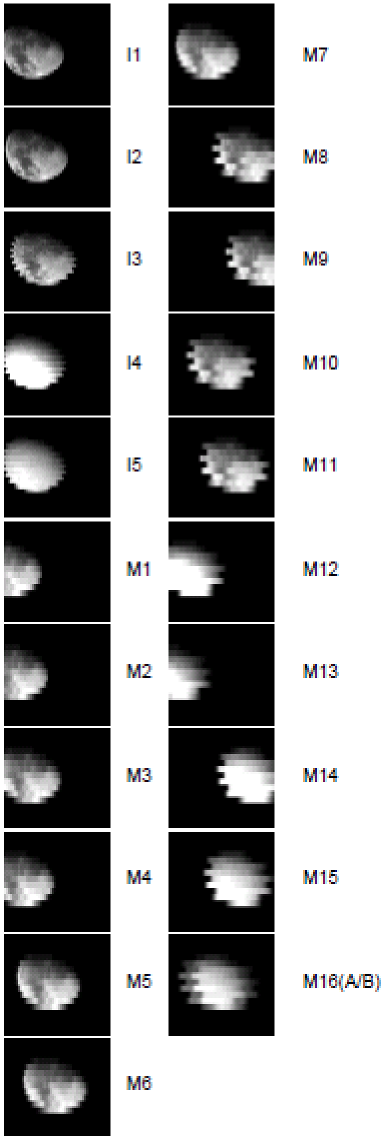

EV Trending

- Earth View (EV) targets can be used to track RSB calibration stability.
- Use NASA Land PEATE reflectance time series from 2012 to 2016.
- The widely used pseudo-invariant sites Libya-4 desert.
- A semi-empirical bi-directional reflectance function (BRDF) consisting of two kernel-driven components (f_1 and f_2):

$$\mathrm{BRDF}\ (\theta,\psi,\varphi) = K_0 + K_1\, f_1(\theta,\psi,\varphi) + K_2\, f_2(\theta,\psi,\varphi)$$

θ, ψ, φ - solar zenith, view zenith and relative azimuth angle

K_0, K_1 and K_2 – site-dependent coefficients

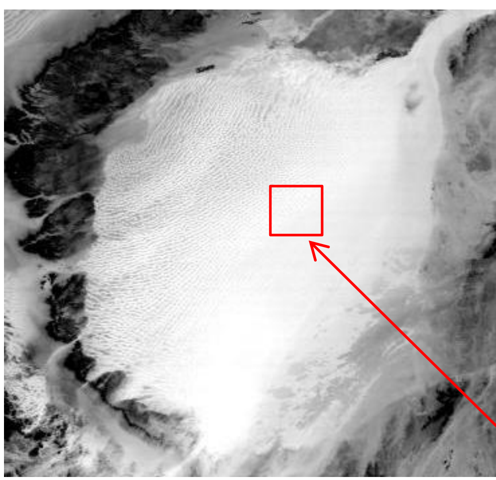

- Good radiometric stability.
- Repeatable orbits every 16 days maintain constant viewing angles.
- Surface measurement and atmospheric correction are needed to conduct absolute calibration.

20 x 20 km

Libya-4 Reflectance Trending

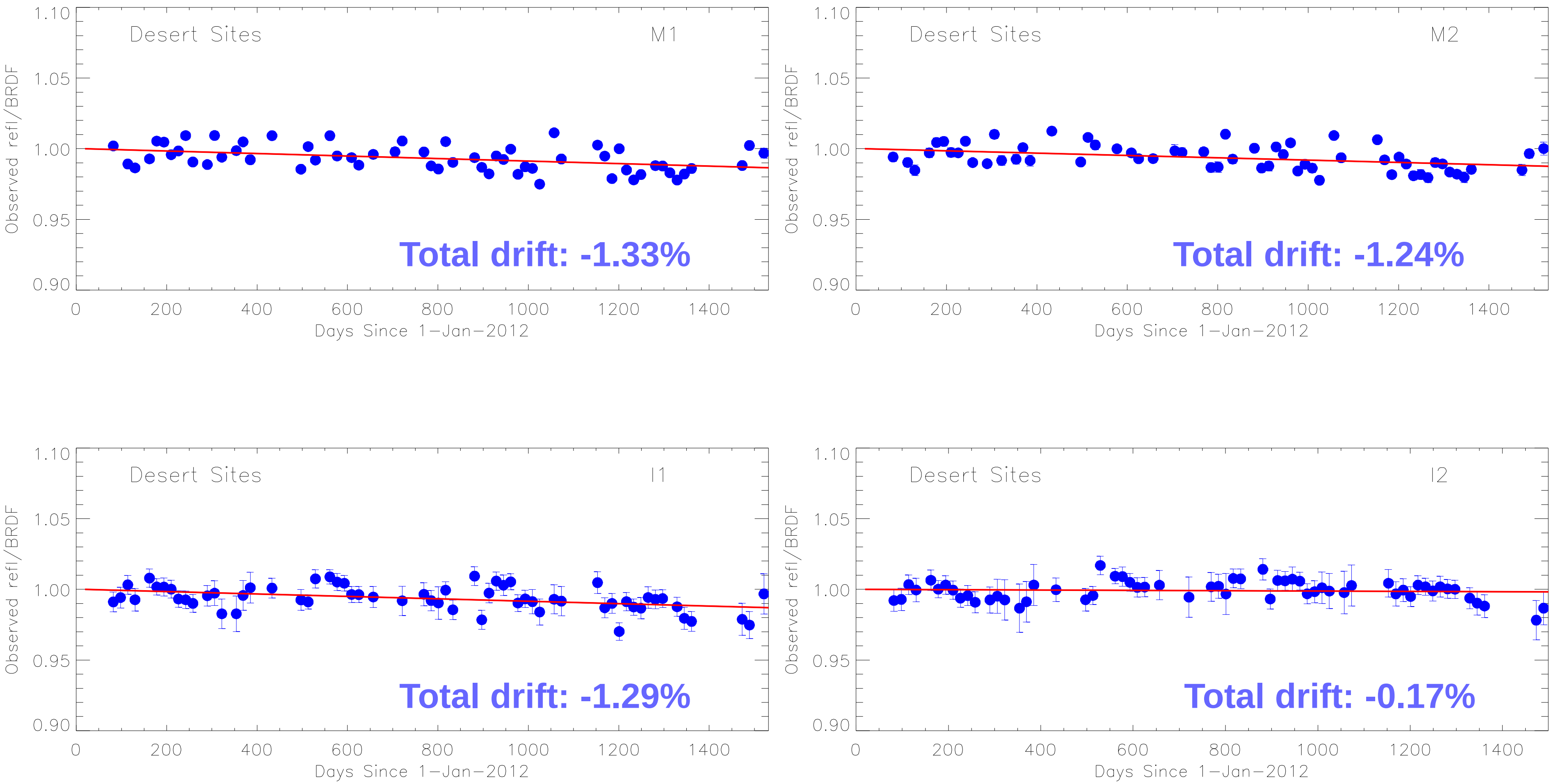

* VIIRS reflectance normalized by its site-dependent BRDF

Libya-4 Reflectance Trending

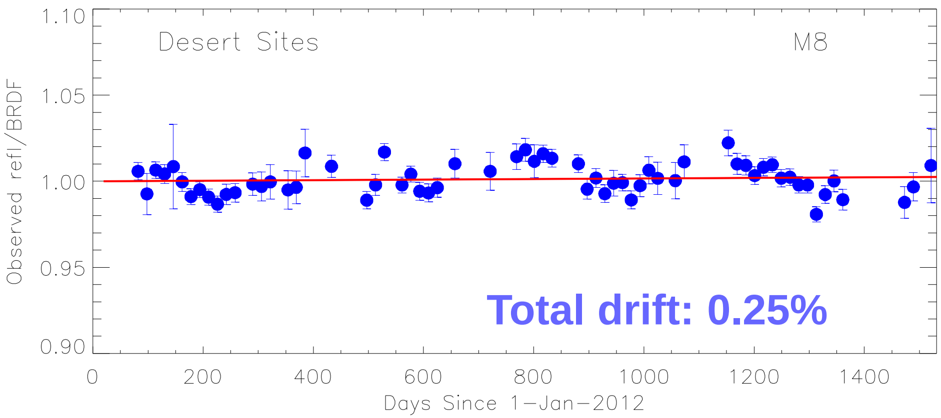

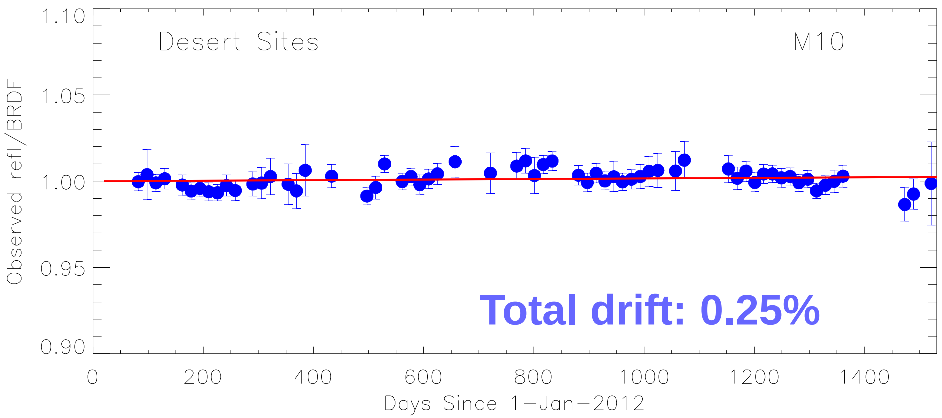

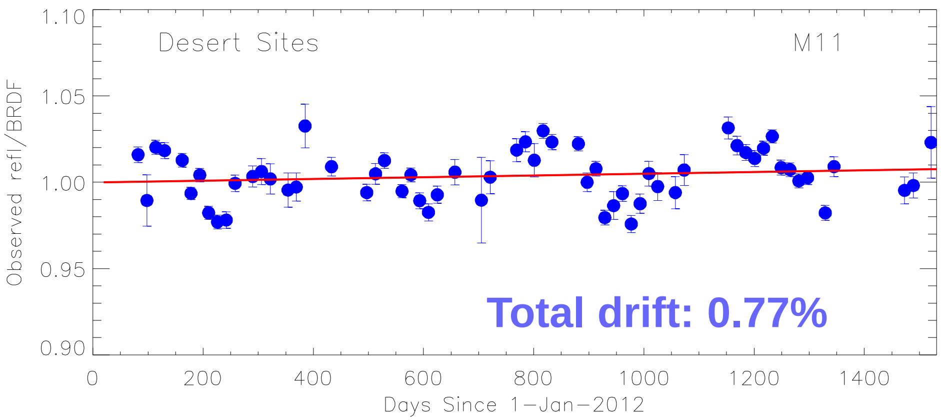

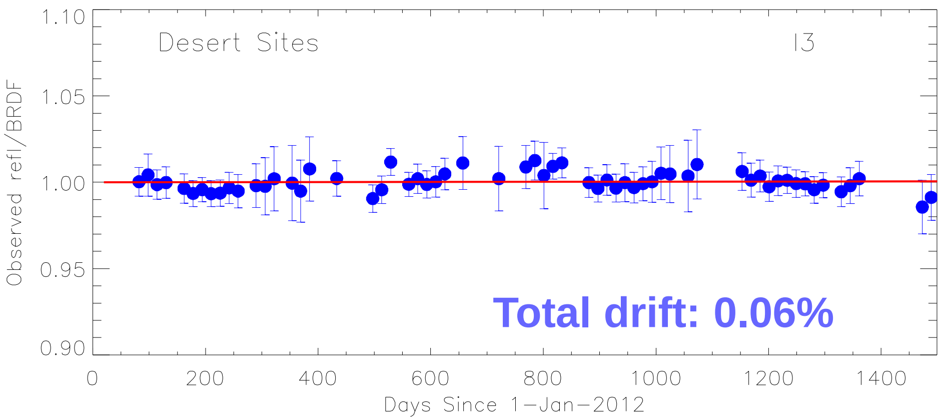

The trending is based on Land PEATE C1.1 data.

Libya-4 Reflectance Trending

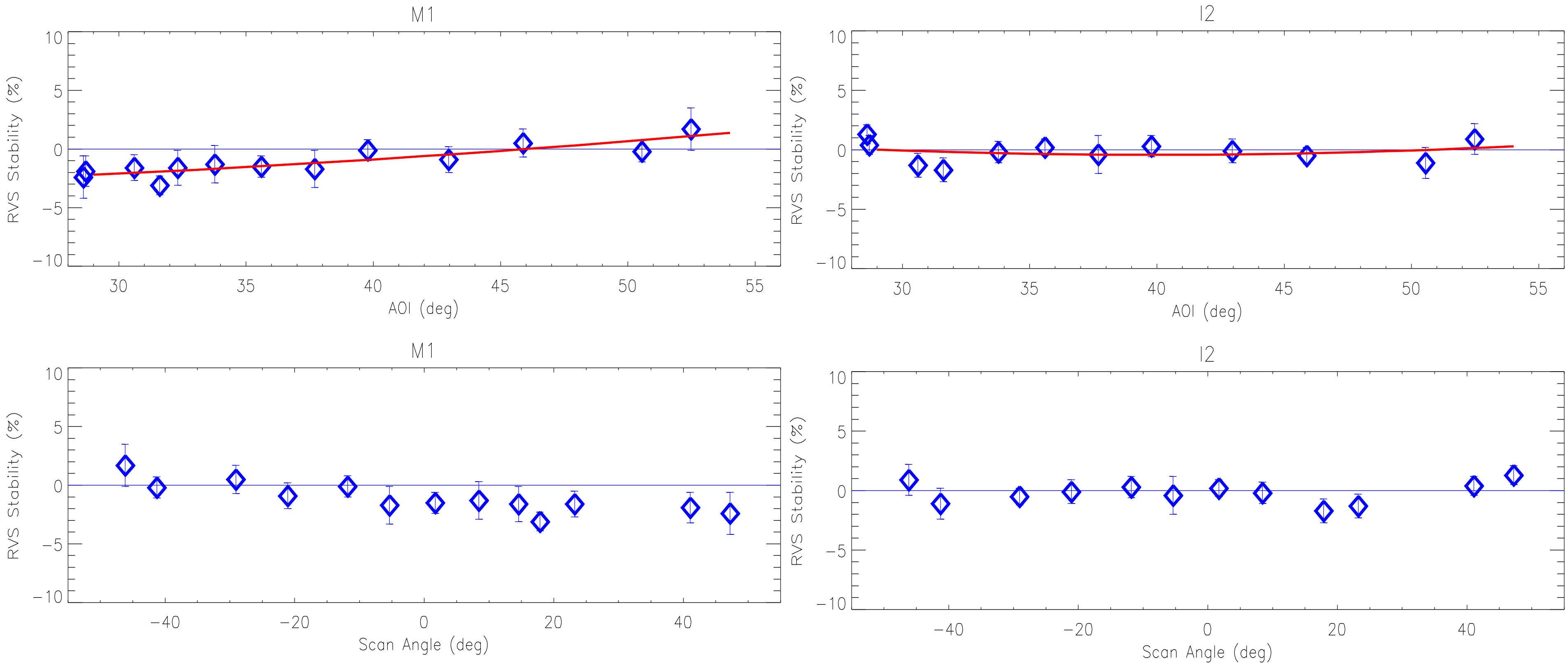

- Long-term EV reflectance trends can track the calibration stability.
- The drift is expected to significantly decrease in new L1B v1 product, using revised SD F-factor.
- The on-orbit response versus scan-angle (RVS) change is measured.

Improved Lunar BBR Trending

• VIIRS on-orbit spatial characterization can use EV scenes and Moon*.

• The BBR offset between two bands is characterized as the centroid displacement between their lunar images.

• The impact of the lunar image rotation to BBR trending is eliminated.

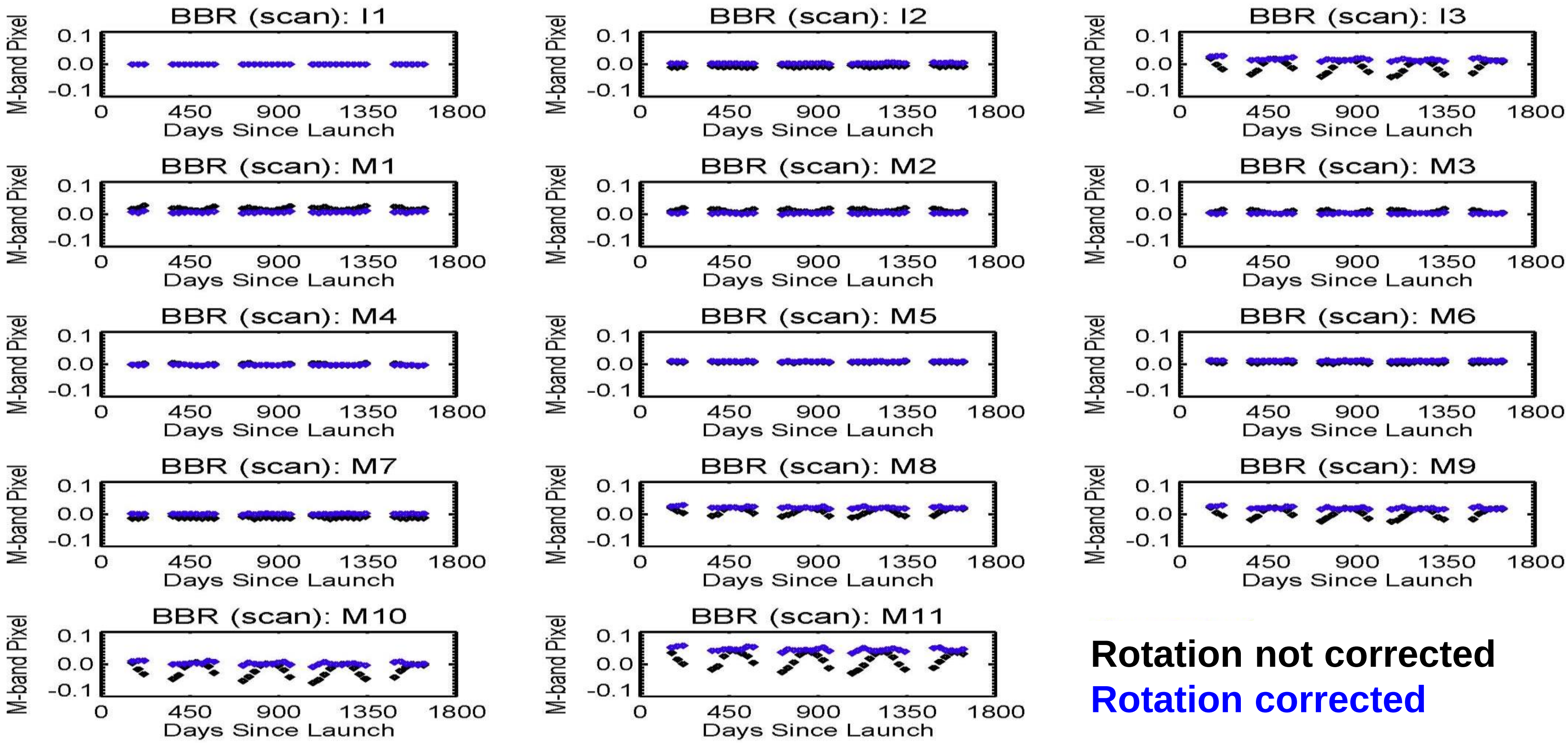

Summary

- Remote objects such as the Moon and EV sites have been used to independently track the stability of S-NPP VIIRS RSB radiometric calibration.
- The trends are consistent for all RSB within the design requirement. Long-term drift of up to ±1% have been observed for some bands.
- Adjustment of SD calibrated gain coefficients based on the lunar data trending has been implemented. Adjustment of RVS based on the EV data trending is feasible.
- Spatial parameters such as BBR have been characterized.
- Unscheduled lunar observations are available and the data can be used to derive lunar F-factor and BBR.
- Conduct absolute calibration with the Moon or EV scenes remains a challenging topic.